Tuning of PID Controllers within Building Energy Systems

PID-Regelungseinstellung
für Gebäudeenergiesysteme

Von der Fakultät für Maschinenwesen der Rheinisch-Westfälischen Technischen Hochschule Aachen zur Erlangung des akademischen Grades eines Doktors der Ingenieurwissenschaften genehmigte Dissertation

vorgelegt von

Johannes Peter Fütterer

Berichter: Univ.-Prof. Dr.-Ing. Dirk Müller
Professor Elias Kosmatopoulos, Ph.D.

Tag der mündlichen Prüfung: 21. September 2017

Diese Dissertation ist auf den Internetseiten der Universitätsbibliothek online verfügbar.

Bibliographische Information der Deutschen Nationalbibliothek
Die Deutsche Nationalbibliothek verzeichnet diese Publikation in der Deutschen Nationalbibliografie; detaillierte bibliografische Daten sind im Internet über http://dnb-nb.de abrufbar.

D 82 (Diss. RWTH Aachen University, 2017)

Herausgeber:
Univ.-Prof. Dr. ir. Dr. h. c. Rik W. De Doncker
Direktor E.ON Energy Research Center

Institute for Energy Efficient Buildings and Indoor Climate (EBC)
E.ON Energy Research Center
Mathieustraße 10
52074 Aachen

E.ON Energy Research Center | 49. Ausgabe der Serie
EBC | Energy Efficient Buildings and Indoor Climate

Printed in Germany
ISBN: 978-3-942789-48-6
1. Auflage 2017

Verlag:
E.ON Energy Research Center, RWTH Aachen University
Mathieustraße 10
52074 Aachen
Internet: www.eonerc.rwth-aachen.de
E-Mail: post_erc@eonerc.rwth-aachen.de

Herstellung:
afterglow - Werbeagentur und Digitaldruckerei
Vaalser Str. 20-22
52064 Aachen

Johannes Peter Fütterer

Tuning of PID Controllers within Building Energy Systems

Danke

allen, die mich auf meinem Weg unterstützt haben oder mich noch immer unterstützen.

Machen wir den Planeten ein kleines bisschen effizienter.

Abstract

Within this thesis, an extended PID auto-tuning algorithm for HVAC systems and building energy systems using the advances in computational power in recent years that is easily applicable to all state-of-the-art building energy management systems and building automation and control systems through the use of cloud-based services and standardized communication protocols is developed and demonstrated.

The algorithm is derived based on a review of theory and related work. A simulation study investigates the main characteristics of the proposed algorithm. Its real-life demonstration takes place in a multifunctional office building during full operation. Conducted in order to enable this research, the thesis presents the extension of the demonstration building's building automation and control system. On the one hand, the system is equipped with an extensive monitoring system; on the other hand, it is extended with an interface system that turns it towards a system that is able to interact with an IP-connected, thus cloud-like, server infrastructure.

The major contributions of this thesis are an innovative PID tuning algorithm, its general configuration suggestions for application within different types of control loops and its demonstration. Its applicability is proved and demonstrated within a simulaton study and real-life experiments.

The results for a classical real-life building automation system and different classically PID-controlled loops show an amelioration of the tuned systems' control performance in 68 % of the algorithm's applications. The application of the algorithm leads to control quality improvements of up to 90 %, accounting for both, simulation and field study, following the integral time-weighted absolute error criterion, ITEA and in comparison to a state-of-the-art adaptive auto-tuning method.

Additionally, in order to investigate the applicability of alternative control infrastructures as they might occur in future cloud-based building control systems, such control infrastructures are implemented and tuned with the proposed algorithm. Their tuning is far less successful, indicating that data resolution and transmission times are important and should be regarded in future applications.

Moreover, a technical structure for cloud-based services towards building operation optimization is proposed and demonstrated with PID control loop tuning as the use case. Finally yet importantly, a real-life demonstration bench for advanced control research as well as a simulation framework for the same purpose are developed.

Kurzfassung

Diese Dissertation widmet sich der Entwicklung und der Demonstration eines erweiterten PID-Autotuning-Algorithmus für Regelstrecken innerhalb der Automation von Gebäudeenergiesystemen. Es handelt sich um einen cloudbasierten Algorithmus, der große Rechenkapazitäten nutzt. Durch standardisierte Kommunikationsprotokolle lässt er sich dabei für alle Gebäudeautomationssysteme, die dem heutigen Stand der Technik entsprechen, anwenden.

Aufbauend auf dem Stand der Technik und Forschung wird der Algorithmus entwickelt und vorgestellt. Die Eigenschaften des Algorithmus werden im Rahmen einer Simulationsstudie analysiert und präsentiert. Anschließend wird dargestellt, wie die Automation eines Gebäudeenergiesystems zu einem Demonstrator für fortschrittliche Regelungstechnik umgebaut wurde. Der Umbau umfasst einerseits den Aufbau eines detaillierten Monitoring-Systems und andererseits die Implementierung von Schnittstellen zur Anbindung von externen Rechnern durch die Nutzung des Internetprotokolls. Als Demonstrator dient ein multifunktionales Bürogebäude, an welchem Feldtests des Algorithmus durchgeführt werden. Die Feldtestergebnisse und die Simulationsergebnisse werden in dieser Dissertation diskutiert.

Der Beitrag der Dissertation liegt in der Entwicklung und Demonstration des neuartigen PID-Autotuning-Algorithmus selbst, der Identifizierung von Standardeinstellungen für typische, in Gebäuden vorkommende Regelkreise und auf der Demonstration des Algorithmus im Gebäudeautomationssystem während des realen Betriebs.

Innerhalb des Feldversuchs erreicht der Algorithmus für verschiedene typische, grundsätzlich PID-regelbare Regelkreise eine Verbesserung der Regelgüte in 68 % der untersuchten und quantitativ vergleichbaren Anwendungsfälle. Je nach Anwendungsfall werden Verbesserungen von bis zu 90 % im Vergleich zu automatisch-adaptiv getunten Regelkreisen, bewertet nach dem zeitgewichteten Fehlerbetragsintegralkriterium, erreicht. Letzteres gilt sowohl für simulative Betrachtungen als auch für im Feldtest durchgeführte Experimente.

Zusätzlich wurde die Anwendbarkeit des Algorithmus auf alternative Regelungsinfrastrukturen getestet. Diese sind zukünftigen, cloudbasierten Systemen nachempfunden und wurden innerhalb des Demonstrators aufgebaut. Bei diesen Regelkreisen ist das Tuning wesentlich weniger erfolgreich, was die Bedeutung hoher Signalauflösung sowie kurzer Übertragungszeiten bei zukünftigen Regelsystemen unterstreicht. Mit den hier verwendeten alternativen Infrastrukturen sind robuste Regelungen nur schwer realisierbar.

Durch diese Dissertation wird eine technische Infrastruktur sowie ein Service zur cloudbasierten Betriebsoptimierung vorgeschlagen und demonstriert. Darüber hinaus werden in dieser Dissertation ein Simulationsprüfstand und ein Demonstrator für fortschrittliche Regelanwendungen entwickelt.

Contents

Nomenclature

Indices and abbreviations

Symbol	**Description**
A/C	air conditioning
AHU	air handling unit
ampl.	amplitude
ANN	artificial neural network
AO	absolute value optimum
ARMAX	auto-regressive moving avarage with exogenous
ARX	auto-regressive with exogenous
ASHRAE	International technical society organized to advance the arts and sciences of heating, ventilation, air-conditioning and refrigeration
BACnet	Building Automation and Controls Network
BACS	building automation and control system
BAS	building automation system
BEMS	building energy management system
BES	building energy system
BJ	Box Jenkins
BMS	building managenent systen
BMSVM	building management server virtual machine
CL	closed-loop
CO_2	carbon dioxide
DIN	German Institute for Standardization
Dist-1	every second changing disturbance signal
Dist-10	every 10 seconds changing disturbance signal
Dist-100	every 100 seconds changing disturbance signal
E.ON ERC	E.ON Energy Research Center
EBC	Institute for Energy Efficient Buildings and Indoor Climate
ER	excitation range

continued on next page

Indices and abbreviations

Symbol	**Description**
ESO	election-survey optimization
Exp.	Experiment
F	filtered
FEC	field equipment controller
FL	fuzzy logic
FOPDT	first order plus dead time
GA	genetic algorithm
GUI	graphical user interface
HVAC	heating, ventialtion, and air conditioning
HVAC&R	heating, ventialtion, air conditioning, and refrigeration
IAE	integral absolute error
ICT	infromation and communication technology
ID	identificaiton method
IDT	identification time
IMC	internal model control
INT	interface
IO	input-output
IP	internet protocol
ISE	integral squared error
ITAE	integral time-weighted absolute error
ITSE	integral time-weighted squared error
JCI	Johnson Controls Inc.
LON	Local Operation Network
LT	lambda tuning
MAE	maximum amount of excitations
MCIS	monitoring control and interface system
MDO	maximum disturbance order
mf	model fit
MIMO	multiple-input-multiple-output
MMO	maximum model order
MonitoringVM	monitoring virtual machine

continued on next page

Indices and abbreviations

Symbol	**Description**
MPC	model-predictive control
NAE	network automation engine
NCE	network control engine
NFL	no-free-lunch-theorem
NRMSE	normalized root meas squared error
OE	output error
OL	open-loop
OLE	Object Linking and Embedding
OPC	Object Linking and Embedding for Process Control
OPT	optimization
OV	overshoot
P	proportional
PB	proportional band
PEBBLE	Positive Energy Buildings thru Better controL dEcissions
PEM	predicted error method
PI	proportional-integrative
PIBO	PI tuned with absolute value optimum
PID	proportional-integrative-derivative
PILrobust	PI tuned with robust lambda-tuning
PISIMC	PI tuned with Skogestad IMC
PIZN	PI tuned with Ziegler and Nichols
PLC	programmable logic controller
PRAC	pattern recognition adaptive controller
PRBS	pseudo random binary signal
RBS	random binary signal
RC	resistor-capacitor
RT	rise time
RWTH	Rheinisch-Westfälische Technische Hochschule
SCADA	supervisory control and data aquisition
SIMC	simple/Skogestad internal model control
SISO	single-input-single-output

continued on next page

Indices and abbreviations

Symbol	**Description**
SO	symmetrical optimum
SQL	structured querry language
SS	state space
ST	settling time
Ste.	step experiment number
STR	sampling time read
STW	sampling time write
SVM	support vector machine
TCP	transmission control protocol
TF	transfer function
TV	total variation
US	undershoot
VCD	volume control damper
VM	virtual machine
VPN	virtual private network
w/a	water to air
w/w	water to water
ZN	Ziegler and Nichols

Symbols

Symbol	**Description**
$\bar{u}_{\mathrm{PID}}$	upper limit of operational range
$\underline{u}_{\mathrm{PID}}$	lower limit of operational range
A	polynominal term
B	polynominal term
C	polynominal term
c(t)	time dependent controller input
C_F	internal factor (JCI)
cp	specific heat capacity

continued on next page

Symbols

Symbol	**Description**
D	polynominal term
E	polynominal term
e(t)	time dependent white noise error term
f	frequency
F	polynominal term
f_{limit}	maximum excitation frequency
G	transfer function plant
h	opening angle
H_0	noise model
jw	frequency domain variable
K	controller's transfer controller
k	proportional gain in time domain representation, alternative meaning: discrete time variable
K_{p}	proportional gain
L	linear stable filter function
$\dot{m}$	mass flow rate
max	maximum
min	minimum
p	pressure
q^{-1}	common variable for contiuous time domain, discrete time domain, Laplace and frequency domain representation
$\dot{Q}$	heat flow
r(t)	time dependent set point
s	Laplace variabe
t	time variable
T	temperature
T_{Σ}	lumped time constant
T_D	derivative gain
T_I	integrative gain
T_I	i^{th} time constant, i = 1,2,3,...
u(t)	time dependent controller output

continued on next page

Symbols

Symbol	Description
v(t)	time dependent disturbance
$\dot{V}$	volume flow
y(t)	time dependent system output
y_0	system output
z^{-1}	discrete time variable

Greek symbols

Symbol	Description
ε	prediction error
Θ	set of parameter vectors
θ	parameter vector, alternative meaning: time delay
$\hat{\theta}$	estimated parameter vector
λ	tuning parameter
ρ	density
τ	time constant
τ_c	tuning parameter
ω	frequency

List of Figures

List of Tables

1 Introduction

Resources like fossil fuels are limited. The idea of consuming something limited seems not to be the best idea without having an alternative–despite thinking of climate change and its environmental consequences. The replacement of fossil energy by renewable energy sources causes high investment costs, positively correlating with the installed capacity. Thus, in order to accelerate the transition to a renewable energy system while and by reducing costs, a good idea is to consume less energy.

As buildings account for at least 30 % of the energy consumption, it is worth looking at the possibilities to reduce their energy consumption. One option is to better match energy demand and provided energy by increasing the control quality. Since buildings are widely proportional-integrative (PI) and sometimes proportional-integrative-derivative (PID) controlled and industry seems to be reluctant in adopting new technologies, a promising approach might be to once more investigate the possibilities of better tuning these controllers with a special focus on building energy systems, refer to Waide et al. [2014].

Even though PI and PID controllers are overwhelmingly used in industry and sophisticated tuning methods and software packages are available, the building automation industry and the heating ventilation and air condition (HVAC) industry still have a high ratio of poorly tuned controllers within HVAC controllers and building energy systems (BES) controllers. Consulting practitioners from industry showed that sophisticated PI- and PID-tuning-methodologies are widely not applied within building and HVAC automation, refer to Fütterer et al. [2015].

Within this work, I develop and demonstrate an extended PID auto-tuning algorithm for HVAC systems and BES using the advances in information and communication technology and especially in computational power within recent years. The proposed algorithm is easily applicable to all state-of-the-art building energy management systems (BEMS) and building automation and control systems (BACS) through the use of cloud-based services and standardized communication protocols. Thereby, the demonstration takes place in a real-life multifunctional office building during full operation. Therefore, the building's BACS was extended towards a demonstration system that enables this research.

This work's structure shows figure 1.1: A literature and state-of-the-art review is given in chapter 2. In chapter 3, the PID tuning methodology is theoretically derived and its implementation is presented. A simulation study, in order to investigate the developed method within a virtual test bed,

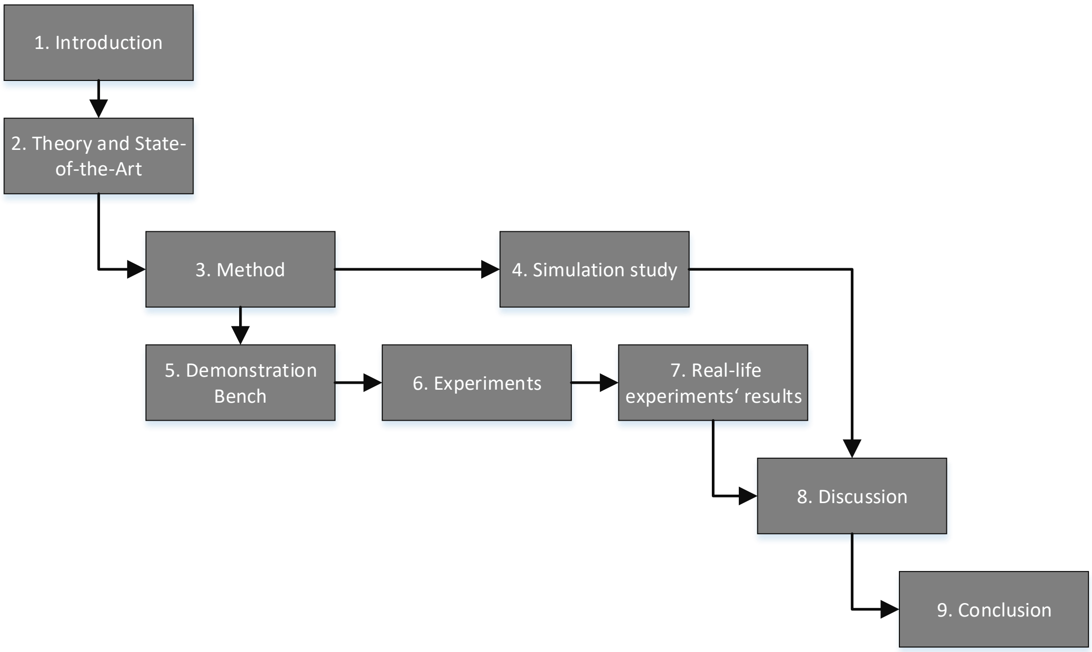

Figure 1.1: Thesis' structure

is presented in chapter 4. In order to conduct a real-life demonstration of the method, the E.ON ERC main building is converted into a demonstration bench for control research, which chapter 5 presents in detail. The methodology is then applied within this demonstration bench. Chapter 6 presents the experiment set up and the results are presented within chapter 7. Chapter 8 presents a discussion on experimental and simulation results. The thesis is concluded in chapter 9.

This work focuses on complex buildings, such as commercial, multifunctional buildings, having a building energy system with a central building automation system and distributed control loops, rather than on small or medium sized houses.

1.1 Motivation

Buildings need thermal comfort within a certain range. Maintaining thermal comfort within a certain range needs energy for air conditioning, heating and cooling. Building energy systems serve for maintaining the thermal comfort within certain ranges via converting energy and transportation of energy and mass flows. Thereby, they must meet the buildings' demand. Any deviation from the defined demand would mean a waste of energy or under-supply. Further buildings' needs can be process heat and cold, as well as services, aiming towards shading, illumination and security. The latter facts also account for those further needs.

Thus, BESs should aim towards consuming as little energy as possible, while producing as little cost as possible in order to fulfill the buildings' demands, which obviously forms an optimization problem. Therefore, BESs use different control approaches and systems to meet the current needs. A proper control strategy is an indispensable ingredient to achieve good performance, see Liu et al. [2011]. Within the BES and given its large part of energy consumption, the effective control for HVAC systems is of primary importance, as Afram and Janabi-Sharifi [2014] conclude in their review on control in buildings.

While advanced control strategies exist in research, the most commonly used control strategy is decentralized feedback control with or without a central supervision or set point control. The most commonly spread controller is the proportional-integrative (PI) and, far less often, the proportional-integrative-derivative (PID) controller[1]. By its nature, the PID controller is limited towards uncertainty, time varying systems and non-linearity, which virtually always occurs in buildings. Therefore, there is a need for performance assessment of theses control loops, see Erbe et al. [2006]. Still, PID control is broadly used. Beside of its given limitations, the control quality of a PID controller depends on its tuning. Not having sophisticated or automated methods, tuning a control loop is a time consuming process. Still, the cost of one single poorly tuned PID control loop may be negligible. This changes with an increasing amount of poorly tuned loops. Poor tuning leads to poor control quality, and accounting for the vast amount of PID controllers within a building energy system, poor control quality becomes a serious problem, since its most important consequence is that it increases operation and maintenance costs–besides CO_2-emissions.

The basic trade off is cost for PID tuning versus benefit of PID tuning. For PID tuning, one needs a certain amount of knowledge and experience. To change business processes within a company towards better PID tuning, certain costs occur for staff qualification, for PID tuning tools, and for the time consumed during the tuning itself. The benefit of PID tuning is contributed by e.g. less energy consumption, better need satisfaction and longer life expectancy of actuators.

For me, the most promising approach to provide most impact in terms of saving energy and cost is to develop a process that provides good control quality with acceptable specific costs and an acceptable amount of a priori knowledge for personnel and staff. Thus: I develop and demonstrate an extended PID auto-tuning algorithm for HVAC systems and BES. The algorithm improves control quality and thereby raises comfort or other need satisfaction indexes while lowering operation costs and saving energy.

The main innovation is that the algorithm uses sophisticated excitation signals (i.e. frequency-shaped, random-shaped and homogeniously/step shaped) to identify a large number of models for the controlled system. Then, it generates different sets of PID parameters and evaluates them

[1] In the following the abbreviation PID is used as a pars pro toto and explicitly including PI controllers for simplicity reasons.

within simulations before testing them in the real system. Therefore, the algorithm uses increased computational power, which is recently more and more available. A cloud-based instance can operate the program, which uses a standardized communication protocol. This makes it, on the one hand, flexible and low-cost applicable, on the other hand, applicable to all-state-of-the-art BACS.

1.1.1 Consequences of poor control quality

The consequences of poor control quality reported in literature, extracted from my own survey, refer to Fütterer et al. [2015], and told by practitioners are considerable and partly severe.

I understand control quality as how well a controller can keep or reach set points of a controlled system, considering the amount of control action. It is possible to measure control quality in different ways, refer to section 2.5. An example: consider that within buildings a certain input has to lead to a correct output. First, the output has to match the current needs, second, this output has to be provided in a way, that is energy efficient and does not cause too high other costs.

Good control quality can lead to little maintenance effort, good energy efficiency and good system demand satisfaction, e.g. appropriate thermal energy flows, thermal comfort, indoor air quality, correct illumination. Bad control quality can e.g. occur as oscillatory behavior of control loops; overshooting behavior; or permanent control deviation; or a combination of two or three of these characteristics, see Salsbury [1999] and refer to section 2.5. Oscillatory behavior leads to higher maintenance efforts due to higher wear and tear in valves, dampers, drives, etc. Overshooting behavior decreases energy efficiency and the systems demand satisfaction ratio. Permanent control deviation leads either to sub-optimal demand satisfaction or even to sub-optimal demand satisfaction and bad energy efficiency in parallel.

Literature considers the main consequences of poor control quality in: discomfort, as e.g. Jetté et al. [1998], Bi et al. [2000], Salsbury and Diamond [2001], and Ghiaus et al. [2007]; in high energy consumption, as e.g. Jetté et al. [1998], Bi et al. [2000], Salsbury and Diamond [2001], Anderson et al. [2007], Lin and Yeh [2007], Afram and Janabi-Sharifi [2014]; increased cost of maintenance due to increased wear and tear, as e.g. Bi et al. [2000], Salsbury and Diamond [2001], Zhou and Claridge [2012]; and in uncertainty in system control, e.g. Zhou and Claridge [2012].

Further, Zhou and Claridge [2012] provides an example of wasting energy:

> The overshoot may waste energy in certain application. Take the discharge air temperature control in VAV application for example. When the space load can be satisfied with the VAV box minimum air flow and the space temperature is close to the heating setpoint, the overshoot or oscillation in the discharge air temperature could invoke reheating in the VAV box and result in reheat and cooling cancellation.

In line with Zhou and Claridge [2012] and from observations of the E.ON ERC Main Building, poor control quality leads to non-interpretable system operation states and, thus, has influence on superior control decisions.

One final example: within a complex BES for a hospital, a PID controller was tuned in a way, that a valve was shifting between fully open and fully closed causing a whole distribution system's defect.[2]

[2] From an interview with a practitioner, Fütterer [2014].

2 Theory and state-of-the-art

2.1 Control in building energy systems

Buildings have demands for e.g. heating, cooling, ventilation, illumination, shading, electric devices, process heat, and or process cooling. The purpose of building energy systems is to fulfill these demands. I define a building energy system (BES) as a system that aims towards fulfilling building's energy demands, caused by comfort demands, e.g. for heating, cooling, ventilation, illumination, shading; utilization demands, e.g. electric energy demands for devices or thermal demands for process heating and cooling; and further demands, e.g. security. For BES providing heating, cooling, ventilation, process heat and or cold, it is possible to introduce a transfer layer, a transport layer, a storage layer and a conversion layer, compare Fütterer et al. [2013].

On the transfer layer, a BES can consist of devices using different principles to transfer energy flows or material flows to its end-use purpose, e.g. concrete core activation, floor heating, radiators, air outlets, active chilled beams, etc. The energy and material transport layer consist of tubes and pipes, dampers, valves, flaps, pumps or fans. On the energy storage layer, a BES consists of different storage for heat, e.g. water thermal storage, latent heat, sorption-based storage, and storage for electric energy, e.g. batteries. On the energy conversion layer, a BES can include e.g. boilers, combined heat and power engines, renewable energy conversion units, such as wind turbine, solar thermal collectors, photovoltaic, heat pumps.

So-called heating, ventilation, and air-conditioning (HVAC) systems are subsets of a BES. In my understanding, a HVAC system is a multi-purpose air handling unit in combination with air transport devices and air transfer devices. For me, it does not include water based heating or cooling systems that do not use air for the energy transport. Thus, e.g. a floor heating or a radiator are not part of an HVAC system.[1] This goes in line with the recent literature's understanding, e.g. Liu et al. [2011]. HVAC&R denotes a HVAC system with a refrigeration extension.

I define an air-handling unit (AHU) as a further subset of a HVAC system. An air-handling is the device that heats, cools, humidifies, and or dehumidifies air. Some air handling units use heat recovering devices. Air conditioning (A/C) or air conditioning unit denominates a decentralized apparatus, that supplies or extract heat on room level via a Carnot cycle process. It is often designed as a split

[1] Still, there are HVAC systems using water-based heat transport and air-based heat transfer, as e.g. active chilled beams, which I would include within HVAC systems.

unit, refer e.g. to Lin and Yeh [2007]. Referring to the definition of the BES, the A/C unit is part of the BES.

It is obvious that BESs have numerous control challenges. On a high level, the control goal is fulfilling the buildings' demands while consuming as little as possible energy. In other words, Naidu and Rieger [2011a] state that the two main requirements of any HVAC&R system are, first, to provide satisfactory indoor comfort (temperature and relative humidity) conditions to the building housing both humans and equipment, and, second, at the same time, minimize the overall energy consumption. This goes in line with Liu et al. [2011] who state maintaining indoor comfort, energy conservation, and environment protection as major control goals. Looking towards a lower level, each BES layer has again its own control goals, e.g. a three-way-mixing-valve that tries to provide a steady supply temperature or an air volume control damper (VCD) that tries to provide a demanded air volume flow. Again on a lower level, an actuator like e.g. the electric drive of the three-way-mixing-valve has again a control goal, namely to provide the demanded opening angle. When talking about a control strategy, one should consider the strategy's scope and level.

In this thesis' understanding, a control strategy is the utilization of rules and techniques to fulfill a control goal. Different authors reviewed and categorized state-of-the-art and recent research control strategies in the BES context. Considering control computing, follwing Ovaska et al. [2002], one can distinguish between two general approaches, hard control and soft control. Hard control has a clear output and needs a complete input to compute the output. Soft control may have an incomplete input and may compute different outputs having the same input[2]. In the sequel, I shortly introduce frequently cited or recent reviews, which appear to me as the most qualitative ones.

Afram and Janabi-Sharifi [2014] categorize between classical control (on-off, proportional ,PI, PID), hard control (gain scheduling PID, nonlinear control, robust control, optimal control, model predictive control), soft control (fuzzy logic control, neural network control), hybrid control (adaptive fuzzy logic control or adaptive neural network control on a higher level and hard control on lower levels, fuzzy PID), and other (direct feedback linear control, pulse modulation adaptive control, patter recognition adaptive control, preview control, bang-bang control[3], reinforcement learning control). They introduce the different approaches and discuss their benefits and shortcomings.
Liu et al. [2011] distinguish between feedback control (single-input-single-output, multiple-input-multiple-output, self tuning by fuzzy logic, neural network, smith predictor-based controller etc.), artificial intelligence control (adaptive neural network control, fuzzy logic control, expert system control), advanced control (model-predicitve control, H-infinity control, decoupling control, adap-

[2]Following Ovaska et al. [2002], soft computing, and thus soft control, includes tolerance for imprecision, uncertainty and partial truth in order to achieve robustness, tractability and low total cost. It differs from conventional hard computing in the sense that, unlike hard computing, it is strongly based on intuition or subjectivity.

[3]Bang-bang control is the common name for a two-parameter switching control, also known as on-off-controller or hysteresis control.

tive control, optimal control). As well, they discusses benefits and shortcomings.
Naidu and Rieger conduct an extensive, two-parted research review towards control in HVAC&R systems in Naidu and Rieger [2011a] and Naidu and Rieger [2011b]. They distinguish between hard control, soft control and hybrid control. Hard control includes PID control, gain scheduling, state feedback, optimal control, model predictive control, robust and H-infinity control as well as nonlinear and adapitve control. Soft control focuses on neural networks, fuzzy logic and genetic algorithms. They understand under hybrid control any possible combination between soft and hard control. Moreover, they introduce attributes like centralized control and decentralized control, discuss recent modeling, testing and validation activities, and summarize recent internet-based HVAC&R research.
Further, Mirinejad et al. [2012] review intelligent control techniques in HVAC systems. They as well state the control problem and discuss recent research directed towards fuzzy control. They then organize fuzzy control with expert knowledge, automated learning and hybrid, i.e. expert knowledge and automated tuning or learning. In order to provide a complete recent overview, I mention the review of Wang Wang and Ma [2008] and Dunis Dounis and Caraiscos [2009] without going deeper into details.

Despite the applied control strategy, state-of-the-art BES have control systems, frequently denominated as building energy management systems (BEMS) on a higher level, building automation system BAS, or building automation and control system (BACS), that consists of actuators, sensors, computational hardware, communication infrastructure, and user interfaces. These systems enable each control strategy. Within this thesis, I further use the abbreviation BACS which is meant to include the other denominations. Section 2.4 provides an overview of recent BACS's structures and capabilities.

2.1.1 Control relevant characteristics of buildings and BESs

Buildings and BESs have certain characteristics that aggravate the challenge to pursue control goals. Reviewing recent literature, important aspects are:

- ▷ **varying, time-depending operation conditions or characteristics**, see Afram and Janabi-Sharifi [2014], Ghiaus et al. [2007], and Seem [1998], thus robustness is hard to guarantee Afram and Janabi-Sharifi [2014]; especially variable load is mentioned by Ghiaus et al. [2007] and Seem [1998], changing operation modes are stated as a problem in Dexter et al. [1990];
- ▷ **non-linearity**, see Afram and Janabi-Sharifi [2014], Homod et al. [2012b], Liu et al. [2011], Ghiaus et al. [2007], Seem [1998], and Dexter et al. [1990];
- ▷ **multi-variable, coupled control**, see Afram and Janabi-Sharifi [2014], Homod et al. [2012b], and Ghiaus et al. [2007], a focus on cascaded loops provides Dexter et al. [1990];

- ▹ **high lag times**, see Homod et al. [2012b], and Liu et al. [2011];
- ▹ **uncertain, time-varying disturbance factors**, see Dexter et al. [1990], and Homod et al. [2012b];
- ▹ **complexity**, in terms of a high number of system parameters and functions, see Lin and Yeh [2007], and due to the fact that it is practically impossible to find an exact mathematical model for HVAC systems, see Mirinejad et al. [2012];
- ▹ **data quality**, poor data due to low resolution of analog-to-digital converter (ADC) devices, sampling rates, accuracy of sensors, and lack of access to network forecasting and environmental information, see Afram and Janabi-Sharifi [2014];
- ▹ **lack of supervisory control**, see Afram and Janabi-Sharifi [2014];
- ▹ **multi-objective optimization**, see Liu et al. [2011]; and
- ▹ **constraints**, as e.g. limited supply air temperatures, see Homod et al. [2012b].

Virtually all systems within a BES are exposed to time varying operation conditions with different time constants, as e.g. weather conditions change on a daily and yearly level, non-modulating energy conversion units can induce oscillations in supply temperature, user occupancy or process needs change during days and so on. Different actuators, such as e.g. valves, dampers, cause non-linearity, on-off operation of energy conversion units and humidifiers induce strong and coupled non-linearity. E.g. controlling thermal comfort is a hardly coupled control problem, as draft effects, CO_2 concentration and temperature matter at the same time. On component level, regarding an air handler, humidity and temperature are coupled. High thermal inertia, long transport or distribution distances, as well as inertia in tubes and ducts cause high lag times. E.g. user behavior is hard to predict and induces uncertainty, the same accounts for weather conditions. These and further issues show that control within buildings and BESs is not a simple task. This aggravates the fact derived from my own observations, that recent BESs do not store data or do not store data with sufficient sample rates on control loops in order to evaluate control quality. Further, information on control parameter adjustments is almost not available.

As seen above, advanced control methods exist, but regarding the state-of-the-art one must accept that the built environment is lacking technological advance. Most of the used control loops are still feedback control loops, e.g. on/off, proportional, PI, and PID, see subsection 2.1.2, while advanced methods are only focus of recent research. Ghiaus et al. [2007] state that PID control is only accepted because of the lack of catastrophic consequences. Conventional on/off operation controls many different components within a BES, e.g. humidifiers, adiabatic coolers, and A/C units, see Lin and Yeh [2007] and Salsbury [2002], which consumes significant power, see Liu et al. [2011]. Afram and Janabi-Sharifi [2014] see one explanation in the simplicity of on/off and PID control.

Current research related to control in BESs focuses on PID control and PID tuning, see subsection 2.1.2 and section 2.2 respectively, as well as on the amelioration, application and further development of advanced control strategies, see mentioned reviews and subsection 2.1.5. Here, high level goals are, following Liu et al. [2011], proper room air temperature or temperature and humidity, reduced energy consumption while improving indoor air quality, as well as systems steady-state performance and robustness. The author's goals in Lin and Yeh [2007] are, among others, that high performance controllers should intelligently adapt to varying operation conditions and load, and expanding single-input-single-output controllers to multivariable control. Further, Lin and Yeh [2007] ask for controllers with satisfactory transient and steady-state performance. Afram and Janabi-Sharifi [2014] claim for an ideal controller, meaning the ability to handle time-varying disturbances, wide operating conditions, actuator constraints, and variable price structures.

2.1.2 Proportional-integrative-derivative control in buildings

Figure 2.1 presents a classical feedback control loop. Ljung [1999] provides the basis for the following nomenclature. $G(q^{-1})$ describes the transfer function of the plant and $K(q^{-1})$ the controller's respectively. The variable q^{-1} represents either the continuous time variable t, the discrete time variable z^{-1}, the Laplace variable s, or the variable $j\omega$ in the frequency domain.

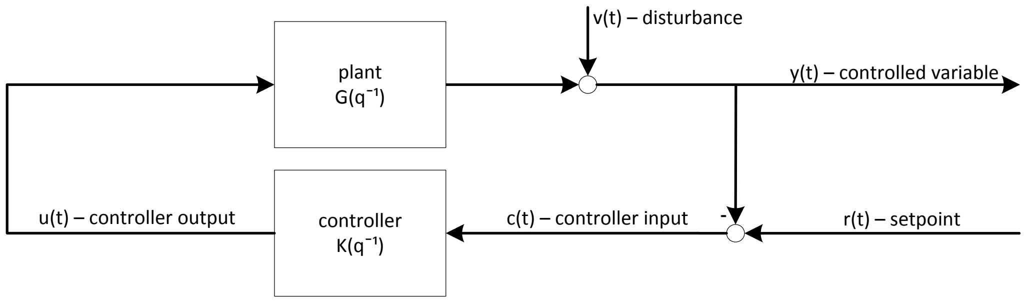

Figure 2.1: Control loop

The equations 2.1 and 2.2 describe the process' input, also denominated as the manipulated variable, $u(t)$, and the plant's output, $y(t)$, of a dynamic system, whereas $v(t)$ denominates a disturbance signal, $r(t)$ the set point signal and $c(t)$ the controller input, also denominated as control deviation.

$$y(t) = G(q^{-1})u(t) + v(t) \tag{2.1}$$

$$u(t) = K(q^{-1})c(t) = K(q^{-1})\left[r(t) - y(t)\right] \tag{2.2}$$

The theoretical and generalized PID control equation in the continuous time domain follows as

$$u(t) = K_{\mathrm{P}} \cdot \left[c(t) + \frac{1}{T_{\mathrm{I}}} \int_0^t c(\tau) d\tau + T_{\mathrm{D}} \frac{d}{dt} c(t) \right] \tag{2.3}$$

consisting of a proportional factorial term, a derivative term and a integrative term, whereas K_P denominates the proportional gain, T_I the integrative gain and T_D the derivative gain. A proportional controller (P) would neglect the derivative and the integrative part etc. Via manipulation of $u(t)$ the PID algorithm tries to keep the control deviation small, accounting for the deviation's magnitude $c(t)$ (proportional), its future development via its slope (derivative), and its history via its integral.

A good PID controller should be stable and robust, it should have a high set-point following and tracking performance at transients, a high regulation performance at steady-state, including load disturbance rejection, it should have high robustness against plant modeling uncertainty, and, finally, it should attenuate noise and be robust against environmental uncertainty, see Kiam Heong Ang et al. [2005]. Further, it should limit the amount of control action for devices where wear and tear is an issue.

PID control is the most frequently used control strategy in buildings, see Ginestet and Marchio [2010], Anderson et al. [2007], Bai and Zhang [2007], Ya-Gang Wang et al. [2001], and Jetté et al. [1998] for instance. For their study Bertil et al. [2005] even assume that a P controller is state-of-the-art in temperature control systems. This is because of well-known advantages of P, respectively PID control, see Bertil et al. [2005]. Mentioned advantages in literature are that the PID controller is most effective, see Homod et al. [2012b], Liu et al. [2011], and Seem [1998], that it is very simple, see Liu et al. [2011], Ginestet and Marchio [2010], and, thus, can be easily understood and executed by practical implementations, see Seem [1998]. Bi et al. [2000] state that PID control is simple yet sufficient. Further, PID controllers normally give better attenuation of low-frequency process disturbances and they give better robustness (less sensitivity to parameter changes) when compared to systems without feedback, see Bertil et al. [2005]. Zhou and Claridge [2012] state that a PID controller is sufficient in a wide range of operation.

My own survey among 58 German practitioners showed, that PID utilization is overwhelming. Advanced methods are rarely known (average over seven suggested so-called advanced methods was 35.71 %). On/Off control, as well as P, PI, and PID control are state of the art, refer to Fütterer et al. [2015]

Even though they are broadly used, PID controllers have certain disadvantages that lead to a poor control quality. A PID controller does not works satisfactorily, when PID parameters are not properly chosen, see Liu et al. [2011]. Reviewing literature, it becomes obvious, that PID tuning is often poor, see Skogestad [2003], which results in either sluggish or too responsive and instable behaviour, see Ghiaus et al. [2007], and might be due to a lack of process knowledge, see Ya-Gang Wang et al.

[2001]. Good tuning is hard to obtain:

> Designing and tuning a proportional-integral-derivative (PID) controller appears to be conceptually intuitive, but can be hard in practice, if multiple (and often conflicting) objectives such as short transient and high stability are to be achieved. Usually, initial designs obtained by all means need to be adjusted repeatedly through computer simulations until the closed-loop system performs or compromises as desired. Kiam Heong Ang et al. [2005]

Although the proportional-integral-derivative (PID) controller has only three parameters, it is not easy, without a systematic procedure, to find good values (settings) for them, as stated in Skogestad [2003]. Furthermore, the tuning of PID parameters in multiple-input-multiple-output (MIMO) plants is difficult to obtain because tuning the parameters of one loop affects the performance of other loops, occasionally destabilizing the entire system Homod et al. [2012b]. Jian Liu et al. [2009] expresse the need of a priori system and process knowledge by finding the reason in the fact, that all of the BAS software comes from developed countries, but on-site engineers did not have the experience of debugging PID parameters: Also, Lin and Yeh [2007] express that thorough system understanding is needed to design an automatic, high-performance controller for a modern air conditioning system. My survey among practitioners unveiled that that only 58 % are satisfied with achieved performance after control tuning, see Fütterer et al. [2015].

Moreover, even if well commissioned, PID controllers do have performance problems due to changing operation conditions, see Liu et al. [2011] and Bai and Zhang [2007], disturbances, significant time delays, and non-linearity, see Liu et al. [2011]. Mentioning non-linearity, Gu et al. [2008] add uncertainty as a further reason. Figure 2.2[4] tries to give an overview of where PID controllers can occur within a recent BES using the above-introduced layers. The sheer possible amount of PID controllers underlines their relative impact in terms of operation cost and energy consumption.

One can argue if PID control is a suitable control strategy, e.g. Bai and Zhang [2007] argues that a PID controller without adaption would not be sufficient, but, it is overwhelmingly used and, since BES industry is reluctant in adopting new technologies, it will be overwhelmingly used in future. Salsbury [1999] states that within industry methods of tuning are faster accepted than replacement of controllers, meaning control strategies in the denomination of this thesis. Moreover, Fütterer et al. [2014] showed that PID control, tuned with classical control rules is able to outmatch an implemented adaptive tuning of a state-of-the-art BES system–the referred system uses a pattern recognition adaptive controller, PRAC, see Seem [1998], as reference for comparison. Thus, the following chapters deal with the status of control loop tuning as it might handle limitations of PID control in

[4] This figure indicates where PID controllers can occur, it does not say that they must occur as indicated. Of course different control approaches might be used or more common at certain places.

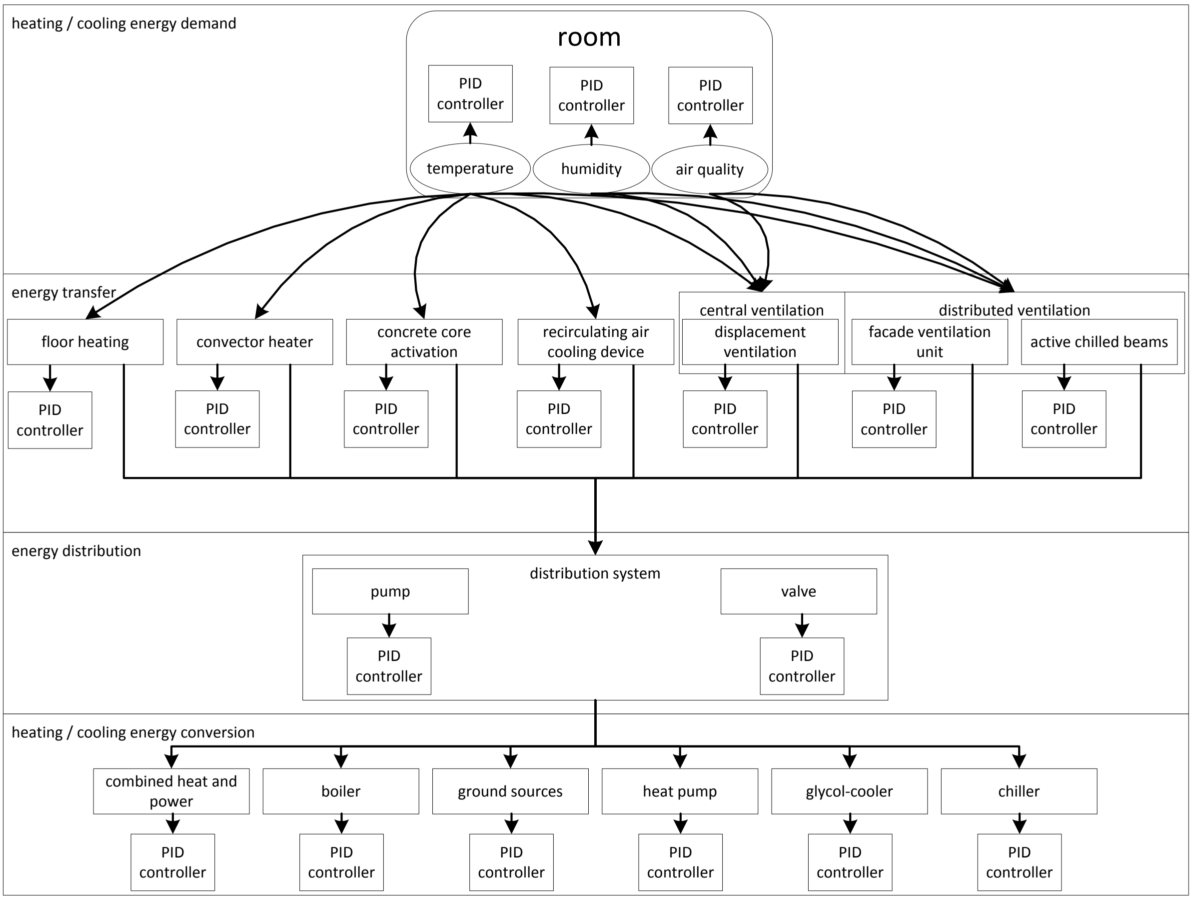

Figure 2.2: Schematic of possibly occurring PID controllers within an examplatory BES, see Kraus [2014]

buildings. After considering the cost of control tuning, subsection 2.1.5 presents possible alternatives and alternatives pursued in literature to improve control in buildings.

2.1.3 Status of control tuning in buildings

Control tuning is the process of adjusting the gains of a controller in order to fulfill certain goals or requirements. Goals and requirements can be expressed in numerical quality indicators or graphical, qualitative indicators. Both presents section 2.5. This subsection provides a brief introduction into the current status of control tuning, namely how it is approached within nowadays BESs, what is its quality, and what are research's foci.

It is possible to extract from recent literature that the industry conducts tuning either manually, see Salsbury [1999], applies self-tuning (also called auto-tuning) methods, see Jetté et al. [1998], or uses adaptive tuning algorithms, see Bai and Zhang [2007]. Considering manual tuning, although many improved PID design methods are proposed, the Ziegler and Nichols (Z&N) methods, see Ziegler and Nichols [1942], are still adopted by many BES control engineers, refer to Bi et al. [2000]. Bai and Zhang [2007] state that finding optimal PID gains by a trial-and error process is one of the most tedious problems faced by a field operators.

Tuning requires deep knowledge and insights into the controlled system, see Homod et al. [2012b] and Ya-Gang Wang et al. [2001], and appears to be hard in practice, see Afram and Janabi-Sharifi [2014], Kiam Heong Ang et al. [2005], and Ya-Gang Wang et al. [2001]. Skogestad [2003] states that PID tuning is not easy without a systematic procedure. Felsmann and Knabe [2002] state that control tuning is hard since implementing personnel does not have sufficient information.

Tuning is time consuming, see Homod et al. [2012b], for a control engineer, it may take up to three days to tune only one air pressure control loop, refer to Ya-Gang Wang et al. [2001]. Bi et al. [2000] state that some control engineers may take one to three days to search for a workable PID controller setting for an air pressure loop in a building. For a temperature loop, the time spent on PID parameter tuning may be even longer.

Further, an initial PID setting should be re-tuned continuously, see Homod et al. [2012b], or retuning should be done repeatedly Kiam Heong Ang et al. [2005], due to several reasons, as e.g. changing operation or usage conditions, aging of components or even due to changing ambient conditions.

The quality of control tuning is often very poor, see Pinnella et al. [1986] and Bi et al. [2000]. Salsbury [1999] found that the performance of control loops such as those associated with air-handling units had to be extremely bad before remedial action would take place. Further, he states that these problems are often hard to discover because they may be masked by others. Also, Ghiaus et al. [2007] consider PID tuning very poor, either sluggish or too responsive and instable. Ya-Gang Wang et al. [2001] find PID control loops poorly tuned due to a lack of process knowledge. Skogestad [2003] states that, in fact, a visit to a process plant will usually show that a large number of the PID controllers are poorly tuned. This might be explained by the fact that BESs are tailor-made systems. Each control loop with each controlled system is almost unique. This makes the control tuning task much more complicated than in retail products, where more time can be spent on their control.

The latter facts go in line with results from my survey on control tuning, where the vast majority of practitioners stated that the potential of amelioration in BACS is very high or high, refer to Fütterer et al. [2015].

E.g. Bi et al. [2000] propose auto-tuning to face the above-mentioned problems. There is a need because analytical models for HVAC systems are hard to obtain accurately, so an auto-tuner should be able to accurately identify and tightly control the processes in HVAC systems. In industry as well as in recent literature auto-tuner exists. This thesis reviews these tuners in subsection 2.2.2.

In general, control tuning can be conducted in an automated manner or manually, with or without excitement, as initial tuning or as re-tuning. Further, different approaches of adaptive tuning exist. Again, surveyed practitioners state that they used manual tuning in the majority of the cases, i.e. 73 %, while 37 % claimed to use automatic tuning. Severely, 12 % do not use any tuning at all, compare Fütterer et al. [2015].

Recent research foci are new auto-tuners, e.g. Soyguder et al. [2009], Jian Liu et al. [2009], Ya-Gang Wang et al. [2001], and Bi et al. [2000], new or improved control tuning rules and heuristics, e.g. Huang and Lam [1997], Nagaraj and Murugananth [2010], Zhou and Claridge [2012], adaptive PID tuning, e.g. Bai and Zhang [2007], or just the application and evaluation of certain PID tuning procedures, e.g. Fütterer et al. [2014], Wemhoff [2012], and Felsmann and Knabe [2002].

2.1.4 Cost of control tuning

The cost of control tuning can be considered as very high, since it is an time consuming task, which can only be conducted by highly trained and experienced personnel. It definitely increases the project's cost and prolongs the project's time. If re-tuning is needed, which is true for many large HVAC systems, the situation is even worse, see Bi et al. [2000]. Auto-tuning can decrease costs by decreasing the temporal effort per tuned control loop. Auto-tuners conduct identification experiments automatically. Still, an auto-tuner needs experienced personnel and their a priori knowledge to reach good tuning results. Thus, it decreases the amount of knowledge but does not make experienced personnel obsolete.

The costs of the process change from classical manual tuning towards auto-tuning and adaptive tuning can be found in higher hardware and or networking requirements and personnel qualification.

2.1.5 Advanced control methods

There is a vast amount of advanced control methods which all are approaches towards amelioration of control quality in terms of being an alternative to PID control. Afram and Janabi-Sharifi [2014] provide an extensive literature review on such approaches, which I suggested to read when questioning the thesis' motivation and approach.

The research approaches do solve inherent problems of PID controllers. They are extensions or basically different approaches. What they have in common is that they all need far more implementation effort, knowledge and experience. The change towards a control strategy that abolishes PID controllers would mean extensively more effort and cost. It is possible to derive that each of the methods, one more, one less, is hard-to-apply. Since BES industry is reluctant in adoption of new technologies and the market environment is very competetive, a sufficient, easy-to-apply, and relatively cheap PID tuning algorithm should outmatch other presented methods and be adopted by the industry.

2.2 PID control loop tuning

PID control loop tuning is the adjustment of the proportional, P, integrative, I, and derivative, D, gain in order to fulfill a design goal, which can be expressed by a control quality criterion or a combination of design criteria. Practical, especially digital implementations of the theoretical PID equation, see equation 2.3, often provide further tuning possibilities, like adjusting the PID algorithm's execution interval, its operation range, its anti-wind up, in order to compensate for raising integrative gain due to continuous control deviation originating from plant issues, its thresholds or its derivative kick attenuation.

The classical manual tuning approach of a control engineer is to gain knowledge about the controlled system by an excitement. Then, the engineer sets the gains according to a certain design rule, which he chooses with respect to his design goal. In order to evaluate the control quality, a closed-loop experiment can be conducted, which forms an extension of the initial tuning process. Thereby, the applied tuning rule is tested against the achieved control quality. If the control quality is not sufficient, the engineer uses either another tuning rule or fine-tunes the parameters via analytically derived heuristics or based on experience. In some cases, control engineers use their experience or heuristics directly to set control parameters. Then, no information gaining or identification of the controlled system takes place.

Aging of controlled systems due to wear and tear, as well as changing loads, change in ambient or other operation conditions calls for re-tuning of control loops. The process of manual re-tuning looks similar to the initial process or to its above-described extensions but takes place later and often periodically or due to certain events during the control loop's life time.

Figure 2.3 tries to categorize and to differentiate the different tuning approaches. The upper branch visualizes the above-mentioned process of manual tuning and manual re-tuning. Since no common denomination or vocabulary exists of terms like adaptive tuning, adaptive re-tuning, hybrid tuning, continuous tuning, automatic tuning and so on, I try and define those terms at least for the scope of this thesis following figure 2.3 in the sequel.

Within figure 2.3, the second branch from top presents self-tuning and adaptive re-tuning. Practical implementations of PID controllers can provide a self- or auto-tuning feature for initial tuning. The control engineer only has to trigger this auto-tuning feature when he implements the PID controller. Then, typically an automatic excitation and model identification takes place. With the gained information the PID controller automatically tunes its gains using a design rule, either fixed-implemented or chosen by the control engineer. A more sophisticated auto-tuner would evaluate different tuning-rules in a simulation environment using the identified model and would then apply the most suitable design rule. Another possibility would be to use an optimization algorithm with the identified model against a single quantitative design criterion or a combination of design criteria.

I define adaptive re-tuning as either a continuous fuzzy-based re-tuning, where heuristic fine-tuning rules are transferred into a fuzzy fine-tuner, or a continuous or periodical identification with or without excitation, which again can be periodical or automated triggered but not continuous. To highlight this, re-tuners either excite the system actively or use system-inherent disturbances or given set point steps. Within this context, "triggered" means that a certain event, which is recognized by the implemented algorithm, triggers something, which can be the excitation itself or the identification due to a step in the set point for example. With the re-identified controlled system, an automated re-tuning process takes place, similar to the above mentioned automated tuning.

The third branch from top within figure 2.3 shows fully adaptive tuning. Such a controller would have pre-defined initial parameters. Either it can use fuzzy-based adjustments or rule-based adjustments to continuously adapt the control behavior. A further possibility is to use the information gained during operation to continuously, or triggered by certain events, identify a model of the controlled process. The latter would then be followed by a continuous, triggered or periodical tuning, i.e. continuous rule-based tuning, periodical simulation- and rule-based re-tuning or periodical simulation-based parameter re-optimization, which all three are similar to above-mentioned related ones and need no further explanation.

The fourth and last branch of figure 2.3 defines hybrid tuning. I.e. manual tuning combined with adaptive re-tuning or an auto-tuning combined with manual re-tuning.

Considering the essentials between auto tuning and adaptive tuning one can state that both have advantages and shortcomings. Auto-tuning excites to get a tuning regime that fits to the desired operation range, while adaptive tuning adepts to a certain operation range. Within buildings, even a sophistic fix-tuned[5] PID controller might under-perform due to e.g. non-linearity and varying operation conditions. Even though researchers investigated and applied adaptive tuning methodologies, these adaptive controllers under-perform in real applications due to different reasons: such as not sufficiently skilled or trained personnel coping with configuration issues; continuous adaption during off operation times; multiple adaption in coupled systems etc.[6] Some kinds of adaptive controllers, i.e. model-based, identifying adaptive controllers need excitation in order to conduct

[5] Regardless whether manually tuned or auto-tuned.

[6] I self-observed all itemized reasons during commissioning of the E.ON ERC Main Building in Aachen

their adaption.[7] I assume that such controllers under-perform during periods with low excitation and might end in an over-adapted, meaning sluggish, state. Even further, when control loops operate at two or more operation points, as it occurs frequently in buildings[8], it is a plausible consequence that an adaption algorithm might over-adapt to one operation point which ends up in under-performance at the other operation point.

A vast amount of software packages for online and offline tuning is available. Also, there is a vast amount of patented tuning algorithms in industry and divers hardware PID tuners available, see Kiam Heong Ang et al. [2005]. Further, Kiam Heong Ang et al. [2005] state a lack within their analysis in 2005 by arising the need for the development of PID tuning software for HVAC systems. They hope that such systems would increase system performance, practicing company's production quality and efficieny without needing to invest a vast amount of time and manpower in testing and adjustment of control loops.

To the knowledge of the author, there is no software package or hardware tuner, that is freely programmable and open source. Thus, the internal algorithms used are not obvious and the understanding of the ongoing procedure would be fuzzy. Even further, to the knowledge of the author, non of these tools has been applied to HVAC tuning in the scope of a scientific publication. Therefore, I derived an open and understandable tuning methodology, which I applied within BEMS and HVAC control systems.

[7]As it is the principle of the so-called ConvCao used in the project "System-Of-Systems that act locally for optimizing globally", "Local4Global", funded by the European Union (EU FP7 611538), conducted at our institute.

[8]E.g. three-way mixing valves used for supply temperature control of a heat transfer device cooling during summer and heating during winter, having different temperature differences between inlet and outlet temperature in summer and winter mode and, thus, different mixing behavior as its transfer behavior.

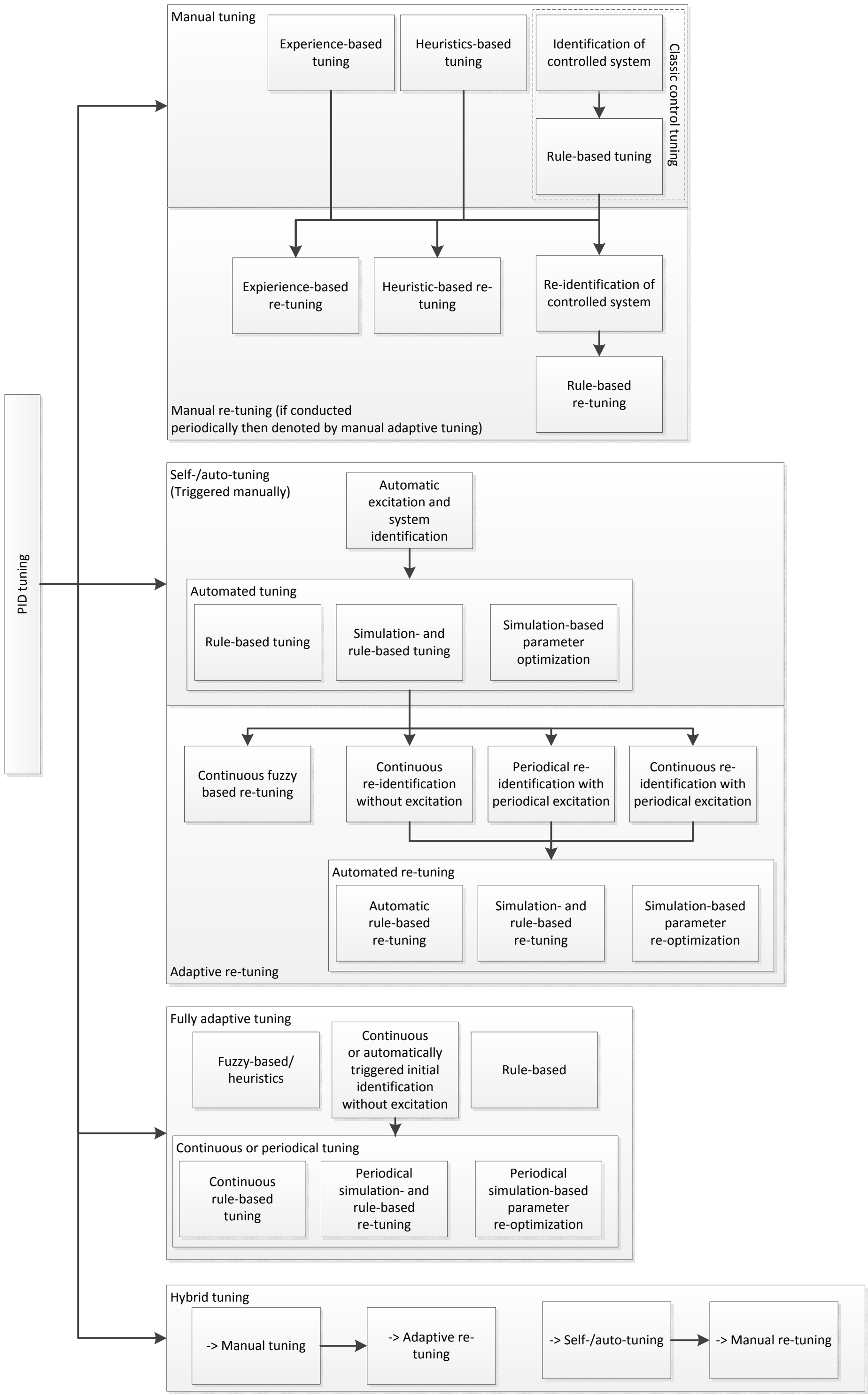

Figure 2.3: Categorization of PID-tuning approaches

In the sequel, I shortly introduce used classical tuning methods. I then review more sophisticated tuning approaches and auto tuners that researchers recently apply. Further, I outline the contributions and innovations of my proposed method. A possible enhancement of this method with an adaptive extension might be addressed in future work.

2.2.1 Classical tuning

A brief history of control tuning provides Bennett [1996]. Relevant for the scope of this thesis is the fact that a vast amount of control tuning approaches exist which evolved over time. My survey showed that over 70 % of practitioners use experience-based, intuitive parameters, which they set without applying any rule. 46 % use classical control rules and 67 % just stick to the delivered standard parameters from the manufacturer and do not conduct any control tuning[9].

The operation principle varies between control rules. There are control rules applicable to open-loop system and closed-loop systems. A further distinction can be made by model-free tuning[10], such as e.g. the tuning rules of Ziegler and Nichols (ZN), refer to Ziegler and Nichols [1942] and model-based tuning. Model-based tuning methods are e.g. internal-model control (IMC), lambda tuning, refer to Åström and Hägglund [2006] and Copeland et al. [2010], and simple/Skogestad internal-model control (SIMC), refer to Skogestad [2003]. Model-based tuning rules have a variety of design criteria, such as pole placement, e.g. the symmetrical optimum method, or designing loops with a pre-defined margin towards Nyquist stability in order to reach certain behavior. Model-based methods such as lambda-tuning have an optimization parameter in order to apply the method while aiming for different control behavior.

Out of surveyed practitioners that apply classical tuning rules, 56 % use Ziegler and Nichols, 45 % use other oscillation approaches, 31 % the absolute value optimum method, and, 15 % use the control rules following Chien et al. [1952]. But still, even if the control loop is correctly tuned, only 59 % state that the control performance is satisfactory.

2.2.2 HVAC control loop tuning research

In their review, Naidu and Rieger [2011a] provide an extensive section on recent PID research. In the sequel I shortly mention some examples for recent PID research with HVAC application.

Some researchers focus on simulation tuning with optimization. Such as Nagaraj and Murugananth [2010] who study the tuning of a PID controller using soft computing techniques, such as genetic al-

[9] Answers are not exclusively demanded, thus exceeding 100 %.

[10] Most model-free tuning rules, such as those of Ziegler and Nichols are in fact model-based, which makes them applicable to proposed algorithm in this thesis. This is because via finding an oscillation time and an ultimate gain, information is available to form a first order plus dead time (FOPDT) model.

gorithms (GA), evolutionary programming, particle swarm optimization, and ant colony optimization. They reach perfect PID tuning results with their (assumed) perfect system knowledge and towards their pre- and self-defined control quality criterion.

Huang and Lam [1997] are using genetic algorithms to optimize controller parameters for HVAC systems. They simulated their system, tuned it with genetic algorihms and compared them to the ZN classical tuning. It turned out that GA ameliorated the control behaviour.

Wenge et al. [2010] present research on PID control parameters tuning based on election-survey optimization (ESO) algorithm. They used ZN tuning to create initial conditions, derived second order models of their controlled systems and applied optimization towards integral absolute error (IAE), itegral time-weighted absolute error (ITAE), integral squared error (ISE), and integral time-weighted squared error (ITSE) criteria, compare 2.5 for further information on these criteria. They conclude that the ESO algorithm outperforms ZN tuning. What I particularly like within their research and considering the fact that buildings are custom made, unique systems is the no-free-lunch-theorem (NFL):

> for each and every optimization problem, a suitable algorithm should be developed since all algorithms are equally good considering the whole search space.

Wemhoff [2012] proposes a new, sophisticated tuning methodology for HVAC equipment. They apply the method on simulation basis within their simulation environment. Via LHVAC and Energy Plus lumped models, they show, that the method is capable of saving energy. Since the method is quite complex and not that easy to apply, compared with the methods presented in table 3.2, this method should be regarded within future research.

Further, Zhou and Claridge [2012] present a new tuning rule for discharge air temperature control based on time constants. First they point out that the PI control principle is sufficient. Then they propose new tuning rule for an air handler control system. They identify the system and use the time constants and the system delay to tune the P gain. Their design criteria is a five minute settling time. Moreover, they suggest a re-tuning heuristic: re-tuing should be done when the system exceeds 20 minute settling time. Here, their suggestion is an online auto tuning but they do not go into more detail.

Auto-tuning research for HVAC systems

Auto-tuning has been widely and successfully applied to many industrial fields, see Åström and Hägglund [1995]. The literature offers different references on auto-tuning for controllers in HVAC systems. E.g. Pinnella et al. [1986] proposed a self-tuning method of an integral-only controller and implemented it for fan static pressure and converter supply water temperature. Brandt [1986] exploits self-tuning control and especially its implementation issues towards application in HVAC systems. Nesler [1986] developed a computer based auto-tuning and self-tuning controller, where the open loop step test of Ziegler and Nichols methods was used to derive the process model and the controller. Wallenborg [1992] proposed a new self-tuning controller for HVAC systems. Bi et al. [2000] develop an advanced auto-tuner with different PID design methods based on step and relay experiments, which give satisfactory performance on HVAC systems. Ya-Gang Wang et al. [2001] apply an auto-tuner for HVAC based on Bi et al. [2000]'s PID design methods.

Moreover, a variety of adaptive tuning methods is proposed in the literature. Since this is not the scope of the thesis, as mentioned before, I just provide one example: Qu and Zaheeruddin [2004] introduced an adaptive tuning method based on H-infinity tuning rules converted to discrete tuning rules. They applied their method to a discharge air temperature control system and showed via conducting simulations that they were able to reach better results towards changes in plant parameters, disturbances and external noise.

To my best knowledge, within the here-proposed method, I have some significant innovations and work done beyond the above-presented state-of-the-art compared with other methods applied to HVAC systems. First, I apply the so-called "identification for control" method, compare Van Den Hof, Paul M.J. and Schrama [1995], for the first time to HVAC systems within an auto-tuning algorithm. I use multiple model structures and a theoretically infinite number of models with different structures and theoretically infinite model orders. Model number and model orders are only limited by computational power and temporal restrictions. I apply a variety of different control tuning rules and compare them later to find the best performing one. Thereby, I use self-identified models for the simulation-based control parameter evaluation. Finally, I practically evaluate the control parameter performance within the real control loop. Furthermore, the here-suggested method has flexible evaluation criteria and, thus, is adjustable towards users' preferences. Additionally, the algorithm is cloud-based, automated and fully scalable. Additionally, the found and reviewed research contributions are mostly use-case driven, meaning that researchers derive a solution starting from a certain problem related to a certain use case, whereas I try and propose a generic method for control loops in buildings, which is then demonstrated towards certain selected use cases. Last, I demonstrate the algorithm within a real-life building under full regular operation, exceeding the technology readiness level of simulation-based or experiment-based research contributions.

2.3 Application limits of PID controllers

For PID application a system needs controllability and observability. In the narrow sense for PID control, controllability means that a systems' influencing device has to be able to transfer the system output from one point to another within a finite time frame. In the narrow sense for PID control, observability means, that it is possible to measure the system output in so far, that the controller has a feedback signal.

Within buildings, multiple input, multiple output, so-called MIMO problems frequently exist. There are many dedicated control approaches for such systems, compare e.g. Ginestet and Marchio [2010] and Anderson et al. [2007]. Still, MIMO systems need an extensive amount of a priori knowledge. When using PID controllers for MIMO problems, one has to decompose the problem and use special PID control tuning methods.

Within buildings, especially heat distribution devices such as concrete core activation[11] do have high inertia which leads to high dead times and, thus, to an offset between influencing variable and controlled variable. For such systems special approaches exist, as e.g. the Smith-Predictor, which is a type of predictive controller for systems with pure time delay, compare Warwick and Rees [1988], Rehrl and Horn [2009] and Bai et al. [2008]. Further, for systems with high time constants, feedforward control approaches for disturbances may solve special problems.

Within building, especially in hydraulic networks, some opening and closing devices, such as two-way-valves and three-way-valves do have hysteretic behavior. PID control is able to cope with some hysteresis but also for this problem there are special control approaches as e.g. model-based controllers, compare Afram and Janabi-Sharifi [2014], and pulse width modulators, compare Salsbury [2002].

Still, for some systems that are in general not PID controllable, PID control is able to provide at least sufficient performance when considering special tuning principles, such as e.g. in sequenced systems, in which one might tune sequenced controllers in a different manner. E.g. a pressure control fan might be aggressively tuned while downstream volume flow controller might be tuned in a sluggish way. Still, such systems remain a multiple-input-multiple-output control problem.

A further issue within buildings is that control loops might operate at different operation points. PID control alone is not the perfect solution for such control loops. A possible option would be to use a gain scheduling PID controller with interpolation of the PID gains between the two designated operation points, compare Afram and Janabi-Sharifi [2014] and Huang [2011]. Still, PID can operate such systems when tuning is conducted in a robust manner.

Moreover, within buildings, many disturbances exists. PID is able to cope with disturbances but an active disturbance handling, like offered by MPC approaches, would ameliorate the control performance.

Finally, the knowledge used for tuning is never ideal. The assumption of ideal system knowledge and an aggressive tuning towards a fitted system model might end in oscillating behavior. The

[11] Sometimes denoted as thermally activated slabs.

robustness-concept, meaning how robust a system reacts towards model parameter changes, provides so-called robustness margins and provides approaches towards this fact, compare Skogestad [2003]. Robustness consideration might enhance the here-developed methodology and should be considered within future work.

As far as I observed during this thesis, my practical experience with different building automation systems, and concluding from the practitioners survey, I assume that PID controllers are applied too frequently in buildings–even for systems that are not PID-controllable or should not be PID-controlled.

2.4 Building automation systems

In the sequel I provide the a short description of BACS. For further information I like to reference to Balow [2012].

A BACS' computational hardware typically consists of hierarchically organized programmable logic controllers (PLCs) with different computational capacity. Hierarchical layers are the management layer, the automation layer and the field layer. First, the management layer covers the system's supervisory operation control. The here-proposed algorithm, if not cloud-based, might be part of this layer. Second, the automation layer covers control logic of the BES. PID control loops are part of this layer which makes this layer the most relevant for the scope of this thesis. Third, the field layer consists of sensors and actuators.

For its communication, BACS use proprietary and standard protocols, such as, frequently, e.g. BACnet, refer to ASHRAE [2012], or LONworks, refer to DIN German Institute for Standardization [7 11]. Its communication infrastructure consists typically of bell wire, BUS-specific wiring and Ethernet[12] wiring, such as Cat-5, 6 and 7 twisted pair. Within the management layer, a frequently used data interface is a server using the object linking and embedding for process control (OPC) protocol, see Mahnke et al. [2009].

2.5 Control quality

In general, people speaking of high control quality of a closed loop system mean that the controlled variable matches its set points over the purposed operation ranges and conditions, thus including transients from one set point to another, noise, and disturbances. To make this vague term of control quality measurable, researchers and practitioners use a variety of graphical, qualitative, and quantitative control quality indicators.

[12] Standards developed by IEEE working group 802.3

For PID control loops, the control quality crucially depends on their tuning. Further, computation issues, like possible maximum PID interval frequency, and communication issues, for example communication service delays can affect the control quality, as Song et al. [2007] show. If control quality is evaluated ex post and not via online data, one has to regard the resolution of the logged data, thus, the data logging frequency, which can influence the control quality indicators and the computational power of the controller itself. For the scope of this work, it is reasonable to assume sufficient computational power for the used PID controllers' computation intervals. I address communication capacity and PID interval times within chapter 3 and chapter 5 respectively.

In line with my observations within the E.ON ERC main building, its test hall, and divers test benches at the E.ON ERC EBC institute, as survey results show, and considering recent literature statements, refer to subsection 2.1.3, PID control quality is very poor in nowadays building energy systems. Even in components like the heat pump, installed within the EON ERC main building, the PID parameters seem to be chosen by hand.

Practically used control quality indexes are e.g.:

- control accuracy steady state/transient
- control variation steady state/transient
- control set point deviation steady state/transient
- settling time
- rise time
- undershoot
- overshoot
- integral absolute error
- integral squared error
- integral time weighted absolute error
- integral time weighted squared error
- total variation of manipulated input
- robustness margins

In literature, authors use unit step set point changes and unit step input (e.g. load) disturbances to excite a closed loop system and calculate control quality indicators. The quality indicators within DIN EN 15500, 2008 are suitable for longer periods and multiple steps in set points and changes in disturbances. Another possibility is that authors define their own quality indicators and use their own approaches to evaluate control performance.

Considering a room temperature control loop, standard DIN EN 15500, 2008, defines the control accuracy with keeping the control variation and the control set point deviation within certain limits. The standard defines control variation as the half of the controlled variable's maximum minus the controlled variable's minimum over a period of time where no set point changes occur–thus, under steady-state conditions. It characterizes the control's ability to keep a certain system output. The standard further defines the control set point deviation as the mean deviation of the controlled variable and the control set points[13]. Lahrech et al. [2002] use and extent these control quality indicators. They define their own limits for control classification and apply the indexes for steady-state as well as for transient conditions. Felsmann and Knabe [2002] also use these indexes.

Figure 2.4 provides an overview of control parameters that can be derived graphically, namely rise time, settling time, overshoot, and undershoot.

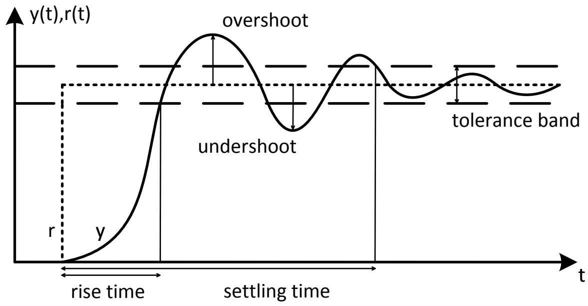

Figure 2.4: Control quality parameters

The rise time is the time the output signal needs to first enter the tolerance band around the new set point. The settling time is the time that it takes for the system from the time of the step in the set point signal to the time, when the output signal enters the tolerance band not leaving it again afterwards. An overshoot takes place, if the system output crosses the tolerance band in direction of the step and leaves it on the opposite side. The value of the overshoot is the maximum of the difference between the output signal and the set point signal on this side. Independent on the direction of the step the overshoot is always defined as positive. If after an overshoot the output signal crosses the tolerance band again and leaves it in the opposite direction of the step, this is called an undershoot. The value of the undershoot is the maximum of the difference between the output signal and the set point signal on this side. The value of the undershoot is defined as a negative number.

Equations 2.4 to 2.7 present the so-called integral criteria. The control error, which is the difference between the system output $y(t)$ and the set point signal $r(t)$, normed and integrated forms the

[13]The referenced version of this standard does have some inconsistency in its Apendix A. The control quality indexes are thus a matter to my interpretation.

integral absolute error (IAE):

$$\text{IAE} = \int_0^{\infty} |y(t) - r(t)| \, dt \tag{2.4}$$

Equation 2.5 defines the integral squared error (ISE):

$$\text{ISE} = \int_0^{\infty} \big(y(t) - r(t)\big)^2 \, dt \tag{2.5}$$

The integral time-weighted absolute error (ITAE) is defined like follows:

$$\text{ITAE} = \int_0^{\infty} |y(t) - r(t)| \; t \, dt \tag{2.6}$$

The last integral criteria, the integral time-weighted squared error (ITSE), shows equation 2.7:

$$\text{ITSE} = \int_0^{\infty} (y(t) - r(t))^2 \; t \, dt \tag{2.7}$$

These aforementioned graphical and integral criteria are output performance indicators and should, in general, be as small as possible. Further aspects of control are its input performance and its robustness.

As a measure for the input performance Skogestad [2003] supposes the total variation (TV) of the input signal $u(t)$ which is the sum of all its up and down movements and hard to compute for a continuous time domain signal. A discretization makes it computable following equation 2.8:

$$TV = \sum_{0}^{\infty} |u(t+1) - u(t)| \tag{2.8}$$

In order to provide a complete picture, going deeper into detail, it is possible to evaluate a control quality by taking a look at its robustness. Used indicators are the gain margin, phase margin and the sensitivity peaks. For further information please refer to e.g. Skogestad [2003].

A system's tuning towards a specific quality criteria influences its behavior. Åström et al. [1993] requests a system response without overshoot for HVAC applications. Zhou and Claridge [2012] state that a controller with a fast settling time and small overshoot is desirable for HVAC controls. Further, overshoot and extended settling time on discharge air temperature control impact the HVAC system control performance adversely in multiple dimensions including wasting building energy, disrupting HVAC system control accuracy, and wearing out control devices. However, an overly tight control performance requirement could reduce tuning robustness. The control performance may deteriorate quickly when the system dynamic changes with the application condition. A controller with acceptable control performance over wide application conditions could provide better overall results than a design condition optimized controller. To indicate the dependance on the design criteria, Hücker [2000] provides the table 2.1 which summarizes the impacts of the integral design criteria towards the resulting overshoot. In general, when designing control loops, one should use a suitable evaluation criterion.[14]

Table 2.1: Relation of the control quality parameters

name	overshoot	characteristic
ITAE	5%	short settling time
IAE	10%	short rise time
ISE	15%	very short rise time

In recent literature, by far, not all authors uses quantitative criteria. Song et al. [2007] use figures to only qualitatively conduct a result interpretation. Jetté et al. [1998] and Bi et al. [2000] proceed in the same way. E.g. Huang and Lam [1997] use settling time, and overshoot, whereas Nagaraj and Murugananth [2010] add rise time to their evaluation. Anderson et al. [2007] try to derive conclusions by just calculating the percentage in settling time change between competing controllers.

Contrarily, Wenge et al. [2010] use four integral criteria, IAE, ISE, ITAE, and ISAE, for evaluating their results in a more sophisticated way. Homod et al. [2012b] proceed in a similar way.

Own quality measures are introduced by e.g. Bertil et al. [2005], i.e. the absolute temperature set point deviation for 24 hours and the total effective energy use. Such measures are suitable for simulation studies or when experiments with exactly the same boundary conditions are possible. Within the PEBBLE project[15], together with co-workers, I used own strategies to evaluate control performance of a new adaptive control algorithm, i.e. a model based control parameter fine-tuning methodology for a nonresidential buildings, compare Constantin et al. [2012].

Skogestad [2003], as developing new control tuning rules, goes deeper towards stability and uses all gain margins, sensitivity peaks, TV and IAE as a joint criterion. Besides control quality, control loop diagnostics and fault detection is a topic within recent research, see e.g. Salsbury [1999].

2.6 Modeling

Within scope of related research, recent studies use models for several applications, e.g. control strategy tuning and development, model-predictive control, PID control tuning, fault diagnostics and so on. Within BES operation, models can serve to increase energy efficiency through better real

[14]The choice of the control criterion used within the proposed method is the ITAE-criterion as explained within section 3.2 on page 38.

[15]"Positive Energy Building thru Better controL dEcissions - PEBBLE", project funded by the European Union (EU FP7 248537)

time control, overall performance amelioration and fault detection. Moreover, models are the bottom line of every simulation study for whatever purpose. One can distinguish between white box, grey box and black box models. Further, a differentiation between the amount of input and output variables is possible, e.g. single-input-single-output (SISO) models, or multiple-input-multiple-output (MIMO) models. The sequel accounts for both:

- ▹ White box models are e.g. physical models, also denominated as forward models. Afram and Janabi-Sharifi [2014] state that physics-based models are based on the knowledge of the process, parameters that can be determined from manufacturer documentation and application of parameter estimation techniques on measured process data. E.g. Lin and Yeh [2007] and Homod et al. [2011] use such, partly highly sophisticated, forward models. Nassif et al. [2008], however, state that within application of PID tuning, it is of practical importance to develop simple, yet accurate and reliable models to better capture the real dynamic behavior of the subsystems and overall system over the entire operating range.
- ▹ Grey box models, are e.g. physical models with fitted parameters, lumped models[16], first order plus dead time (FOPDT), second order plus dead time (SOPDT), etc., derived by a plant analysis, e.g. graphical modeling in bond graphs, refer to Lin and Yeh [2007], or functional charts, see figure B.6 within appendix B. Those models are e.g. used by Bi et al. [2000], Ya-Gang Wang et al. [2001], Jian Liu et al. [2009], Anderson et al. [2007], Ginestet and Marchio [2010], and Zhou and Claridge [2012].
- ▹ Black box models, alias called data-driven models fit linear and non-linear mathematical functions to measured data, e.g. artificial neural network (ANN), compare e.g. Kusiak and Xu [2012] and Chen et al. [2011]; fuzzy logic (FL), refer to e.g. Homod et al. [2012a] and Soyguder and Alli [2009]; support vector machines (SVM), see Lixing et al. [2010]; n^{th}-order models with or without dead time, when shapes are not physically derived, refer to e.g. Bi et al. [2000] or for a 4^{th} and 5^{th} to Lahrech et al. [2002]; and statistical models, see Yiu [2008]. Afram and Janabi-Sharifi [2014][17]

Ya-Gang Wang et al. [2001] state that precise models are neither practical nor necessary for control tuning. Jian Liu et al. [2009] mention that FOPDT and SOPDT are sufficient for PID tuning. Data-driven models are in general regarded as more accurate than forward models, compare Nassif [2014]. Still, high data quality is needed to achieve well fitting models, see Afram and Janabi-Sharifi [2014].

[16] Since thermal networks are analogous to resistor-capacitor (RC) networks, one can link the resistances and capacities. For a detailed definition refer to Afram and Janabi-Sharifi [2014].
[17] This item bases on Afram and Janabi-Sharifi [2014]. I re-reviewed and extended it.

2.7 System identification

I found many publications for “identification for control” in the recent Literature, still I suggest reading Forssell’s dissertation on closed loop identification, Forssell [1999]. MacArthur and Zhan [2007] state that yet no simple and robust identification method exists, the basic scheme in practice is still “trial and error”. “Identification for control” is understood as identification exactly suitable for control loop tuning and not for other purposes, such as diagnosis, forecasting, and detailed plant simulation. Within identification for control, the system is excited, a data-driven model is derived and used for application of a control tuning rule. Figure 2.5 shows a flow diagram of this procedure. The procedure crucially depends on the a priori knowledge for the excitation experiment design, model selection, and choice of mathematical identification method.

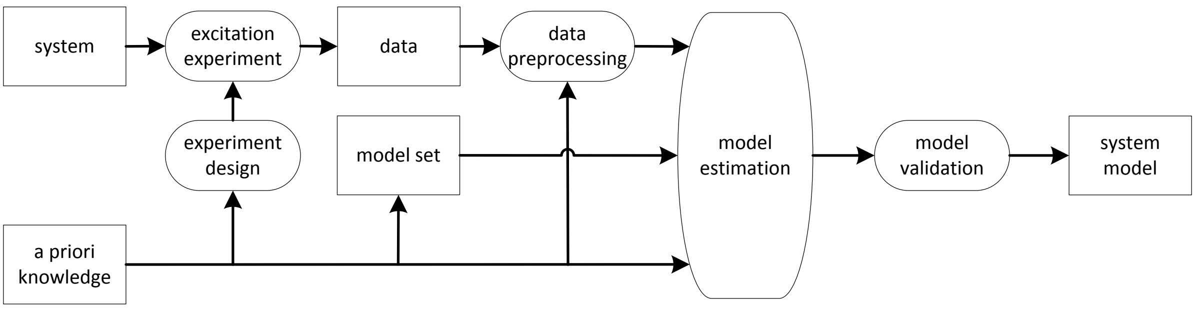

Figure 2.5: System identification procedure, depending on a priori knowledge for experiment design, model selection, and choice of mathematical identification method

In general, excitation for system identification is possible in open-loop, meaning directly to the system and closed-loop, including the control loop and exciting the control set point.

2.7.1 System excitation and identification experiments

The aim of the identification experiment is to gather data from the real system in order to derive a system model within the model estimation. Forssell [1999] sees the identification experiment as the most important aspect of the system identification.

Crucial for the identification experiment is setting up the input signal, also denoted as excitation signal. It is possible to vary the signal in terms of its energy, its power, and its frequency spectrum, e.g. assessed by Fourier transformation. Figures A.2 and A.1 in the appendix provide two examples of different input signals.

In general, the amount of gathered information increases with power and experiment time. Thus, theoretically, shaping must orientate towards as much power as possible and as long as possible experiment time, which is, of course not always suitable.

Typical input signals might be band-limited white noise, random binary signal (RBS), compare figure A.1 in the appendix, and pseudo random binary signals (PRBS). Optimal input signals are typically specified in their spectral properties, compare Rojas et al. [2007]. Goodwin et al. [2008] proposes a $1/f$ signal, whose amplitude decays with its frequency, as such signals provide higher identification robustness. In general, the input spectrum of the whole frequency range is of interest, but not more than three decades of time constants should be identified in one attempt. Thus, Ljung [1999] proposes to use multiple identification attempts in such a case.

When assessing the cost of an automated identification experiment, for buildings, performance degradation during experimentation is far less important than the experiment time and connected energy consumption or service effects, such as e.g. lower thermal comfort. Bombois et al. [2006] raise the question of finding the least costly identification experiment for control. Thus, it is important to find economically reasonable experiment lengths meeting the trade-off between model fit and cost.

Data collection and preparation are further important issues in the literature. The choice of the correct sampling time is always a trade-off, as discussed in chapter 8.2.1. Thereby, an important aspect to regard is the prevention of aliasing effects, e.g. by cutting of the frequencies above the Nyquist frequency. In the opposite direction, filtering, e.g. low pass filters like the Butterworth filter, compare Butterworth [1930], might be a good way to prevent fitting towards measurement noise.

2.7.2 Model estimation

There are three basic identification structures in identification for control: the direct approach, the indirect approach, and the joint input-output approach. A explanatory figure provides 2.6.

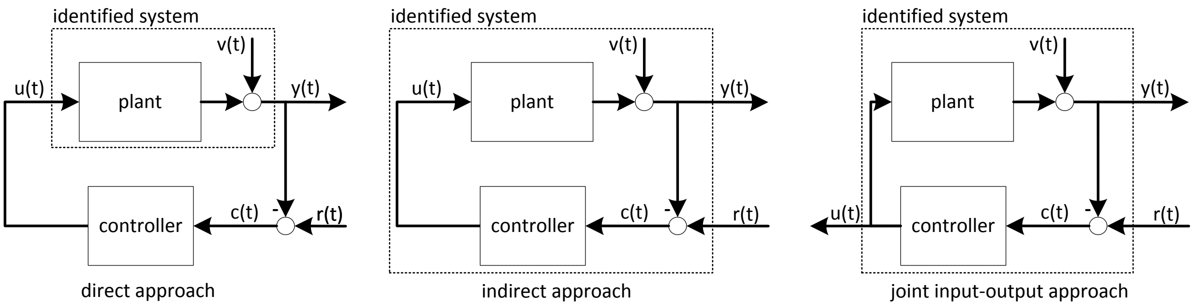

Figure 2.6: Approaches for system identification: direct, indirect and joint input-output approach. Figure taken from Kraus [2014], who drew it following Agüero et al. [2011].

The direct approach provides consistency and optimal accuracy, further, it has optimal statistical properties, and, it is practical, since data availability is given and this approach inherits certain advantages. The indirect approach needs perfect knowledge of the controller which cannot be achieved over multi-vendor BACSs. See Agüero et al. [2011] for further explanation and a discussion on advantages and disadvantages for each approach, including the input-output approach or the virtual closed-loop method.

In order to fit input-output data towards models, literature offers various methods and approaches. Most of them stick to one of the following common principles:

- ▹ Minimization of the posterior probability of the probability density function of the model error (e.g. predicted error method, PEM),
- ▹ the correlation of the model error with specific signals and aiming at non-correlation (spectral analysis methods), and,
- ▹ the minimization of a scalar valued function of the model error (know as “subspace identification approach”), compare Ljung [1999].

Spectral analysis are older techniques and non-parametric, whereas subspace identification approaches are susceptible towards measurement noise and input correlations in close-loop identification. To fit models suitable for the identification for control method, the prediction error method is quite common in the field of system identification applications and easily applicable, compare Åström [1980] and Ljung [2002].

2.7.3 Model validation

In general, the aim of a model is to meet the real plants output. The engineering question rises about the following: the effort that can be spend on the model validation adds a dimension of complexity to the persistent trade-off between effort of modeling and computational time towards accuracy of the model in respect to the model’s actual use case.

One can conduct a variety of numeric and non-numeric investigations, meaning visual investigations. E.g. comparing the model’s output data to the real plant’s output data directly, deriving residuals, investigating and comparing models and plants spectral characteristics, investigating the residuals via confidence intervals and auto correlation, etc. It is literally possible to drive the effort of comparing a model to the system to infinite. In practice, the task is to find a good-enough model validation method for the respective use.

In building control reseach, in order to validate models, many different approaches are part of the the literature. Afram and Janabi-Sharifi [2014] concisely and pointedly state the following:

> Performance metrics are defined to compare prediction results of different models and their deviations from measured data. Models are compared using absolute error, maximum absolute error, mean absolute error, mean bias error, mean squared error, ab-

solute percentage error, mean absolute percentage error, standard deviation of absolute error, standard deviation of absolute percentage error, coefficient of determination, root mean square error, coefficient of variation, goodness of fit, relative mean error, mean absolute relative error, coefficient of multiple determination, and correlation coefficient, compare Kusiak and Xu [2012], Henze et al. [2004], Kusiak et al. [2010], Soyguder and Alli [2009], and Kumar and Kar [2009].

For data driven models, a common procedure is the application of a cross-validation method. Within cross-validation, an available data set is split into identification and validation data. The model is then compared to the part of the data which is left out of the identification procedure.

2.8 Model order reduction

As model order reduction, this thesis understands the reduction of the mathematical complexity of the applied numerical models in order to suit for the applied control tuning methods.

It exist a variety of model order reduction approaches. The majority of methods are projection-based, e.g. the proper orthogonal decomposition. Thereby, the main directions of the model's transfer behavior are identified and projected to a smaller dimension, e.g. a three dimensional space might be projected to a planar surface using direct projection with manipulation of the coordinate system.

Another technique is a balanced turncation of time constants. E.g. neglecting them, adding them to dead times or distributing them to other time constants. Application of such techniques inherits certain risks, i.e. neglecting important information, and an argumentation for the method is needed, e.g. it is known that the model has one major time constant and other identified time constants might originate from disturbances or system noise.

Skogestad [2003] suggests a special model order reduction technique with certain rules on how to handle time constants in order to achieve models suitable for his PID tuning rules.

2.9 Own research history and methodology

The problem of dissatisfying control quality became obvious to me, when I tried and developed control strategies for the new E.ON ERC main building within different projects[18]. In order to ame-

[18] "Energy Concept for the new E.ON ERC Main Building", funded by E.ON gGmbH, refer to Fütterer and Constantin [2014]; "Positive Energy Building thru Better controL dEcissions - PEBBLE", funded by the European Union (EU FP7 248537), refer toConstantin et al. [2012]; "exergetically optimized HVAC control with dynamic and flexible integration of a monitored geothermal borehole heat exchanger field", funded by the German Federal Ministry of Economics and Technology funded project (03ET1022A), refer to Michalski et al. [2014]; and "System-Of-Systems that act locally for optimizing globally", "Local4Global", funded by the European Union (EU FP7 611538), refer to Schild et al. [2015].

liorate the operation at all building automation system's levels, i.e. field, automation and management, the building was transferred into a demonstration bench for control research, refer to Futterer et al. [2013]. Having the test bench developed, I postulated that classical control tuning rules would outmatch the implemented adaptive controllers. The proof-of-concept was successful, refer to Fütterer et al. [2014], thus, the automation of whole methodology with attention to scalability and using the advances in information and communication technology was the next step, refer to Futterer et al. [2015]. The simulation study provided detailed insights, refer to Fütterer et al. [2016]. Having the fully automated control tuning algorithm, I conducted an experimental study, whose results are presented within this thesis for the first time. Finally, I jointly analyzed and discussed the simulative and experimental results.

Research methods can differentiate towards their implementation level. Ranked by practical implementation level in increasing order, researchers use simulation studies, software-in-the-loop approaches, test benches, test benches coupled with software or simulations, namely hardware-in-the-loop approaches, or demonstration benches, closely linked to field test. In general, the level of technicality, thus the technology readiness level, rises with the implementation level, which pushes the research issue closer to industrial implementation and adoption. The presented research uses simulations and a demonstration bench, which is a real-life building under full operation conditions, thus, it has the highest technology readiness level amongst research methods.

3 Method

As stated in the introduction, see chapter 1, my goal is to ameliorate the control performance of PID control loops within HVAC system and BESes using the advances in information and communication technology and especially in computational power within recent years.

This goal clearly addresses PID control loops since they are widely applied and their performance is crucial for the overall performance of nowadays state-of-the-art buildings, as shown in chapter 2. One might argue that there are more advanced control principles which should be applied but removing all PID control from BESes seems not to be likely to happen within upcoming years. Thus, having good performance in PID control loops remains crucial.

In order to achieve the above-mentioned goal one can pursue many approaches, such as e.g. better education of personnel manually tuning PID control loops, the application of auto-tuning algorithms, of adaptive tuning algorithms, and hybrid tuning approaches. A variety of PID-tuning approaches and principles exists, see figure 2.3 and its explanation in section 2.2.

For me, having an applicable PID auto-tuning algorithm, on the one hand, provides the most promising solution to achieve the goal, and on the other hand, if exists, is able to provide a better basis for any adaptive controller compared with any standard configuration. The here-developed methodology can be used in any state-of-the-art HVAC or BES, which cannot be easily the case for an adaptive methodology, which either would have to be implemented on a system's programmable logic controller (PLC) or on a cloud-based-device that would have to be permanently connected to the BES. Further, any tuning, even adaptive tuning, anyways, needs a certain amount of excitation in order to develop a good parameter regime, thus, there is a reason to focus on the excitation signal's properties and on the most promising exploitation of the gathered data, as included in the here-developed algorithm. Adaptive tuning approaches have further shortcomings as explained in section 2.2. Still, adaptive extensions might be beneficial to this method and thus remain a topic for further work.

The presented method cannot solve PID tuning problems that are due to misplaced or misused PID controllers. Such misplaced or misused PID controllers occur frequently in HVAC and BES, see section 2.3 on the application limits of PID controllers.

This chapter presents the developed algorithm with focus on the methodological aspects. The application aspects are addressed in chapter 5.

3.1 Implemented algorithm

The presented algorithm, refer to figure 3.1, considers both possible initial conditions: stable and unstable control loops. If the aim is to find an initial controller parameter configuration, it uses open-loop experiments. If the algorithm's purpose is to re-tune a controller in order to improve the control quality, it first estimates the current control quality with the execution of a closed-loop step experiment with the aid of different common performance indicators.

Then, it conducts an identification experiment in order to find a large amount of system models which are afterwards used for finding control parameter combinations. Therefore, no matter in which way, either open- or closed-loop, it collects input-output data of the system by exciting the system following different excitation signals. The gathered output data is then used for the system model estimation. The identification uses different model structures and model orders to identify a large set of system models.

After that, the algorithm ranks the system models by applying a so-called fitness function in order to evaluate the models. Thereby, it uses the cross-validation method. The algorithm selects a subset of useful models for the further procedure. Thus, the ranking is used to reduce the number of models for computational capacity reasons, since this saves simulation time for the sequel steps.

The next step is the PID parameter calculation. The identified system models serve for the calculation of several PID parameter configurations with different tuning methods.

Then, a simulation analyzes each combination of system model and parameter set for the respective closed-loop system by estimating the combination's control quality. A transformation of the ranking according to the control quality estimation's results takes place, with an indication of the best simulation-based PID parameter model combinations.

In the last step, the user chooses an arbitrary amount of PID parameter sets to be tested in the real plant. A comparison between the resulting real plant's control qualities for each parameter set and with consideration of the initial plant's control quality provides the most advantageous set up.

For the documentation of each experiment, the algorithm provides results via comprehensive figures and data sheets. Thereby, the most important result is the comparison of the initial control quality with the new control quality. Further, figures of the control loop's step experiments in order to investigate its transfer behavior manually.

The user is now able to decide whether the achieved control quality is sufficient and the transfer behavior of the loop is acceptable for the overall system operation. If it is considered as sufficient, the user may use the documentation as a certificate for the conduction of control tuning. If the result is not sufficient, the algorithm's input parameter might be adjusted and further algorithm runs conducted. Of course, a rerun of the algorithm in total, e.g. in order to improve the results or whenever it might be necessary due to changes in the system, is also possible.

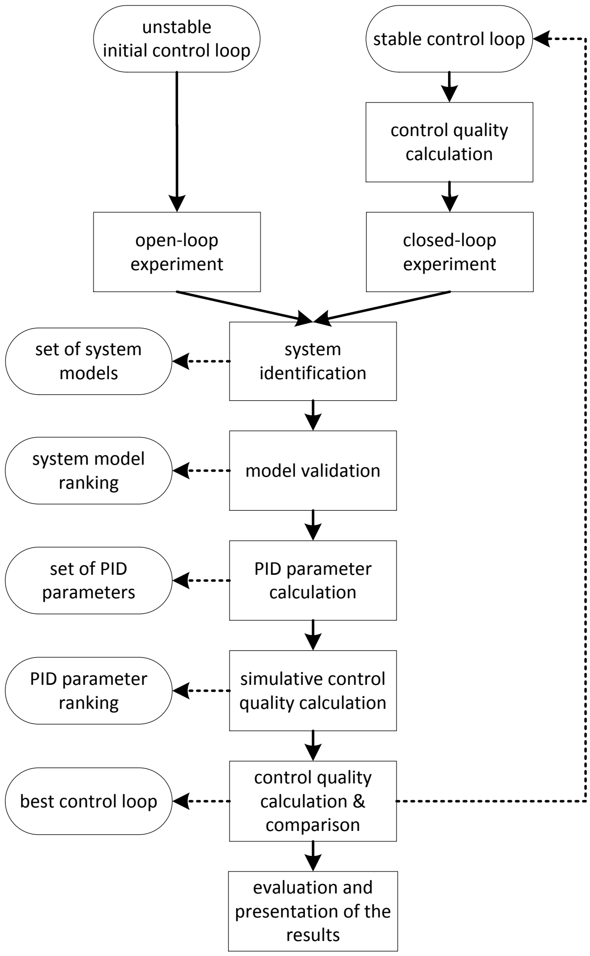

Figure 3.1: Proposed controller auto-tuning process

The steps from the model validation up to the control quality calculation with the real plant are an adoption of the so-called identification for control method, refer to Van Den Hof, Paul M.J. and Schrama [1995]. Its idea is that only an implementation and a test of the controller in the system assures that the quality criterion for the identified model is sufficient, see Forssell [1999], and Forssell and Ljung [1999].

In the sequel, I describe the main parts of the algorithm in detail.

3.2 Control quality estimation

As shown in Figure 3.1 and explained before, the first task in the algorithm is the estimation of the system's initial control quality. Simple closed-loop step experiments provide the used indicators and therefore, they are easy to apply and have comparable conditions among different executions. The rise time, the settling time, the undershoot, the overshoot, and the integral parameters like integral absolute error (IAE), integral squared error (ISE), and integral time-weighted absolute error (ITAE), are calculated in order to provide all the information for the user, refer to section 2.5. The indicators were chosen due to the fact that these indicators suffice in order to describe a control loop's behavior.

For the ranking of the different controller configurations the algorithm uses the ITAE criterion, see equation 2.6 on page 27, as it leads to small overshoots and short settling times, which HVAC applications request in general, refer to Åström and Hägglund [2006] and Hücker [2000] and refer to section 2.5. However, the choice of the quality criteria or a weighted combination of quality criteria is possible. The algorithm user can define the control quality calculation towards his own control requirements.

When calculating integral criteria, sampling times of gathered data get crucial. Therefore, when comparing the control quality results of algorithm runs with different data logging sampling times (in the following denoted as sampling time read, STR), mathematical calculations are conducted to guarantee for comparability.

3.3 Modeling

Within the method proposed, I use a data-aided model selection applied to statistical models, where different model structures are fitted towards the data of the process. The idea behind is that with data-aided model selection, less a priori knowledge is needed for the algorithm user and the algorithm itself gets more general. Further, since computational effort and applicability for the scope of this thesis play a role, I renounce artificial neural networks (AANs), fuzzy logic (FL), and support vectro machines (SVMs).

The model structures cover a variety of models and model orders. The used model structures cover auto-regressive moving average with exogenous (ARMAX), auto-regressive with exogenous (ARX), Box-Jenkins (BJ), and output error (OE) in a discrete time domain. Further, I applied state space (SS) and transfer function (TF) estimations within both, continuous and discrete, time domains. Refer to table 3.1 for the mathematical model descriptions. The latter statistical models are standard models suggested by and used within related work, compare Yiu [2008].

Table 3.1: Used model structures

name	structure	time domain
ARMAX	$A(q^{-1},\theta)y(k,\theta) = B(q^{-1},\theta)u(k) + C(q^{-1},\theta)e(k)$	discrete
ARX	$A(q^{-1},\theta)y(k,\theta) = B(q^{-1},\theta)u(k) + e(k)$	discrete
BJ	$y(k,\theta) = \frac{B(q^{-1},\theta)}{F(q^{-1},\theta)}u(k) + \frac{C(q^{-1},\theta)}{D(q^{-1},\theta)}e(k)$	discrete
OE	$y(k,\theta) = \frac{B(q^{-1},\theta)}{F(q^{-1},\theta)}u(k) + e(k)$	discrete
SS	$\dot{x}(t,\theta) = A(q^{-1},\theta)x(t) + B(q^{-1},\theta)u(t)$ $y(t,\theta) = C(q^{-1},\theta)x(t) + D(q^{-1},\theta)u(t)$	both
TF	$A(q^{-1},\theta)y(t,\theta) = B(q^{-1},\theta)u(t)$	both

For each model, the signal $y(t)$ is the output of the system, $u(t)$ the input, $v(t)$ the disturbance entering the system, and $e(t)$ a white noise signal. The coefficients A, B, C, D, F represent polynomials of the variable q^{-1} and with a certain parameter vector θ. The index 0 for the transfer functions and signals of the true system is used whenever it is necessary to distinguish between the true system and the model.

These structures can be centralized in the following equation

$$A(q^{-1},\theta)y(t,\theta) = \frac{B(q^{-1},\theta)}{F(q^{-1},\theta)}u(t) + \frac{C(q^{-1},\theta)}{D(q^{-1},\theta)}e(t) \tag{3.1}$$

where the model of the system is also represented by the equations

$$y(t,\theta) = G(q^{-1},\theta)u(t) + v(t,\theta) \tag{3.2}$$

$$v(t,\theta) = H(q^{-1},\theta)e(t) \tag{3.3}$$

and the true system is described by the equations

$$y_0(t) = G_0(q^{-1})u(t) + v_0(t) \tag{3.4}$$

$$v_0(t) = H_0(q^{-1})e(t) \tag{3.5}$$

The disturbance signal $v(t)$ covers the measurement noise, process disturbances, non-measurable input signals and effects of system linearization. Its dynamic behavior gets reproduced by transforming a white noise signal $e(t)$ with a noise model $H(q^{-1})$.

These definitions are used for the explanation of the applied model estimation algorithm, PEM, compare A.1 within the appendix.

3.4 System excitation and identification

The aim of the system identification is to provide suitable models for the applied PID tuning rules, see section 3.5.

After the initial control quality evaluation the algorithm tries to identify the above-mentioned model structures. To do so, it needs so-called input-output data. In order to gather this data, the algorithm uses an active system excitation. The here-applied method widely follows the practical multistage method for fully automated closed-loop identification of industrial processes, suggested by MacArthur and Zhan [2007][1]. Another approach, without active excitation, might be to use monitoring data over a certain period of time, hoping for sufficient information in order to derive system models. Such an approach would inherit the above-discussed shortcomings of an adaptive control approach, see discussion in section 2.2 on page 18.

3.4.1 Excitation signal and experiment

The identification experiment has to be set up, in other words, the excitation signal has to be shaped and the length of the experiment has to be set. The adjustment of the experiment's length is important due to the wide range of controlled systems with very different dynamic behavior in buildings. Hence, the identification experiment length is a input parameter of the algorithm. The design of the excitation signal is also crucial for the success of the identification method, refer toMacArthur and Zhan [2007]. For the length of the excitation experiment, the user has to meet the trade of between sufficient accuracy and acceptable excitation cost, see subsection 2.7.1 on page 31.

For building-use, the assumption is that the amplitude of the excitation signal should be limited to excite the system around a certain operation point. For given amplitude, binary signals have the maximum power, refer to Ljung [1999]. Thus, the algorithm considers only binary signals.

However, beside the amplitude, the frequency spectrum characterizes the excitation signal. The distribution of the excitation signal's energy over the frequency range of interest is important for the identification experiment, see Ljung [1999].

[1] For a broader discussion of the identification for control method and the applied identification methodology, compare Kraus [2014], master thesis, which is available upon request. For the scope of this thesis I try to point out the most relevant things. Interested readers have to refer to the mentioned literature, such as Van Den Hof, Paul M.J. and Schrama [1995], Forssell [1999], and MacArthur and Zhan [2007].

The user of the algorithm has the possibility to choose from three different signal types. The first one is a random binary signal (RBS). The RBS has high energy in the frequency range from zero to the upper limit frequency, f_{limit}, which defines the minimal pulse width of the RBS. I introduce the limit frequency as two times the frequency of an excitation signal consisting of alternations only with the minimal pulse width. Figure A.1 within the appendix shows the frequency spectrum of the RBS signal. The minimal excitation pulse width leading the maximum excitation frequency, f_{limit}, is an user-defined input parameter of the algorithm called sampling time write, STW.

The second excitation signal is shaped to a spectrum with a frequency decay of $1/f$. Within a chosen range the power of the signal decays with $1/f$, as Goodwin et al. [2008] considers this kind of excitation signal as most suitable. Rojas et al. [2007] show, how to design such a signal. The signal's power is caped low outside of this range between the lowest and highest frequency. In case of the algorithm, the lower limit of the range is set very close to zero and the upper limit to f_{limit}, to be consistent to the RBS spectrum.

The part of the excitation signal with high energy should cover the frequency range of interest for the identification. Therefore, the algorithm provides the possibility to adjust the minimal pulse width of the excitation signal. Furthermore, the user is free to choose the amplitude and the mean value of the excitation signal. Figure A.2 within the appendix shows the frequency spectrum of the $1/f$ signal.

The third excitation signal consists of uniform steps. The algorithm's user is able to define the steps as he does for the step experiment with settling value, step value, settling time and waiting time. Additionally, it is possible to set the number of step repetitions.

In open-loop mode, the excitation signal is equal to the system input signal; in closed-loop mode it is equal to the set point signal. As described above, if possible, the algorithm should executes a closed-loop experiment which, however, remains an algorithm parameter to choose. This mode of operation shapes the frequency spectrum of the input signal in a control relevant way. Thereby, the controller prohibits an unlimited system output, compare Forssell [1999].

3.4.2 Data pre-processing

Figure 3.1 does not show the pre-processing of the experiment data as a single step. It is part of the system identification step. The algorithm provides the possibility to remove the means from the data. The usage of a low-pass filter before or within the system-model-estimation-method is possible as well. It is reasonable to choose the time constant of the filter in relation to the highest frequency of the excitation signal. The algorithm calculates the limiting frequency, f_{limit}, with the smallest pulse width. It does not use higher frequency parts in the binary signals. Thus, these frequency parts have significantly lower amplitude in the frequency spectrum of the input signal.

Therefore, with high probability, the higher frequency parts in the system's output signal do not mainly originate from the input signal, but from disturbances and noise. The algorithm filters all measured signals automatically and cuts off all frequencies above f_{limit}. The user is also able to choose a sampling time for the experiments in relation to the analyzed system, which should be chosen at least two times f_{limit} to prevent aliasing effects following the Nyquist–Shannon sampling theorem.

3.4.3 Applied system identification

For the system model identification in closed-loop mode, there are three different approaches: direct, indirect and joint input-output approach, refer to subsection 2.7.2. The algorithm uses the direct approach as the transfer functions in commercial BEMS controllers are not always fully known or not known to a sufficient extent, see section 3.6. Further, the direct approach is preferred to advanced methods such as the virtual closed-loop method Agüero et al. [2011], because it is easy to apply.

Hence, in both operation modes, open-loop and closed-loop, the algorithm uses the plant's input and output signals and directly identifies the open-loop system behavior. For the identification, it uses six different model structures, that table 3.1 shows, in order to provide a wide range of models to maximize the chance of a successful identification. The model's time domain is either discrete or both, meaning used in a continuous and discrete domain.

In order to fit the input-output data to the proposed model structures, the prediction error method is used. Spectral analysis are older techniques and non-parametric, whereas subspace ID approaches are susceptible towards measurement noise and input correlations in close-loop identification. To fit models suitable for the identification for control method, PEM is quite common in the field of system identification applications and easily applicable, compare Åström [1980] and Ljung [2002]. A mathematical explanation of the applied estimation algorithm, PEM, is attached in the appendix, section A.1 within the appendix.

For all structures, the algorithm estimates multiple models with varying model and disturbance orders. The models with the lowest order are first-order models. The highest considered model order is a parameter that the user chooses in the algorithm. It depends on the system of interest and it may be higher than the expected order of the dynamic system. The algorithm provides continuous as well as discrete system models. For some control loops, measured disturbances are further inputs for the system estimation method. The order of the additional transfer functions is free to choose, independently from the order of the transfer function of the system model. The algorithm uses the prediction error method to estimate the parameters of all model structures. In general, the algorithm generates a bunch of models and looks for the most effective ones to use in the further procedure, as MacArthur and Zhan [2007] propose.

3.4.4 Model validation

The algorithm automatically divides the data record of the identification experiment into two parts. The first part, two thirds of the data, serves for the model estimation method and the other part, one third of the data, serves for the model validation. That means that the algorithm applies a cross-validation method.

In general, Forssell [1999] does not recommend using a residual analysis of the estimation error for evaluation purposes, if one needs a reliable statement about the quality of the model. In this case, he recommends a frequency-depending criterion. Those criteria are not within the scope of this thesis due to their complexity. Further, following the literature's idea of the identification for control method, such as the one presented in this thesis, it is suitable to use a residual analysis.

The first reason is that the aim is not to search for the best model but for the best control parameter configuration. The second reason is that the algorithm uses a large number models[2] out of the total identified number of models to calculate the PID parameter configurations. Thereby, the residual analysis just provides a relative ranking in order to choose which models to use for the further process.

For the first reason, anyways, the algorithm validates the quality of the model through the control quality reached with the new control parameters later. The aim here is a general model validation and it is not to identify the best model. It is sufficient to identify those models, which are obviously not usable. Therefore, the assumption is that the usage of the residuals, as introduced in subsection 2.7.3, equation 3.6, is suitable for this good-enough evaluation.

For the second reason, the residuals serve as criterion for the ranking of the identified models. Beside of that, the number of neglected models is an adjustable parameter of the algorithm, which represents the trade-off between computational resources and possible higher control quality.

Thus, for the scope of this thesis the algorithm uses residuals and the derived so-called model fit for a ranking of models within the "identification for control" method, refer to Forssell [1999]. The normalized root mean squared error (NRMSE) is defined as follows:

$$\text{NRMSE} = \frac{\sqrt{\frac{1}{n}\sum_{t=1}^{n}\left(y(t,\theta) - y_0(t)\right)^2}}{y_{0,max} - y_{0,min}} \tag{3.6}$$

[2] 150 models per standard experiment within this thesis.

Here y_0 is the output of the system and y the output of the model. In respect to this definition, a fitness value can be calculated which will be used within the framework of this thesis.

$$\text{fit} = 100\% \cdot \left(1 - \frac{\sqrt{\frac{1}{N} \sum_{t=1}^{N} \left(y(t,\theta) - y_0(t) \right)^2}}{\sqrt{\frac{1}{N} \sum_{t=1}^{N} \left(y_0(t) - \bar{y}_0 \right)^2}} \right) \tag{3.7}$$

$\bar{y}_0$ is the mean value of the system output and defined as

$$\bar{y}_0 = \frac{1}{N} \sum_{t=1}^{N} y_0(t). \tag{3.8}$$

3.4.5 Model order reduction

For applicability reasons, the algorithm uses simple procedures to fit the derived models into a suitable form for the different tuning methods. Furthermore, the model reduction methods from Skogestad [2003] have been implemented and used. Further or more sophisticated model order reduction methods might be in the scope of future research. If a PI controller is used ($T_D = 0$) the ZN and LT methods approximate the system by a first-order model with time delay ($PT_1 T_d$). Thereby, a possibly identified second time constant is added to the time delay. Further time constants are neglected. In case of the absolute value optimum (AO) and symmetrical optimum (SO) methods all time constants, except of the largest one, are added to the parameter T_Σ. The system is here approximated by a PT_1 model as a possible time delay is neglected. All methods mentioned above do not consider nominator time constants (zeros in the transfer function of the system).

This is not the case for the Skogestad internal model control (SIMC) method, refer to Skogestad [2003], as a model order reduction algorithm is applied, which is proposed in combination with the actual controller parameter tuning rule. Here, the system is approximated also by a $PT_1 T_d$ system, but all time constants in nominator and denominator are considered automatically. The method also includes a tuning parameter τ_c in the equations. Within the framework of this thesis this parameter is fixed to $\tau_c = \theta$ as recommended for a fast and robust controller tuning. For further details see [Skogestad, 2003].

The situation is similar, if the parameters for a PID controller are searched. The only difference is that the AO, SO and SIMC methods then approximate the system with a second-order model. The way how the remaining time constants are considered stays the same.

3.5 PID parameter calculation

As Figure 3.1 shows, the next task is the calculation of the PID controller parameters. For each considered model, the algorithm calculates a variety of parameter sets for the PID controller according to various classical tuning rules, i.e. Ziegler-Nichols, Lambda Tuning, absolute optimum method, symmetrical optimum method, and a more recent one, namely Skogestad IMC, see Skogestad [2003] and compare subsection 2.2.1.

Those tuning rules approximate the systems as PT_1, PT_1T_d, PT_2 or PT_2T_d systems, which is reasonable for the analyzed control loops. However, the considered tuning rules work only with continuous time models. Therefore, it is necessary to transform the discrete models, shown in 3.1, to continuous models by a zero-order-hold interpolation, which was implemented by using the "System Identification Toolbox"/MATLAB.

For the proposed algorithm, the aim was to use a variety of control methods in terms of their functional principle. Therefore, I chose to apply the classical tuning rules of Ziegler and Nichols, refer to Ziegler and Nichols [1942], representing heuristically found methods. Further, I use the absolute value optimum method and the symmetrical optimum method, refer to Abel [2009]. As recently well cited and referenced methods, I apply the PID lambda-tuning method (using three different lambda parameters), refer to Åström and Hägglund [2006] and Copeland et al. [2010], and the Skogestad internal model control, SIMC, refer to Skogestad [2003]. Practitioners refer especially to lambda tuning as relatively simple, intuitive, and bullet-proof, see VanDoren [2013]. All of these tuning methods are applicable without advanced system knowledge and easy to calculate.

For PI controllers, the above-mentioned tuning rules for application within the proposed method presents table 3.2, i.e. Ziegler und Nichols (ZN), lambda-tuning (LT), absolute value optimum (AO), symmetrical optimum (SO), and SIMC. The additional tuning rules for PID controllers are attached in the appendix, see table A.1.

The basis for the applied control rules are the controller parameters K_P, T_I and T_D, which are calculated for the ideal PID controller equation, refer to equation 3.9 for a Laplace representation.

$$K(s) = K_P \cdot \left(1 + \frac{1}{T_I\ s} + T_D\ s\right) \tag{3.9}$$

The dynamic system is represented by the following equation (second-order system as example) where k is the process gain, T_1 and T_2 are the dominant time constants and θ is the time delay, refer to equation 3.10.

$$G(s) = \frac{k}{(T_1\ s + 1)\,(T_2\ s + 1)} e^{-\theta s} \tag{3.10}$$

Table 3.2: Parameter calculation for PI controller

tuning rule	process model	K_P	T_I
ZN	PT_1T_d	$\frac{0.9}{k}\frac{T_1}{\theta}$	$\frac{10}{3}\theta$
LT	PT_1T_d	$\frac{1}{k}\frac{T_1}{\theta+\lambda}$	$max(T_1, 3\theta)$
AO	PT_1	$\frac{1}{k}\frac{T_1}{2T_\Sigma}$	T
SO	PT_1	$\frac{1}{k}\frac{T_1}{2T_\Sigma}$	$4\ T_\Sigma$
SIMC	PT_1T_d	$\frac{1}{k}\frac{T_1}{2\theta}$	$min(T_1, 8\theta)$

The LT method is named after the tuning parameter λ in the equations. There are three different values for λ considered

- $\lambda = T_1$ - aggressive tuning
- $\lambda = 2T_1$ - normal tuning
- $\lambda = 3T_1$ - robust tuning

so that there are seven different parameter sets for both controller types PI and PID.

3.6 Simulation

The simulation of the closed-loop system's step response is the next step and it is realized in the simulation framework SIMULINK. The conditions are the same as in the real step experiment. The identified model, from which the tested PID parameters are calculated, approaches the dynamic system. Models in a continuous time domain are simulated in a continuous time simulation and models in a discrete time domain are simulated in a discrete time simulation respectively. In case of a continuous model, the simulation uses a continuous, ideal, classical PID controller block.

For the discrete time simulation, the simulation should be as close as possible to the controller used in the real building, thus, the simulation has to use a model of the real PID controller implemented in the building. The practical implementations of the ideal PID controller equation, compare equation 2.3, vary among different BACS manufacturers. The implementation found in the demonstration building, described in detail in chapter 5, represent equations 3.11, 3.12, 3.13, and, 3.14.

As equation 3.11 shows, the discrete PID implementation is the sum of of a proportional discrete, integrative discrete and derivative discrete part, whereas k is the discrete time variable.

$$u_{\mathrm{PID}}(k) = u_{\mathrm{P}}(k) + u_{\mathrm{I}}(k) + u_{\mathrm{D}}(k) \tag{3.11}$$

Within the equation for the proportional part, PB is the so-called proportional band, a variable handed over to the system, representing a reciprocal normalized P gain with $\bar{\mathrm{u}}_{\mathrm{PID}}$ as the upper limit and $\underline{\mathrm{u}}_{\mathrm{PID}}$ as the lower limit of the operational range.

$$u_{\mathrm{P}}(k) = \frac{\bar{\mathrm{u}}_{\mathrm{PID}} - \underline{\mathrm{u}}_{\mathrm{PID}}}{PB} \cdot \big(y(k) - r(k)\big) \tag{3.12}$$

In the equation for the integrative part, $T_{\mathrm{I,JCI}}$ is the practical implementation for the integrative gain.

$$u_{\mathrm{I}}(k) = u_{\mathrm{I}}(k-1) + \frac{\bar{\mathrm{u}}_{\mathrm{PID}} - \underline{\mathrm{u}}_{\mathrm{PID}}}{PB} \cdot \big(y(k) - r(k)\big) \cdot \frac{1}{T_{\mathrm{I,JCI}}} \tag{3.13}$$

The implementation of the derivative gain represents $T_{\mathrm{D,JCI}}$. Whereas $\mathrm{C_F}$ is a internal factor, which was not documented.[3]

$$u_{\mathrm{D}}(k) = (1 - \mathrm{C_F}) \cdot u_{\mathrm{D}}(k-1) + 2 \cdot \mathrm{C_F} \cdot \frac{\bar{\mathrm{u}}_{\mathrm{PID}} - \underline{\mathrm{u}}_{\mathrm{PID}}}{PB} \cdot \big(y(k) - y(k-1)\big) \cdot T_{\mathrm{D,JCI}} \tag{3.14}$$

In general, it is not always possible to capture all internal states of the controller and all additional mechanisms, like anti-wind-up since the manufacturer's PID block documentation does not always offer full information. In this case, the unknown state of the P, I, and D parts of the PID implementation at experiment starts sometimes lead to slightly different results. For the demonstration within this thesis, figure 3.2 shows the PID Simulink model output in comparison to a real controller having the same input values and step changes.

Still, while applying the algorithm to further BACS, the user has to be aware that the algorithm needs a numeric model of the PID algorithm implemented in the respective BACS.[4]

[3] Compare Kraus [2014] for a mathematical derivation of this factor.

[4] Despite the very implementation of a certain manufacturer whose controller have to be tuned, I assume that method achieves comparable results as long as the very implementation is known or a model has been reverse-engineered and is fitting the real-life controller's output. This means that the results of this thesis are fully transferable with only a few limitiations: if the implementation differs from the general PID controller structure and if the model is not fitting to the real-life controller the method would not work. If the implementation differs from the general PID controller structure but the model still finds outputs alike with the real system, I assume that on the one hand, the method's results would get arbitrary since the proposed parameters will have, in the worst case, random meanings, but on the other hand that the method would still work, since the best parameters of the simulation experiments would be handed over to the system.

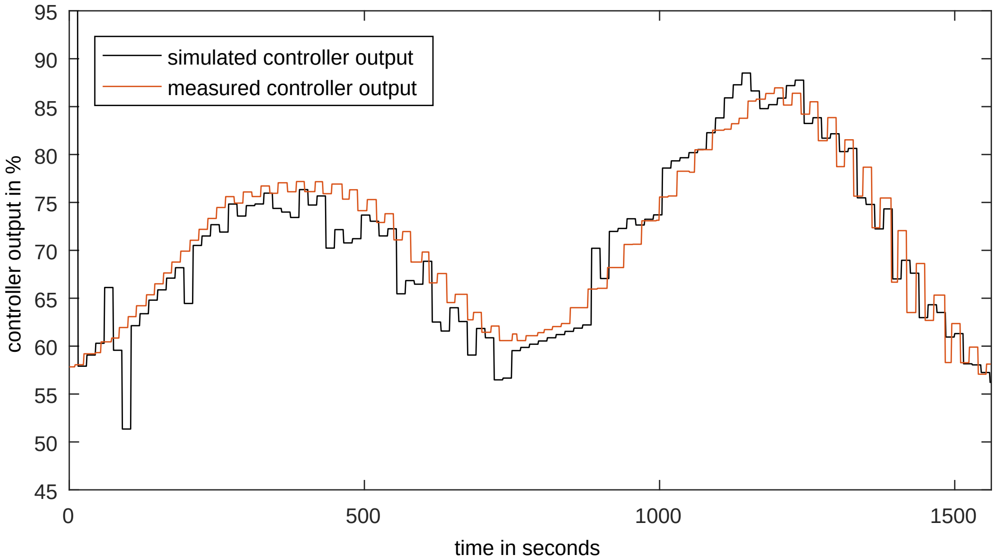

Figure 3.2: SIMULINK PID controller model

3.7 Needed a priori knowledge

For the experiment set up, the algorithm's user needs to adjust the following parameters according to the experiment and, thus, according to the investigated control loop. There are the following nine parameters to adjust: sampling time of measurements; the minimal pulse width of the excitation signal; the system's settling time, settling and step value for the step experiment; the tolerance band around the new set point; the experiment mode, either closed-loop or open-loop, depending on either the algorithm tunes a stable system or it searches for an initial configuration; the mean and the delta value of the excitation signal; and, finally, the experiment start and end time. Further, the user can adjust standard parameters if necessary. Generally the following seven parameters can remain unchanged: the number of real step experiments for control quality evaluation; the model structure constraints, i.e. considered model structures, maximal model and disturbance orders; the shape of the excitation signal, either RBS, $1/f$, or uniform steps; the time domains; and the number of periods of the excitation experiment, if a signal repetition makes sense.

4 Simulation study

To evaluate and optimize the method towards advantageous configurations for specific controlled systems, simulation experiments offer great opportunities, since the optimization complexity is enormous–with a number of 614,432 non-numeric possible algorithm configurations. Sensitivity analyses become a challenging task. Real-life experiments are time-taking and not always successful, refer to section D. Further, a comparison between experiments is not always perfectly possible, since ambient conditions vary among experiments. A whole run of the method needs e.g. up to seven to nine hours on thermal control systems. Simulations have the benefit to hold the "ambient" conditions, ensure comparable results and perform experiments in less time, also due to high computational power and thus simultaneous executions for one control system. In the following, I give a short summary of the conducted simulation study, its methodology and its results. For more details please refer to Fütterer et al. [2016]. This simulation study covers 1950 single experiments within ten physically-modeled control loops under variation of eight parameter types and integration of nine disturbance models. Further, it investigated the algorithms capability of identifying black box models with and without disturbance.

A simulation control-tuning-test-environment is developed to link the algorithm with simulation models of control systems. The models are validated and adapted based on additional real life experiments in the considered building. After guaranteeing the simulation algorithm's similarity to the real algorithm and an extensive result comparison, sensitivity analyses of important configuration parameters are conducted. Reasonable algorithm configurations from real life experiments serve as a starting point for these analyses. The investigation of the algorithm's behavior under exposition to different disturbances is a further research question. Therefore, different disturbance models are developed and systematically applied to the algorithm. Figure 4.1 shows the part of the algorithm that is replaced by simulation, i.e. the building and the database.

Figure 4.2 shows the signal flows of the algorithm interacting with the building, figure 4.2(a), and the signal flow as found in the simulation environment, figure 4.2(b). For the simulation control-tuning-test-environment, all connections between the algorithm and the database as well as the between the algorithm and the building automation system are linked to the simulation environment.

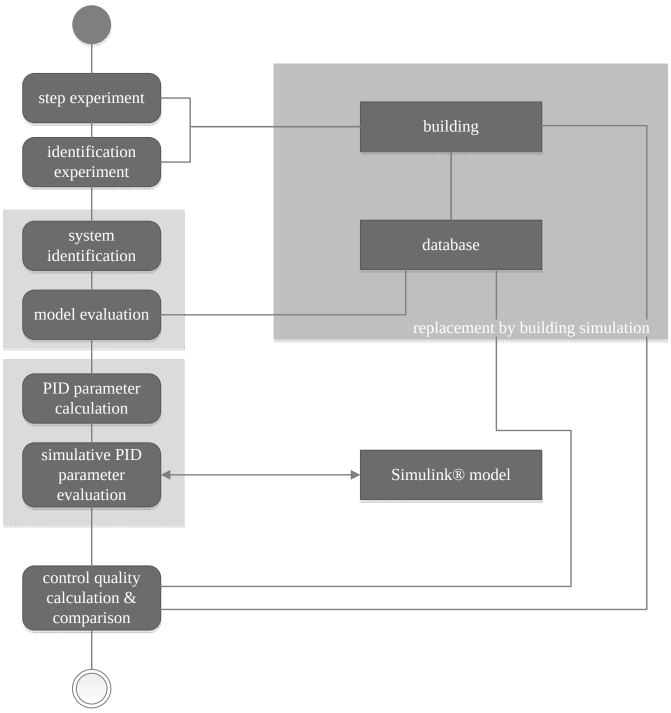

Figure 4.1: Algorithm with replacement by simulation (light grey part)

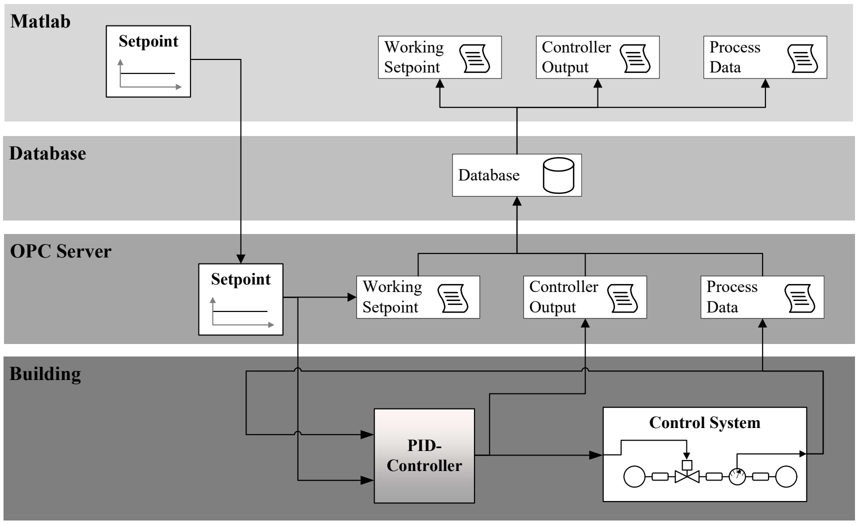

(a) Algorithm's communnication - real case (w/a)

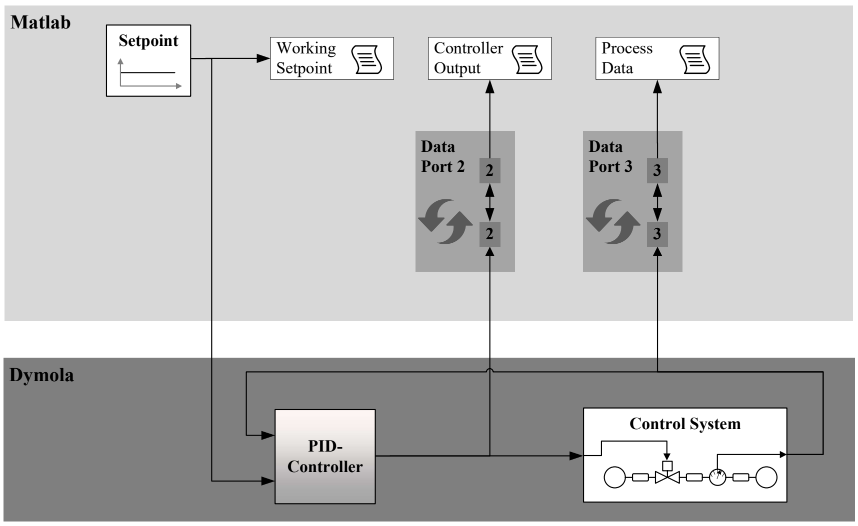

(b) Algorithm's communication - simulation study

Figure 4.2: Comparison of algorithm's communication

4.1 Modeled systems, varied parameters, and introduced disturbance models

Developed simulation models use available Modelica classes from the open-source building library AixLib, compare Fuchs et al. [2015], the Buildings library, refer to Wetter et al. [2014], both are based on the IEA EBC Annex 60 Modelica Library, compare Wetter et al. [2015], and additionally from the standard library of Modelica, see Modelica Association [2015]. Design data and data from real experiment data served to adjust precisely the behavior of the simulation models. The final study covered ten physical models.[1]

Within the simulation study eight algorithm input parameters were varied, i.e, sampling time write (excitation signal pulse width), closed loop vs. open loop identification, the excitation values (mean and amplitude), excitation signals (RBS, 1/f, step), filtering, model order, number of transferred models, control quality criteria.

In order to investigate the algorithms disturbance handling capabilities, three time-variable disturbances were developed, which change the disturbance value every second (Dist-1), every ten seconds (Dist-10) and every 100 seconds (Dist-100).[2] The 100 seconds disturbance, represents a systemic disturbance, the 10 seconds disturbance a short non-systemic disturbance and the 1 second disturbance the classical white noise. Every disturbance has two occurrences, one with a minimum (Dist-xxx-min) and one with a maximum (Dist-xxx-max) standard deviation.[3] Additional to the disturbances for the measurement, inlet-temperature-disturbed models for heat exchangers' water and air sides is added.

4.2 Exemplary results - Two-way-valve air temperature control over heat exchanger(w/a)

Since presenting all results of this study would exceed this thesis' scope, I present a choice of exemplary results for an air handling unit's heating coil, which should represent the AHU 04 pre-heater, refer to section 6.1.2 for a description of the physical system and subsection 7.1.2 for practical results.

[1] Four times temperature control, i.e. models representing AHU 04's pre-heater, re-heater, and cooler, as well as a three way mixing valve temperature controller, representing K08Y02; four times pressure control, i.e. AHU01's and AHU04's supply and exhaust pressure; and two three-way-valve volume flow control loops representing concrete core activation mixing valves from the demonstration building.

[2] Between the time intervals, the disturbance value is interpolated according to the respective simulation sampling time.

[3] Standard deviation in limits between 0.5 % and 10 %

4.2.1 Results towards the identification process

For the algorithm's identification, experiments with different excitation signals, i.e. 1/f, RBS, and step, and varying disturbance models took place. Uniform steps show good identification results with model fits up to 95 % at undisturbed models. Still, excitation frequency ranges might be tight, because the excitation signal has always the same frequency. At a Dist-100-min disturbance the bandwidth limited "1/f" signal shows approximately, with a difference of 2 %, the same identification results than uniform steps. Overall, RBS provides the worst identification results at this disturbance.

The experiments towards open loop versus closed loop identification provided the following results. At undisturbed experiments, a closed loop identification shows slightly poorer identification results compared to an open loop identification. Also, an open loop excitation, in the total operating range (valve position 10 % to 90 %), appears as the best choice under the disturbance model Dist-10-min, providing model fits up to 83 %. Thus, considering the identification process separately, an open loop experiment should be recommended for temperature systems. However, the model fit is just one indicator of the tuning process that determines the control quality.

The experiments towards a variation of the excitation signal's values, i.e. the amplitude and the mean of the excitation signal, generates mixed results. At undisturbed experiments, variations show almost the same results with a total fit difference of 4 %. In disturbed systems, the algorithm demonstrates best identification results with a model fit of 77 % at a delta value of 10 to 15 K. During the variation of the sampling time write, it turned out that the model fit decreases with lower sampling time write (20 to 50 seconds) with a minimum value of 60 % and increases at higher sampling time write (>1000 seconds) with model fits exceeding 80 %. The variation of the overall number of excitations, i.e. the length of the identification experiment, did not provide better results with longer identification times compared to the default minimum identification time, which lies in the range of 40 maximal possible excitations.

The variation of the model order provided that model orders higher than four show good model fits, with fit values up to 85 % for undisturbed models. Above a model order of four the increase of model fit is approximately one to two percent per model order. This goes in line with the observation made by turning filtering on an off. The difference between an experiment with and without activated filter reached up to 30 %. The difference lowers with rising model orders, as these higher model orders cover filtered frequency ranges. Thus, a filter can obsolete higher model orders or, in turn, using lower model order necessitate filtering.

At consideration of all experiments, experiments analyses determined the following ranking of all model structures: Box-Jenkins, Output Error, ARMAX, ARX, and state space estimation.

4.2.2 Influences of the identification experiment on quality control

As seen from the practical experiments, the configuration of the identification experiment has a high influence on the controller's setting and the resulting control quality.

Uniform steps show the best identification results compared to other excitation signals, however, uniform steps fail during the control quality calculation. Only for systems disturbed by a Dist-100-min disturbance these signals show the best results with an ITAE decrease of 15 %, however, only 25 % of the proposed PID-parameter-sets led to stable systems. In contrast, 1/f and RBS produced at 90 % of the experiments stable configurations. At all other disturbances, mostly 1/f or more rarely RBS showed a better relative ITAE reduction. Figure 4.3 shows this circumstance exemplary with the disturbance model Dist-1-min.

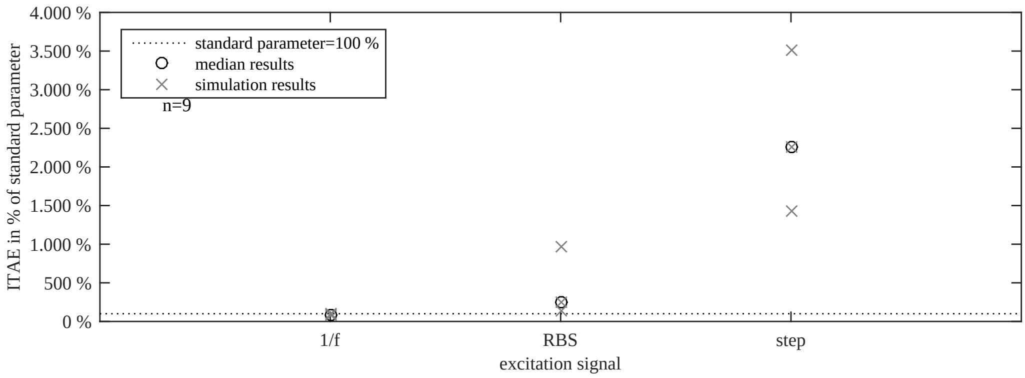

Figure 4.3: ITAE control quality values in percent of standard parameter's ITAE values among different excitation signal types for an AHU's heating coil under disturbance model Dist-1-min

A sampling time write of 50 to 200 seconds was the best choice for seven out of nine disturbance models. For undisturbed models, these sampling time write decreased ITAE values up to 45 % compared to higher sampling time write, refer to Figure 4.4. The results became worse at sampling time write higher than 300 seconds. However, in contrast, sampling time write higher than 300 seconds were particularly successful for disturbance models with higher standard deviations.

As Figure 4.4 further shows, the control quality raised with sampling time write approaching the user-set waiting time of the step experiment (1800 seconds). This is a phenomenon, also observed during the system identification: the model fit raised with sampling time write reaching the waiting time.

As Figure 4.5 shows, closed loop identification produced a reduction of the ITAE criterion at the disturbance model Dist-1-min up to 10 %, while the excitation values were set in range of maximum excitation for the operating range and in range of the values of the step experiment. However, the

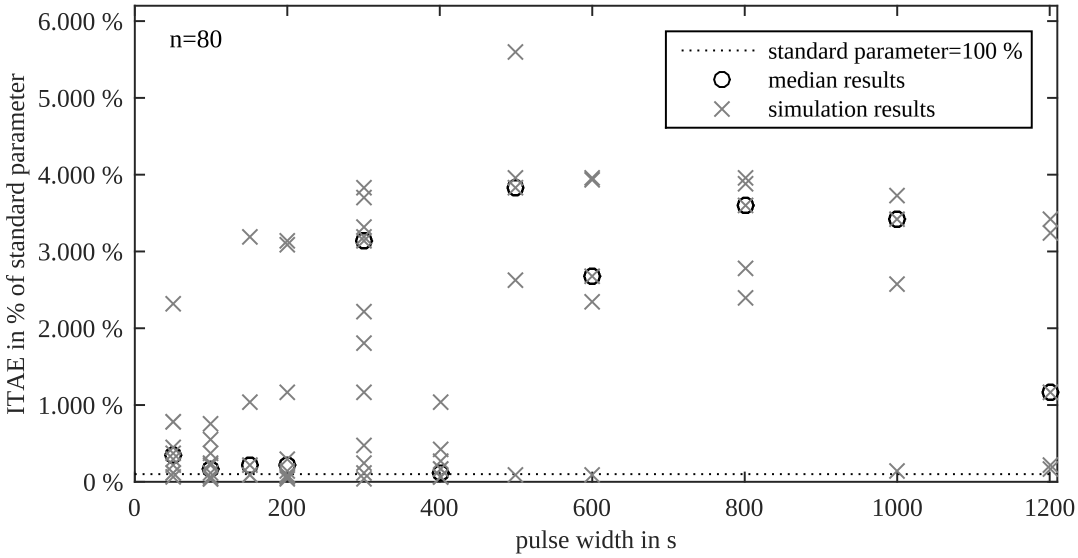

Figure 4.4: ITAE control quality values in percent of standard parameter's ITAE values among different excitation sampling time write for an undisturbed AHU's heating coil system

results of open loop identification in range of maximum excitation in the operating range (valve position 1 % to 90 %) achieved significant better values with a reduction up to 20 %, and also more stable configurations. For other disturbance models than Dist-1-min, within open loop identification, all other excitation experiment configurations were less suitable. Across all experiments, the closed loop identification was more successful for all disturbance models.

4.2.3 Influences of system identification on control quality

There are only a few parameters of system identification, which can be configured in the algorithm. Regardless, these parameters are decisive for the resulting control quality.

Results show that the higher the model order the better the control quality. A model order of 8 provided a decrease in ITAE criterion of 46 % at undisturbed model and 19 % at Dist-1-min, which conforms to white noise.

A low-pass filter is capable to improve the results of system identification and, thus, also the resulting control quality. As presented in Figure 4.6, the gap in the ITAE value between an activated and deactivated filter decreases with a higher model order and approaches to zero. Results show this phenomenon at nearly all disturbance models.

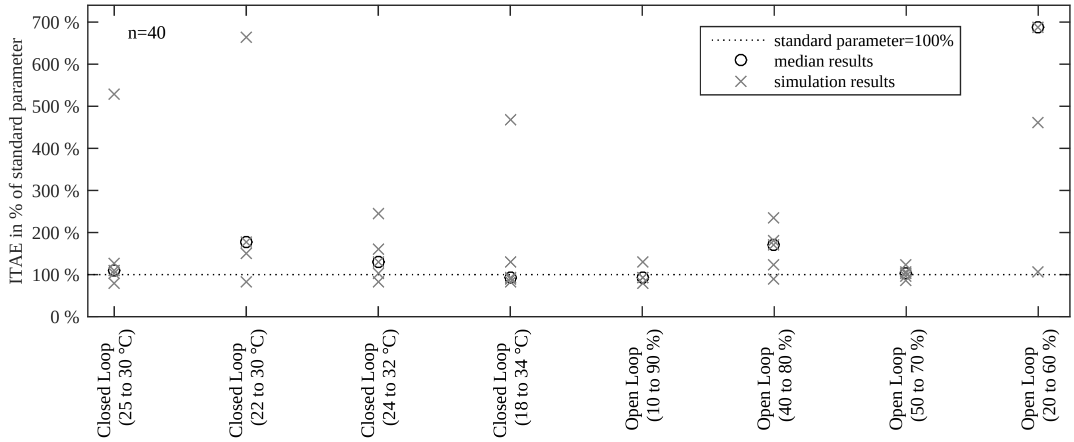

Figure 4.5: ITAE values in percent of standard parameter at different excitation values in AHU04 pre-heater with disturbance model Dist-1-min

4.2.4 Influences of tuning rules and chosen quality criteria on control quality

At the undisturbed and disturbed model, lambda tuning and symmetrical optimum convinced. In addition, Ziegler-Nichols shows good results at several disturbance models, but not at all.

In only 7 % of the cases, ISE as sole quality criterion produced stable control parameters. A relation between rise and settling time is notable. A reduction of rise time follows usually an increase of settling time and vice versa. The inclusion of settling time into control quality calculation leads to a reduction of the ITAE criterion up to 16 %. Altogether, other considered control qualities are not as successful as the ITAE in terms of visual investigation of desired control behavior.

4.3 General results

Over all simulation experiments, the highest improvement of ITAE criteria was up to 97 % without disturbance and 51 % for disturbed systems. Further, the analysis of the examined experiments shows, that the parameterization of the identification experiment and the subsequent system identification has high influence on resulting control quality of proposed PID parameter sets.

Each of the analyzed control systems has individual optimal algorithm input parameter combinations or input parameter ranges. Depending on and within a certain type of control systems, the values of optimal parameter ranges show a similar nature. That can be explained by the systems' analogous dynamic and static transfer behavior, i.e. the rise and settling time range in a comparable segment.

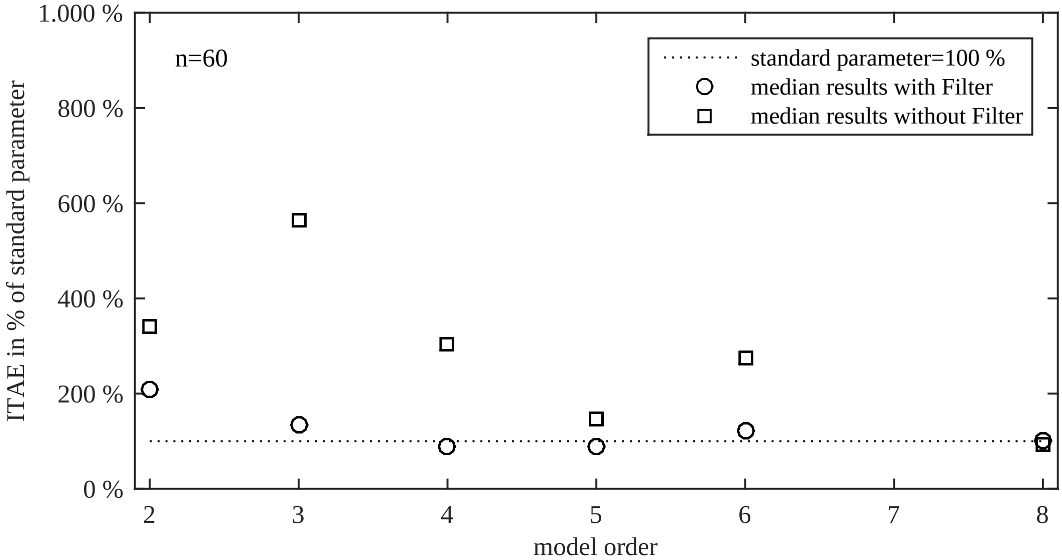

Figure 4.6: ITAE values in percent of standard parameter at different model orders with and without filtering in AHU04 preheater with disturbance model Dist-1-min

With identical algorithm input parameter, the algorithm provides identical PID parameter sets and system models in the majority of the cases – which is not evident since the excitation signal has a random nature. Moreover, the results for identical algorithm runs with considered randomized disturbances show the same behavior, even though the ratio of equivalence is reduced. On black box models the outcome is exactly consistent.

4.3.1 General results towards the identification experiment

The algorithm achieves excellent results via identification in open loop mode for strong disturbances. On the contrary, an identification in closed loop mode convinced for experiment with no disturbances and weaker disturbances.

Two different extreme-edge excitation signals are thinkable for investigation: a maximum excitation in the operating range and an excitation with values in the range of the step experiment. In open loop mode, a maximum excitation in the operating range (valve input from 10 % to 90 %) was more successful than an excitation with values in the range of the step experiment, except in one case. Contrary, in closed loop mode, an excitation with values in the range of the step experiment reached higher reductions of ITAE criteria. In general, a maximum excitation in the operating range led to more stable control parameters compared to an excitation with values in the range of the step experiment. Even though such an excitation shows occasionally excellent results, while, in contrast, excitation values between these two ranges tended to instability.

On the one hand, for a maximum excitation in the operating range the identification process produces a linearized model over the whole physically-possible operation range. The algorithm applies this acquired model over the whole operation range during control parameter evaluation. Therefore, such an excitation signal leads to PID parameter sets with higher over-all stability. On the other hand, an excitation with values in the range of the step experiment provides an appropriate linearized model exact in the range of the respective step experiment and thus leads to higher ITAE control quality within these ranges but minor stability outside the respective step experiment's operation range.

In conclusion, the configuration of the excitation experiment turned out to be essential for the whole tuning process. Poor or insufficient parametrizations caused high deviations in control quality.

It is not possible to specify one first-best choice for the sampling time write for any specific type of control loops, since sampling time write heavily interacts with other parameters influencing achievable control quality. However, results can indicate a range of values, where the algorithm achieved outstanding results. An approximately linear correlation between rise time and dimension of sampling time write is observable.

Goodwin's bandwidth-limited 1/f-signal type convinced in all considered cases as excitation signal's shape. However, the random binary signal (RBS) was close to 1/f in many configurations or could even outperform it in some cases. Uniform steps were able to reach outstanding model fits but the tuning process achieves stable control parameters only in occasional cases with the associated limited identification data, as also explained by Ljung [1999].

4.3.2 General results towards system identification

The number of models, for which the algorithm calculates PID parameters has only an indirect influence on the achieved control quality. However, the model fit is the decisive factor. At thermal control systems, the results indicate that a model fit of 30 % is at least required to reduce ITAE criteria. Pressure control systems seem to need lower model fit values to be ameliorated. In contrast, real life experiments within the demonstration building showed that a model fit value above only 10 % can suffice in order to ameliorate the quality criteria.

In experiments with disturbance, the usage of a low-pass filter showed consistently better results than the experiments without this filtering. In contrast and as expected, the filter did not consistently yield to better results in experiments with ideal models without any disturbance. Since all real systems are exposed to disturbances, i.e. at least white noise in the measurements, the usage of low-pass filtering for smoothing curves is strongly recommended in order to achieve good tuning results.

For disturbed black box models[4], results proved that the tuning algorithm is able to find their characteristics with an accuracy of more than 99 %. Therefore, it is evident that the algorithm is able to remove disturbances from the time series and extract the meaningful controlled system models.

For all experiments, a model order of eight reached good model fits and led to sufficient associated PID parameters. In most cases, a model order of four shows adequate results. At pressure controlled systems, second order models already achieve good controller parametrizations. For this kind of controlled systems, an explanation might be found in the modeling technique for the simulation, which consists of the attachment of a PT2-element to a static table-based model, nevertheless, this goes in line with the practical results of e.g. figure C.4 for an armax(2,1,0;18;d)-model fit and figure C.10 for a bj(1,2,2,2;3;d)-model fit.

4.3.3 General results towards controller setting

In terms of applied control rules, the results did not indicate an overall-superior tuning rule. For heating coils, results showed that the symmetrical optimum method and lambda tuning convinced, whereas for pressure controls, Skogestad internal model control and absolute value optimum method played a decisive role. Such at different controlled systems varying convincing tuning rules are justifiable due to the controlled systems' deviating dynamic behavior.

In contrast, the results did not determine model-tuning-rule combinations, which perform significantly better. Still, as expected, Box-Jenkins and output-error-model-structures performed better than other models, maybe due to their separate disturbance models.

Further, the study shows that the algorithm finds better results in the case of a more sluggish initial controller than in the case of an initially oscillating controller. An initial unstable control loop deteriorates the results of quality control, especially in closed loop mode. In these cases, users should switch to open loop mode.

[4] i.e. a further investigation conducted in order to find out wether the algorithm is capable of finding the characteristics of a black box model.

5 Demonstration Bench

I demonstrate the algorithm by conducting experiments within the E.ON Energy Research Center Main Building at the RWTH Aachen University in Aachen, Germany. The building is multifunctional, integrating office spaces, staff facilities, seminar and conference rooms, laboratories, and common areas.

This chapter describes the initial building automation equipment, then it describes all extensions of its building automation system which are necessary for the development and demonstration of the proposed method. Further, the chapter provides minimum prerequisites for an application of the proposed method within other state-of-the-art buildings.

5.1 Energy concept

The building's energy concept meets the trade-off between fulfilling all energy demands while maintaining highest possible energy efficiency. As shown in figure 5.1, the concept consists of different energy conversion and distribution units. The system's heart is a turbo compressor driven heat pump. A glycol cooler and a field of 40 borehole heat exchangers keep the energy balance of the heat pump's hot and cold side throughout the whole year. A co-generation plant provides electricity, mainly used for the heat pump, and also high temperature heat for integration into a heat-to-cold shifting sorption process, or for direct use in laboratories or for additional heating energy. A detailed description of the building's energy concept can be found in Fütterer and Constantin [2014].

5.2 Initial building automation

The building provides a state-of-the-art building automation system with PID control loops at all levels.

The initial system had a classical Johnson Controls BACS with field, automation and management layer. The field layer connects sensors and actors, while the automation layer offers the possibility to program the system logic within programmable logic controllers of different sizes, like field equipment controllers (FECs), network control engines (NCEs) and network automation engines (NAEs), in increasing order of computational capacity. Each NCE integrates a bunch of FECs and has the

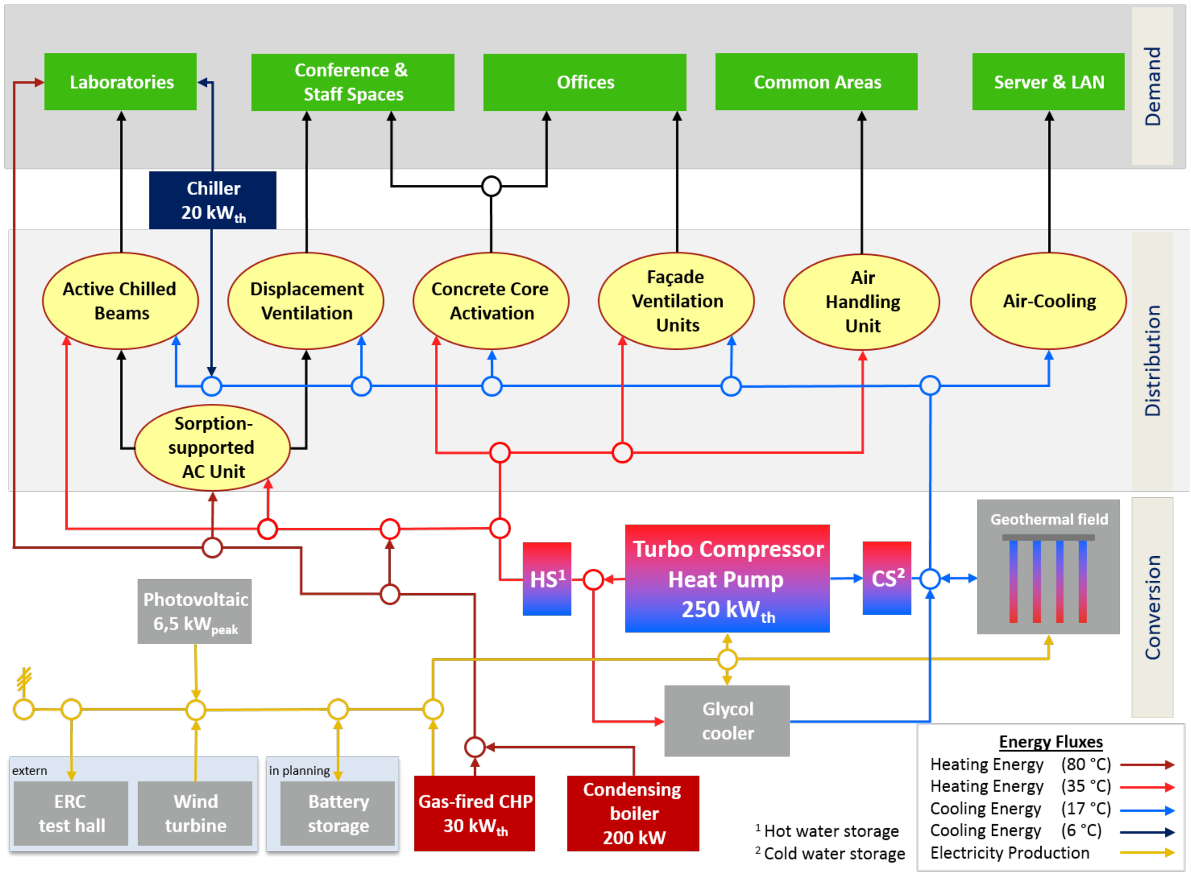

Figure 5.1: Demonstration building's energy concept

capability to communicate over BACnet/IP with other components on the management level. The NCEs and the NAE provide all management layer functionality. The NAE serves as the a central control and hosts a meta-system configuration tool for all integrated NCEs. All three types of controllers are able to directly integrate literally all kind of field devices. Important for the scope of this thesis, all three kinds of controllers operate PID-controllers at different levels throughout the automation system. Furthermore, via the hierarchical integration structure, it is possible to push forward data objects towards the BACnet/IP management level communication. Thus, it is in principle possible to read and write each PID-parameter, controller output, controlled system output, set point, thus, controller input, and all further relevant data objects from an superior, e.g. cloud-based, instance.

5.3 Extension towards a test bench

The initial system was extended towards a so-called monitoring, control and interface system (MCIS) offering all functionality to conduct literally all kinds of control research. Futterer et al. [2013] de-

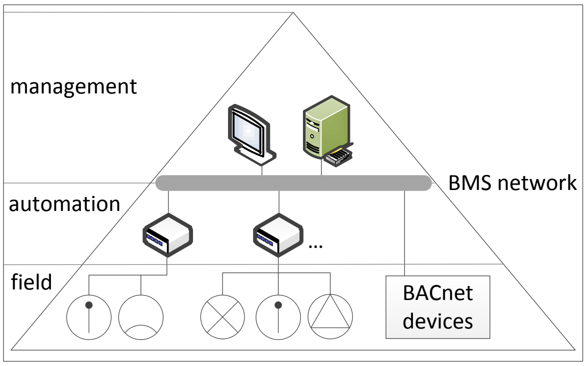

Figure 5.2: Building automation schematic

scribes the system on a high level and Fütterer and Constantin [2014] go deeper into the system's details. Within this chapter and for the scope of this thesis, I present only parts, which are used for the application of the proposed control tuning method itself and for its development. I.e. the extension of the network topology, the integration of a building management server, the integration of an OPC-server, the integration of a data logging and storage system, the integration of engineering stations for PLC reprogramming, the integration of an interface that allows for direct TCP to OPC communication, and, as an overview, the set up of a physical and virtual server architecture providing computational power for the algorithm's execution.

5.3.1 Test bench's network topology

The new E.ON ERC main building is part of the RWTH Aachen University. The network infrastructure needed for the MCIS is integrated into the RWTH Aachen University's network topology which is expanded by two networks. The so-called monitoring network and the building management network. The networks are connected to each other. Access rights can be controlled via firewalls. To administrate different users with different access permissions, a flexible virtual private network (VPN) gateway is implemented.

Figure 5.3 visualizes the network topology on a high level. The office network of the E.ON Energy Reseach Center consists of all computers of the center's scientific and administrative stuff. Computers for test benches and students as well as automation infrastructure for test benches are placed within the laboratory network. The user-added monitoring hardware, the weather station, the promotional display, the wireless sensor network sink and user-added automation components are attached to the monitoring network. The building automation network is operating the management layer of the building automation system. It connects all programmable logic controllers with BACnet-components of the technical building equipment, such as the heat pump, the air handling units, and façade ventilation units. Touchscreens for direct user control and supervisory control are also part of the building management network.

A fully virtualized, cloud-like server infrastructure is installed between the building management network and the monitoring network in order to enable domain free connection to building automation components and connections to office network participants while not connecting to the building management network. For security reasons only some workstations are permitted to access the building management network directly.

MCIS databases are placed in the RWTH ICT department's intranet and redundantly in the cloud server infrastructure, which is part of the monitoring network and as well of the building automation network as mentioned above.

All components have connection to the world wide web via the intranet of RWTH Aachen University's ICT department and can also be accessed from the internet, administrated via firewall rules. The whole building and the whole RWTH Aachen University campus offer a wireless network called eduroam and a VPN. Connecting to eduroam or to the RWTH VPN provides access to all MCIS databases hosted at the central RWTH Aachen University's ICT department.

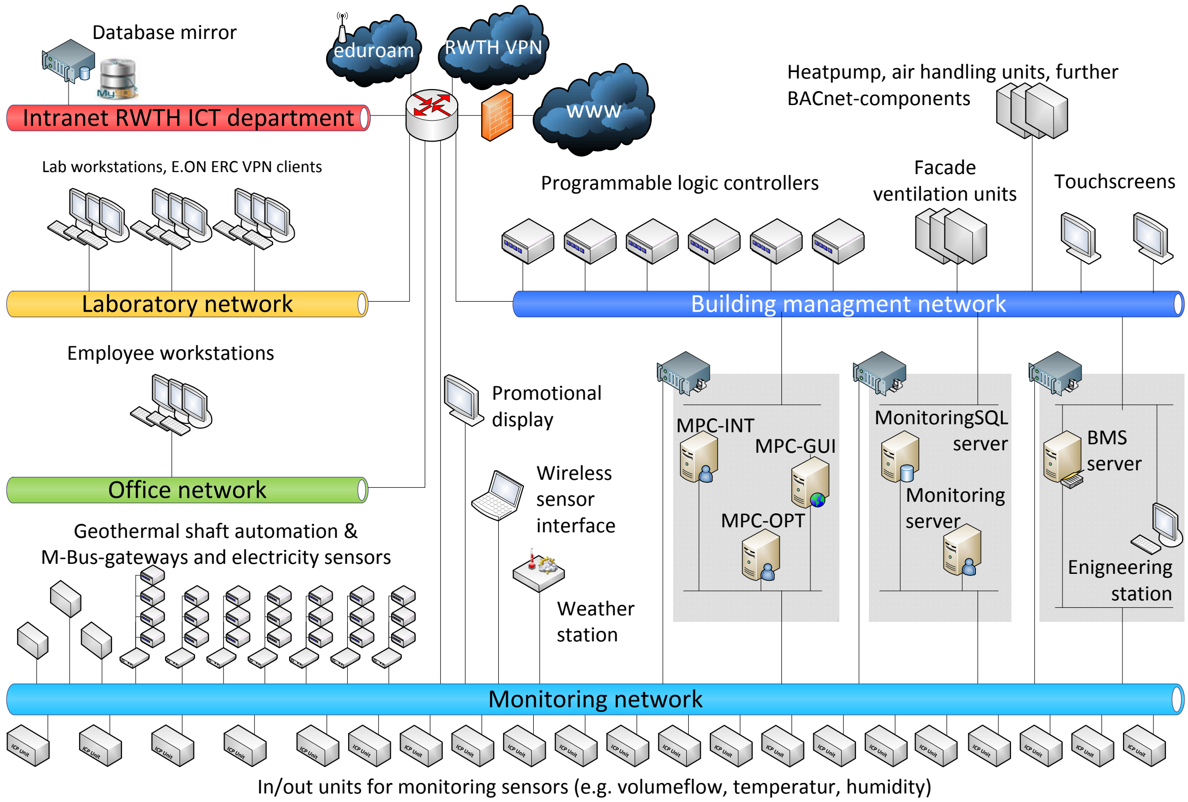

Figure 5.3: Network topology

5.3.2 Implementation of a building management server

Within the initial system, there was no supervisory control system. The management layer consisted of a live-view application, hosted web-based by the NAE. This was a proprietary system, which was not open for the integration of further services, e.g. data logging, communication interfaces, external control applications. Thus, a building management server (BMS) was integrated, which is a Windows server system that offers all flexibility for services and further servers. Previously to the virtualization, this server operated on a physical server provided by Johnson Controls.

5.3.3 Implementation of OPC servers

The PLCs in the system are able to push forward all data objects to the BACnet/IP management communication level. For used software or algorithm development environments, e.g. MATLAB or Phyton, and further service software, a direct BACnet communication is hard to realize. An OPC server provides the possibility to read and write BACnet data points from external devices. It uses the OLE standard. Its purpose is to provide access to data points of the BACS. Further, JCI offers a supervisory control and data acquisition (SCADA) system based on OPC. Thus, JCI integrated a BACnet-OPC-Server, providing access to all data points that are part of the BACS's BACnet. This server offers access to all available BACnet-data-point-attributes, but only has a limited data point integration capability. In the system's final extension stage, it operates two BACnet-OPC-servers on two virtual Windows servers, separating JCI and third party BACnet-devices. A so-called MPlus-OPC-server again integrates these two BACnet-OPC-servers.

Having this OPC infrastructure now allows for the OPC-based communication between the building and external services, such as the data logging server and the OPC2TCP-Interface described in the sequel.

5.3.4 Data logging and storage system

A self-developed C++ service[1] parses all data points integrated within the MPlus-OPC-server. It stores a data point list in a database, which is cloud-based hosted within the virtual server infrastructure, explained in subsection 5.3.7. For each data point a change threshold determines the amount of change that defines when a new value is stored. The data base offers the possibility to freely adjust this change threshold for each data point. Having the change threshold available, the service checks the change of value for all data points in a certain frequency, i.e. the system log cycle time, also denoted as sample rate. Thus, freedom exists in adjusting the change of value threshold

[1] The service was developed by the former EBC software developer Achim Wilden.

and the sample rate. The service stores its measurement data in two data bases, one hosted within the virtual server infrastructure at the MonitoringSQLServer and one hosted at the RWTH Aachen University's ICT department server infrastructure, refer to figure 5.3.

Setting up the standard configuration is a trade-off between network traffic and speed, data storage costs, and data processing costs. For experimental purpuses, a MATLAB-function sets the sample rate down from 30 to one second and activates a threshold regime, that is designed for low network traffic. Then, it sets the change thresholds of all relevant data points down to near zero. The outcome is very highly resolved monitoring data during an experiment's duration.

The data model of the data bases accounts for low storage costs. It is an event-based model, which, in contrast to sample-based data models, helps to save storage capacity. Fütterer and Constantin [2014] present further descriptions.

5.3.5 Engineering stations for PLC reprogramming

All programmable logic controllers of the building automation system are freely programmable via two engineering stations. These engineering stations are implemented as virtual machines in order to have accessibility from every work station within the E.ON ERC network and a safe operation environment at the same time.

The engineering stations do have tools for controller configuration and system configuration. The controller configuration enables their users to e.g. push forward relevant PID-parameters to a BACnet level. With the system configuration tool, it is possible to integrate these BACnet objects at the management level.

5.3.6 Multi-threading TCP2OPC-interface

TCP communication is a more common type of communication for software languages and mathematical software like MATLAB than direct OPC communication. Software or programming languages used at the institute like e.g. Phyton, MATLAB and Excel provide inherent TCP functionality. Thus, a software tool which interfaces between TCP and OPC was developed. Since control tuning experiments endure up to several hours, one should have the possibility to conduct different tuning experiments in parallel. Thus, the TCP2OPC-interface was equipped with multi-threading functionality.

For the algorithm's application two Matlab functions allow for write and read commands for all data points attached to the interface. Data point management and access permission management takes place in a proper data base hosted within the MonitoringSQLserver, refer to figure 5.4.

5.3.7 Physical and virtual server architecture

In order to host all necessary services and in order to provide the needed functionality the E.ON ERC ICT team, an EBC software developer and I designed and implemented an own server infrastructure. The server infrastructure between the building management network and the monitoring network consists of four VMware EXSi physical servers hosting nine virtual machines with different operating systems. The building management server virtual machine (BMSVM) server hosts the building management server (BMS), refer to subsection 5.3.2. Its main purposes are operating the SCADA system and the OPC server, refer to subsection 5.3.3. The BMS server hosts the OPC data logging service, refer to subsection 5.3.4. Further, it hosts the TCP2OPC-interface, refer to subsection 5.3.6. Coming back to higher level, the BMSVM hosts two engineering station, refer to subsection 5.3.5. It is possible to expand the whole data network and server system of the building automation system for any thinkable use.

The monitoring virtual machine (MonitoringVM) server hosts two virtual machines. It hosts the monitoring server which collects data from an user-added monitoring equipment and other data sources, such as weather station, weather forecast and TCP/IP sensors. It further hosts the MonitoringSQLserver, which serves as the local database for gathered data as well as for configuration data, refer to subsection 5.3.4.

The so-called model-predictive control virtual machine[2] (MPC-VM) server hosts three virtual machines, an interface machine (MPC-INT), providing an interface between the OPC server and the the optimization server (MPC-OPT). A further virtual machine (MPC-GUI) hosts an Apache web server offering a graphical user interface for configuration of data points and system elements for model predictive control. All experiments conducted within the scope of the thesis use the MPC-INT as main operation machine that executes the control tuning algorithm.

5.4 Preparation of proposed method's demonstration

In the special case of the demonstration bench, the following steps were conducted to apply the method. The first step is the re-programming of the PID-controllers at the FEC, thus, the automation level. Here, re-programming means to deactivate the existing and as benchmark serving JCI adaptive controllers and make all relevant data points, as e.g. the P, I and D gains, controller input and outputs, and so on, available for the management layer. Second, the new data points have to be integrated into the BACnet at management level and then, third, into the BNOPC- and MPlus-OPC-server. The fourth step is to attach the new OPC-objects to the TCP2OPC-interface. Fifth, the new

[2] The name originates from an EU research project, where I, together with colleagues from different countries, set up a MPC environment to demonstrate a MPC algorithm, compare Futterer et al. [2013] and Constantin et al. [2012].

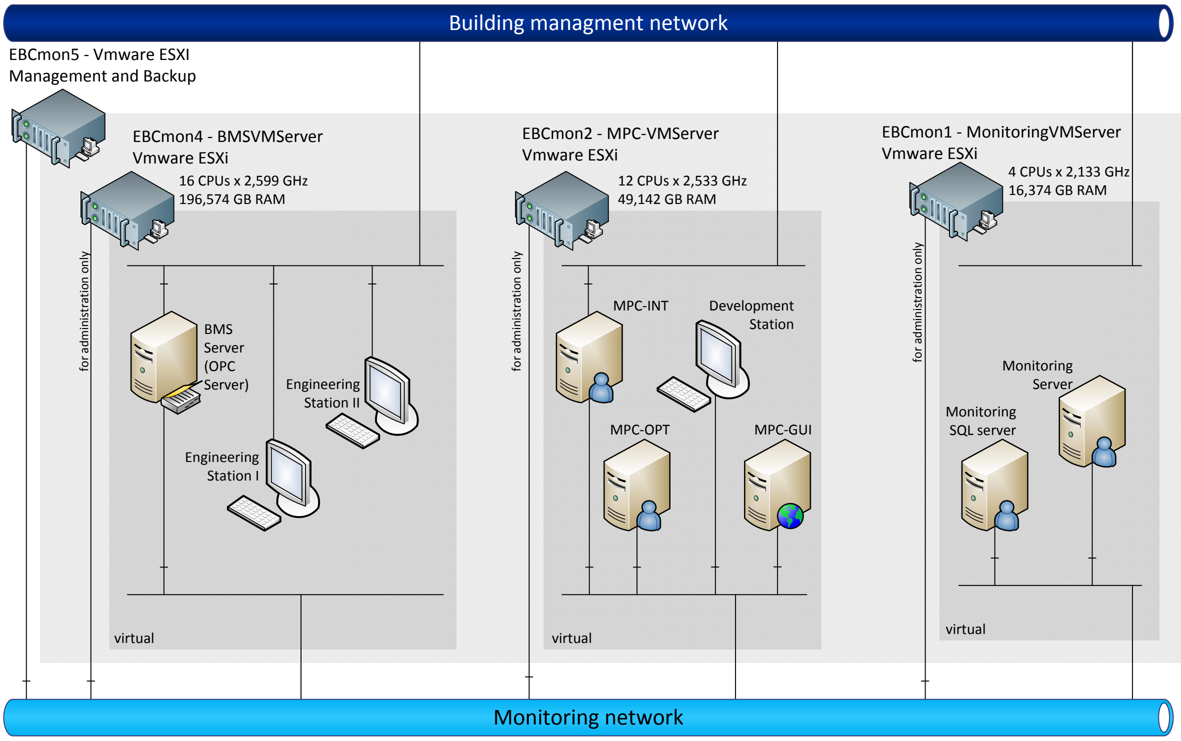

Figure 5.4: Physical server and virtual machine infrastructure

TCP-objects have to be linked to the relevant pins in the algorithm configuration sheet. Finally and sixth, a function to change the log cycle time, i.e. the sampling time of the monitoring system, for selected data points involved in a experiment[3] was developed.

Almost every building automation equipment manufacturer implements the theoretic PID-algorithm in his own way. The here-proposed tuning algorithm needs the exact mathematical model of each manufacturers PID-controller for its simulative PID-parameter evaluation, refer to section 3.6. Thus, for each manufacturer an individual Simulink model has to be developed and validated. This has to be done one time for each type of controller.

[3]Despite the implemented monitoring system has change of value threshold, the typical sampling time within the implemented monitoring system is 30 seconds. Putting down every of the more than 9000 data point to a near-zero sampling time results in sampling times of about five seconds. Selecting data points according to experiments and neglecting the other data point while decreasing the log cycle time set points achieves actual sampling times of below one second.

5.5 Test bench limitations

A limitation of the test bench is that it was not possible to test all resulting parameter configurations within the real system, since the manufacturer holds certain PID parameter constraints within its hardware. Still, this fact had only minor consequences for the results.

Further, physical limitations occurred, which led to non-successful experiments. As physical limitation I denote e.g. an air temperature control loop, where the controlling device, e.g. an air cooler, is not able to influence the controlled variable, e.g. room temperature, due to capacity reasons, e.g. not enough power. Also, these limitations have neglectable consequences for the core results. Still, they prohibited the method's application on several control loops within the building, see chapter 6.

5.6 Requirements for retail application of the proposed method

Since an algorithm for a simple, easy-to-apply and cloud-based control tuning has significant marketing potential, when assuming 1.8 million non-residential building within Germany alone, the prerequisites for retail use are a very interesting topic. The prerequisites for the development, demonstration and evaluation of a control tuning method are fulfilled by the above-described extensions. This section outlines general requirements for a non-research application of the proposed method. Thus, how the method can be applied towards a state-of-the-art building and what it needs.

The control tuning method requires different functionality from the BACS. First, the BACS either needs a (e.g. OPC) data access server for communication or the management level should follow the BACnet standard. In the second case, an own OPC server or a direct BACnet communication can be provided. Second, the proportional, derivative, and integrative gains of controllers that are to be tuned must be available on the communication interface. Thrid, the architecture of the PID-controller has to be known, especially the PID controller's PID algorithm execution interval, and further parameters like e.g. operation ranges, anti-wind-up functionality or derivative kick suppression, compare section 5.4. Fourth, the BACS needs the ability to log relevant data, like e.g. controlled variable, controller output, set point etc., or the algorithm has to be extended with an integrated data storage functionality for the relevant data objects. A rule of thumb would be the higher the resolution, the better the identifcation results, refer to chapter 8, subsection 8.2.7. To prevent anti-aliasing, to assure comparability of results, and for validation of the PID-controller model validation, the the data logging interval should be at least twice the PID controller's PID algorithm execution interval.

For retail use, also adaptations on the algorithm side are neccessary. First, the BACS manufacturer's PID-controller has to be modeled. Second, the algorithm has to be adapted to the BACS's communication interface. This is not necessary, if the BACS provides TCP communication. In general, also a direct communication to BACnet should be possible, but, this was not performed within the scope of this work. Third, either an adaption of the data base interface or an extension of a integrated data storage functionality is necessary.

6 Field test experiment design and investigated control loops

As argued in chapter 2, a variety of physically-different controlled systems exists in a building. Their transfer behavior differs and has different time constants. The systems face different ambient and/or supply conditions. Disturbances differ and the communication system of the controlling BACS is not always the same. Multiple single control loops exist for each of those controlled systems.

For all experiments, I compared the control performance of the proposed PID-parameter sets against the control performance of the PID-parameter set found by the previously installed JCI-adaptive-controller[1], which had at least three month to adapt its operation conditions. I used the ITAE criteria for comparison of control quality, as argued in chapter 2, section 2.5.

This chapter introduces the controlled systems and summarizes the conducted experiments.

6.1 Controlled systems

The thought of developing a control tuning method that is applicable to all state-of-the-art BACS and as generic as possible in order to be suitable for all possible controlled systems within BACS leads the process of choosing controlled systems to be investigated. I started with all occurring controlled systems in the E.ON ERC Main Building's BACS, then, I evaluated the importance of each controlled system towards maintaining the buildings operation, especially for the case of an unforeseen algorithm crash. Finally, I prepared 29 single control loops out of 16 controlled systems for experiments. In order to evaluate the influence of communication dead times, I designed three controlled systems with two kinds of alternative communication infrastructures (included in the latter numbers). Among them, one controlled system alternative redundantly occurs in two control loops. For the other two controlled systems alternatives, one control loop each serves as experiment object.

First tests, a re-elavuation of systems' impact on operation performance[2], and just the fact of not enough temporal availability[3] of the controlled system for sufficient experiments, decreased the

[1]Using the pattern recognition adaptive control (PRAC) framework, see Seem [1998].
[2]E.g. the humidification of laboratories had too much influence on the laboratory users and test benches.
[3]E.g. for dehumidification the time frame when outdoor humidity is high enough for dehumidification operation.

amount of investigated controlled systems to eight, with 19 remaining single control loops[4] for investigation.

All single control loops are systems of a system, in the following called super-system[5]. I use an automated function to set the operation of the super-system in exactly the same condition for each experiment. All flaps and valves of e.g. an air handling unit operate at exactly the same position during each experiment. This allows for maximum comparability between experiments.

6.1.1 AHU air pressure

An air pressure control loop controls the air pressure in a ventilation duct by adjusting the rotational speed of a fan by adjusting the frequency of a frequency transformer for the fan's electric motor. Thereby, the controller output is an analog signal, which is the input for the frequency transformer. A sensor measures the over-pressure compared to ambient pressure which is the controlled variable.

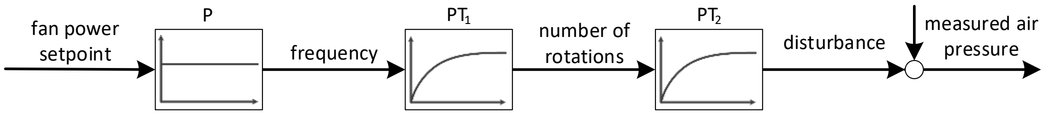

Figure 6.1: Air handling unit functional diagram for pressure control

All downstream air volume flow controllers disturb the system by influencing the duct system's pressure drop by altering their opening angle. Within the scope of the thesis, I neglect this disturbance. On the one hand, it would be a lot of effort to integrate all opening angles of downstream air volume flow controllers and not suitable for practical use. On the other hand, during operation hours, I assume that the air demand is almost constant.

The level of tuning's robustness depends on the tuning of the downstream controllers, since this could be a source of system-inherent oscillations. Since there is no perfect information and the tuning parameters of downstream air volume flow controllers are not known, I observed there behavior. All downstream controller operate robust, thus, good ITAE performance appears to be a good choice for the tuning optimization criterion.

All air-handling-unit-supply- and -exhaust-pressure-control-loops do have a certain dead range at the beginning of their operation range as well as a slight hysteresis. Figure 6.3 shows the assessment

[4]This comes down to 14 when neglecting the room air control loops.

[5]Refer to Schild et al. [2015] for further information about the System of Systems theory as a new perspective on building control.

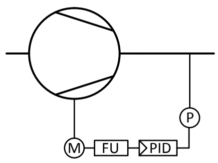

Figure 6.2: Air handling unit schematic for pressure control

of the operation range of the supply pressure control loop of air handling unit AHU01. Its dead range evolves from 0 to approxemately 35 % of the operation set points. Its slight hysteresis represents the area within the forth (lower curve) and back (upper curve) pressure curve. The appendix provides further figures on hysteresis experiments of air pressure control loops for AHU01 exhaust, AHU04 exhaust, and AHU04 supply pressure, compare figure B.1, figure B.2, and figure B.3 within the appendix.

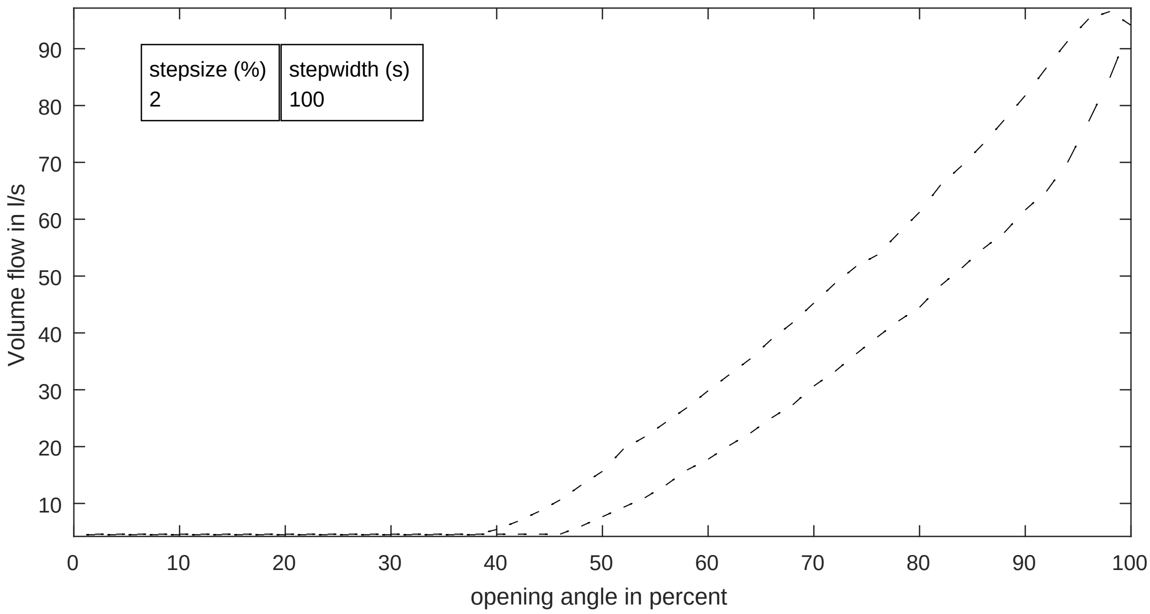

Figure 6.3: AHU01 supply pressure 2015-09-01: AHU01 supply pressure operation range assesment; step size describes the change of the opening angle in percent, step width describes the time between two changes of the opening angle

6.1.2 Two-way-valve air temperature control over heat exchanger (w/a)

A standard component of an air handling unit is a heating or cooling coil. This water to air heat exchanger controls the temperature of an air flow passing through it with the adjustment of the water flow using the opening of a two-way-valve. Figure 6.4(a) presents its schematic. The PID controller uses the coil's exhaust air temperature as input for adjusting the opening angle of a motor-driven two way valve in order to control the volume flow of a fluid, A.

Air volume flow and pressure, inlet air temperature, and inlet water temperature disturb the system. For the experiment, the algorithm used inlet water's temperature as well as inlet air temperature as disturbances. Air pressure and air volume flow are considered negligible, since they are more or less static over the experiments' time.

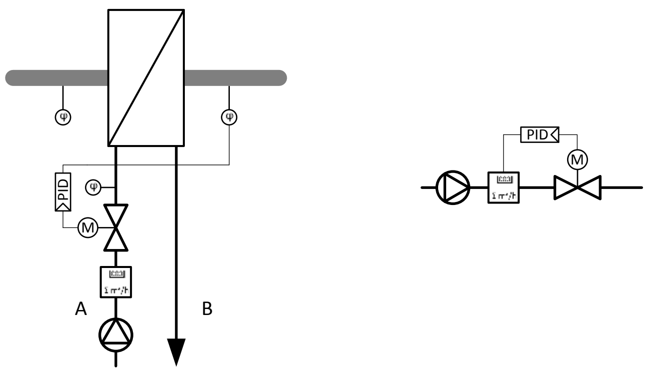

(a) schematic of a cooling or heating coil - heat exchanger (w/a)

(b) volume flow control

Figure 6.4: Two-way-valve control loops

6.1.3 Two-way-valve flow temperature over heat exchanger (w/w)

Within this control loop, in heating mode, the water exhaust temperature at a heat exchanger's cold side is controlled by variation of the water volume flow at the heat exchanger's hot side. In cooling mode, the volume flow of the cold side influences the exhaust temperature of the hot side. The controller adjusts the opening angle of a two-way-valve, in order to vary the the fluid volume flow on the hot or cold side respectively, in order to control the respective temperature. Disturbances are the both fluids' inlet temperatures as well as the volume flow at the hot or at the cold side respectively.

In the conducted experiments, the algorithm uses measured temperatures as disturbance for identification purposes. It neglects the volume flow, even if measured in the E.ON ERC main building

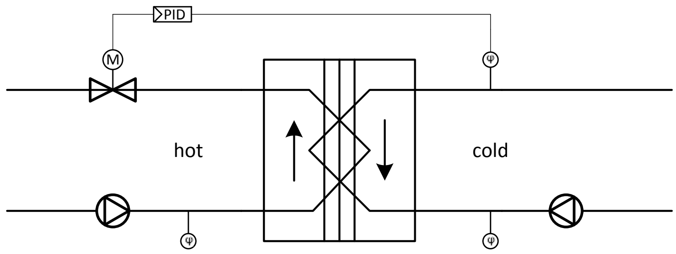

Figure 6.5: Schematic of two-way-valve flow temperature over heat exchanger (w/w)

due the fact that most state-of-the-art BACS do not measure such volume flows[6].

6.1.4 Three-way-valve flow temperature

Figure 6.6(a) shows a schematic of a motor-driven three-way-valve, controlling the inlet temperature of a system's inlet flow, B, by mixing a supply flow, A, with a system's outlet flow, C, having a temperature difference between A and C. This principle suits for heating up, if the supply flow, A, has higher temperature as the outlet flow, B, and for cooling down, if the supply flow, A, has a lower temperature as the outlet flow, B, likewise. The motor receives the controller output and moves the valve into the proportional position. The position again acts on the volume flow, whereas this transfer behavior is non-linear and, in some cases, has significant hysteresis. The system's non-linearity and its hysteresis show figure B.4 and in figure B.5 in the appendix.

The algorithm used the supply flow's, A's, and the outlet flow's, C's, temperature as disturbances during the system identification. All occurring pumps are pressure-difference-controlled.

I used three-way-valves to conduct the proof-of-concept that classical control tuning rules are able to outmatch adaptively tuned PID-control loops[7] within Fütterer et al. [2014]. The reader can find an extensive functional diagram within the appendix, refer to figure B.6, and a full mathematical description in the referenced paper.

[6]Further, the volume flow measurements in the E.ON ERC main building are part of the user-added monitoring system. Thus, a different control infrastructure would bias the results, please refer to subsection 6.1.5 and respective results in 7.3.2.

[7]In the referenced study, I applied the same evaluation criterion: the adaptive controller were JCI controller that use the so-called pattern recognition adaptive control algorithm, refer to Seem [1998] and had at least three month time to adapt their specific operation.

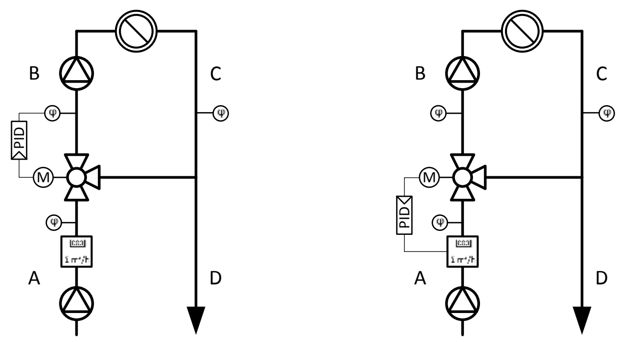

(a) Supply Flow temperature control (b) Injection volume flow control

Figure 6.6: Three-way-valve control loops

6.1.5 Three-way-valve volume flow control - user-added monitoring

Figure 6.6(b) presents the schematic of the injection volume flow control, which is a three-way-valve controlling the supply volume flow, A. From a functional point of view, this control loop represents a more direct loop compared with the latter loop. Here, the controlled variable is the supply volume flow, A, itself and not its temperature, which should make the system simpler. The volume flow directly depends on the valves' opening angle. Still, hysteresis and valve's non-linearity complicates the controlled system.

For three-way-valve volume flow control experiments, the algorithm neglects all disturbances, such as the static pressure of the fluid in front of the valve. The generating pump uses a differential pressure control algorithm. Thus, it is assumed, that the static pressure in front of the valve remains constant.

I chose this system having two thoughts. First thought: having shown temperature control with three-way-valves is possible with better control quality than in adaptively controlled systems, it should be possible to achieve even better results by simplifying the system. Second thought: having a system that I assume to be easily controllable, it should be possible to test the influence of an alternation of the communication structure and, thus, adding communication-caused time lag and uncertainty. Here, the volume flow sensor is part of the user-added monitoring system, compare subsection 6.2. Compare figure B.5 in the appendix for a operation range assessment, i.e. volume flow over opening angle, of a three-way-valve volume flow control loop.

6.1.6 Two-way-valve volume flow control - user-added monitoring

Figure 6.4(b) shows the even more streamlined control loop of a two-way-valve controlling the volume flow through a pipe, measured by a volume flow sensor. The volume flow sensor is part of the user-added monitoring, thus, its specific characteristics apply, compare subsection 6.2 and the communication infrastructure's schematic in figure 6.7(b).

The only disturbance in this system is the positive net suction head of the pump which acts on the static pressure in front of the valve and which I assume to be static as all pumps are differential-pressure-controlled. Consequently, this disturbance is neglected.

Different two-way-valves from different manufacturer differ in hysteresis and non-linearity. For the experiments conducted here, I used a two-way-valve that had significant hysteresis and non-linearity, see figure B.4 in the appendix. Unfortunately, only these kinds of valve offered the opportunity to conduct experiments with this specific communication architecture.

6.1.7 Two-way-valve volume flow control - BACnet 3rd party control integration

This experiment set up consists of a two-way-valve as described in subsection 6.1.6 with a communication infrastructure as shown in figure 6.7(c). Further, this two-way-valve almost has no hysteresis and has an almost linear transfer behavior due to it's special construction. Despite of these issues, all before-mentioned issues for two-way-valves apply.

6.1.8 Room temperature control

For experiments on room temperature control loops, I used five different rooms with three different energy distribution concepts.

- ▷ One staff facility room, which has concrete core activation and displacement ventilation in combination with cooling coils.
- ▷ Two laboratories that use active chilled beams for heating, cooling, and ventilation.
- ▷ Two laboratories that use active chilled beams in combination with circulation air coolers.

The staff facility room is situated in the inner building, having no contact to outdoor walls. The control task is to cool down internal loads induced by humans, electronic devices and lightning. A central air handling unit provides a constantly conditioned air volume flow to the displacement ventilation, transferring it to the room. A decentralized cooling coil, situated in the air duct, cools down the temperature of the supply air before it enters the room. The controller adjusts the room temperature by controlling the supply air temperature by controlling the opening angle of the cooling coil's valve, and by adjusting the supply air volume flow in parallel. A functional chart of this principle provides the appendix, see figure B.7. The concrete core activation has a central control. Its is supply temperature controlled with an almost constant temperature set point, however slightly depending on the ambient temperature. I include a controller signal flow diagram of this control loop and a functional schematic of the controlled system in the appendix.

Disturbances are the thermal conditions of the room's surroundings, the variation of internal loads and possible oscillations within the supply temperature of the concrete core activation[8]. The algorithm does not use any disturbances for system identification, since the BACS does not measure any of them.

The laboratories either have a certain number of active chilled beams, or a combination of a number of active chilled beams and a number of circulation air coolers, if they face higher internal loads due to experiments or server equipment. The room temperature PID-controller adjusts in parallel the volume flow, the opening angle of the circulation air cooler, as well as the opening angle of the active chilled beam's cooling and heating valves.

Disturbances of the laboratories include waste heat from experiments and internal loads caused by humans. On system level, the supply temperature of circulation air coolers as well as active chilled beams on their hot and cold side disturb the control quality. Despite these temperatures are measured and available, the algorithm neglects them with respect to the system's high inertia. Higher frequent disturbances should be well damped. Further, their impact is far less important than the impact of waste heat from experiments.

6.2 Communication infrastructure variation

A further investigated issue is due to two facts. The first fact is that it appears more and more suitable to add additional sensors, e.g. wireless sensors, to a system and change control logic. Adding not-native[9] sensors leads to further issues. To investigate consequences, I designed an emulating control infrastructure.

The second fact is that exchanging control logic to external intelligence becomes more and more relevant within cloud-based control and due to further thinkable system configurations while implementing agent based control system in building automation systems. Therefore, I tried to control a 3rd-party device with a native controller which emulates a thinkable retrofitting for agent based control demonstration.

[8]However, the concrete core activation has very high inertia, damping oscillations induced by minor control quality of e.g. the three-way-valve controlling the concrete core activation's supply temperature.
[9]Native means all building automation manufacturers' OEM parts and further parts, directly integrated into the BACS.

Figure 6.7 shows three different communication infrastructures. Within all three systems, the PLC, $K(q^{-1})$, receives its set point via the supervisory control system. The sub-figure 6.7(a) shows the standard system, where a sensor and an actor are integrated via analog communication. The PLC, $K(q^{-1})$, receives the set point, r(t), uses analog communication to send the control action, u(t), to the plant, $G(q^{-1})$. The sensor measures the controlled variable, y(t), and sends the measured value, y'(t), to the controller. The y(t) equals y'(t) minus the measurement uncertainty.

Sub-figure 6.7(b) shows the so-called "communication infrastructure one", (com inf 1), which uses a sensor of the user-added monitoring system that measures y(t) as y'(t). A decentralized analog-digital-converter provides the digital measurement value y"(t') from y'(t). Every analog-digital-controller has a certain sample rate and thus the time t of the physical measurement deviates from the time t', where t' is larger than t. A Labview-service gathers the analog-digital-converter's value, y"(t'), via TCP/IP communication and communicates it, later at the time t", according to its inherent sample rate, via direct OPC communication to the MPOPC-server, which again uses BACnet in order to communicate the y"(t"') to the PLC. The PLC $K(q^{-1})$ uses analog communication to control the actor, while it derives u(t) using r(t) and y"(t"'), meaning that this infrastructure adds two uncertainties and three additional time set offs.

Sub-figure 6.7(c) introduces a "communication infrastructure two" (com inf 2), which uses a fully digital, BACnet-based communication between the controlling PLC $K(q^{-1})$, and the integrated 3rd-party PLC, $K(q^{-1})_{Belimo}$. In this case, the 3rd-party PLC serves with forwarding and converting u(t) to u'(t'). Due to a conversion error the actual plant produces a response that I denote as y'(t'), since it would not exactly be the same response as it would be produced with u(t) as direct input. A sensor, connected with the 3rd-party PLC, measures y"(t') from y'(t'). The 3rd-party PLC then forwards and converts y"(t') to the actual PLC as y"'(t"). This infrastructure adds two time set offs and three uncertainties to the control system.[10]

6.3 Conducted experiments - overview

Including each and every run, the algorithm ran 583 time from July 3rd 2014 until November 20th 2015. Thereby, the algorithm performed 1541 single step and identification experiments[11]. Up to eight experiments performed in parallel thanks to experiment type clustering in order to avoid inter-system effects. The result section presents results from 398 algorithm runs, while I neglect experiments that use a continuous time domain identification, compare subsection E.

[10]Further remarks: Time lags exist within the PLC $K(q^-1)$ itself. For the PLC, $K(q^-1)$, within the all three systems, these time lags are the same and, thus, neglected. The standard system converts the analog y'(t) value to a digital value internally, which sub-figure 6.7(a) does not show for clarity reasons. Thereby a analog-digital-conversion fault is unavoidable, too. Still, the external analog-digital-conversion fault may differ from the internal. In all three system, the analog-digital-conversion fault of the controlled variable occurs only once.

[11]These runs and experiments do not include any simulation ones, compare chapter 4.

The algorithm's complexity becomes obvious when considering the fact that the algorithm offers 614432 combinations of input factors. Following the goals mentioned at the beginning of this chapter, the first input combinations followed from theory and cognitive intuition. Interpreting the results made input parameters variations possible, in order to investigate their effect and in order to find superior control quality. For each experiment, chapter 7 presents the most important input parameters and the experiment's step configuration. The configuration and full results for each of the 583 algorithm runs are included within the online documentation.

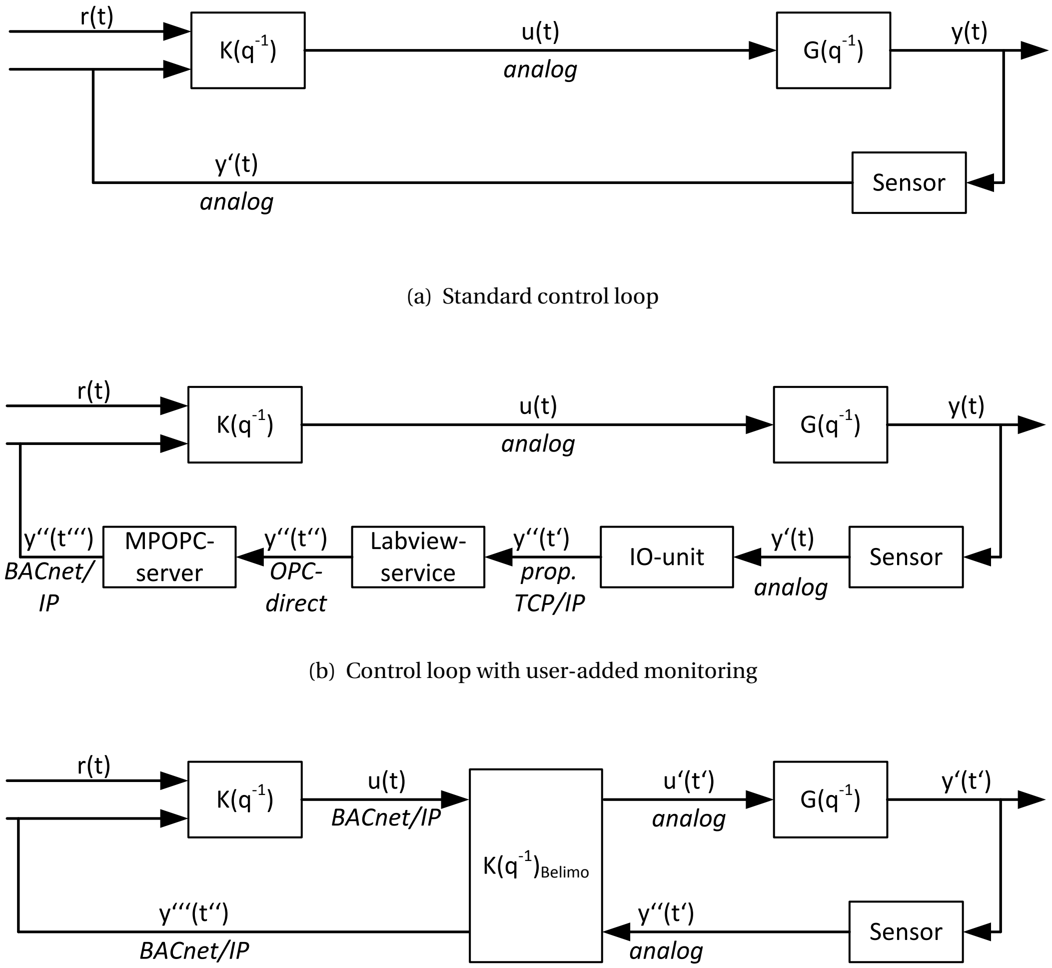

(a) Standard control loop

(b) Control loop with user-added monitoring

(c) Control loop with 3rd-party BACnet device

Figure 6.7: Alternative communication infrastructures

7 Field test results

This chapter presents the results of the experiments for different control loop types and different control loops.

Its aim is to provide a holistic view of the results achieved while it cannot present each and every experiment. It presents a condensed experiment overview for each type of control loops, while facing the fact that many experiments had setups that served for investigation of e.g. the influence of certain input parameters. The first experiment presented here is described in detail in order to provide insight into the applied method.[1]

The results of the different identification experiments are comparable, if the investigated plant with all its operation conditions remains exactly the same and if the step experiments' configuration, i.e. step height, its relative position within the operation range, and waiting time unless settled, is equal. Such characteristics can be found in simulations. This leads to the fact that for the used controlled systems of chapter 4, simulation study, the sensitivity analyses are fully comparable. Since the field test experiments took place at different times, well spread throughout 2014 and 2015, this cannot be achieved for all identification experiments, because e.g. maintenance workers changed filters, thus, pressure conditions change, or maintenance for valves took place, thus, their effective operation range changes, etc. This accounts for absolute and relative criteria. Keeping this in mind, it is still possible to compare experiments with moderate uncertainty.[2] Thus, within the following chapter, besides prooving that the algorithm is generally and practically capable to improve control quality, the results serve to prove the general tendencies of parameter variations shown via simulation, see chapter 4, and further discussed in chapter 8.

[1] Denotation remarks: As already seen in chapter 3, one identification experiment uses the data of the initial step experiment and the data gained by excitation of the to-be-identified system. Thus, the "identification experiment" consists of the initial step experiment, the system exitation and the model identification. Further, "initial step experiment" denotes the step experiment with the initial PID parameters and "step experiment" denotes to step experiments with tuned parameters.

[2] However, it is not always possible to account for having the same operation conditions, since this is a sophisticated task within a field experiment. The assumption is that systems operate in their normal or set operation conditions during step experiments. The configuration, e.g. a long-enough settling and waiting time, tries and accounts for disturbances.

7.1 Experiment results

7.1.1 AHU air pressure

The algorithm ran 177 times in four different air pressure control loops, whereas 89 runs served for code and method development, 38 did not finished due to errors presented in section D within the appendix. The following subsections of this section present 50 successful experiments.

For this type of control loops, out of 39 evaluable experiments 27, 69 %, ameliorated the ITAE control performance, whereby 60 out of 127, 47 %, proposed and tested PID-parameter sets were advantageous.

AHU 01 exhaust pressure

Taking the algorithm's development and further development experiments into account, the AHU 01 exhaust pressure control loop served for 52 identification experiments. 33 experiments served for code development, seven experiments did not finished. A distinctive analysis investigates all different reasons for not-finishing, thus, unsuccessful experiments, in section D within the appendix. In the following the twelve remaining experiments that were successful insofar as they the algorithm proceeded without any errors are analyzed.

Table 7.1[3] shows the most important input variables for each of these twelve experiments. In the following, the combination of input variables is called experiment configuration. Each experiment conducts steps with the real system – the initial step experiment and the step experiment for evaluation of the proposed PID parameter sets – and simulation-based steps. 61 step experiments have been conducted towards the real system. The experiments provided the evaluation basis for twelve initial PID combinations and 49 proposed PID parameter sets.

Each step experiment has four characterizing input variables. The step response and its control quality criteria depend on these four variables, on the PID parameters used and on the conditions of the physical system. In general, it is possible to quantitatively compare PID parameter sets via step experiments if the four input variables are the same. If the input variables differ, only qualitative comparisons make sense[4]. Thus, if control quality criteria are compared in the following, this is only done for steps having exactly the same configuration. In the following a certain combination

[3] Nomenclature starting from left: Experiment (Exp.), sampling time write (STW), sampling time read (STR), maximum model order (MMO), maximum distrubance oder (MDO), identification time (IDT), maximum amount of excitation (MAE), identification method (ID), mean and amplitude (ampl.) of the excitation signal, shape of excitation signal, and number of respective step configuration.

[4] As e.g longer step lengths include deviation that occurs after exceeding the shorter step lengths; longer settling times offer more opportunity for the PID controller to unload its integral and or its derivative gains; and different settling and step values investigate different operation ranges.

Table 7.1: AHU 01 exhaust pressure: experiment configurations

Exp.	STW	STR	MMO	MDO	IDT	MAE	ID	mean	ampl.	shape	Ste.
-	in s	in s	-	-	in s	-	-	in % or Pa		-	-
1	10	1	4	4	9000	900	CL	85	65	rbs	1
2	10	1	8	8	600	60	CL	85	65	1/f	1
3	10	1	4	4	1440	144	CL	85	65	rbs	1
4	10	1	4	4	1440	144	CL	85	65	1/f	1
5	200	1	4	1	4140	20.7	CL	105	50	1/f	2
6	200	1	2	2	4140	20.7	CL	105	50	1/f	2
7	200	5	2	2	25640	128.2	CL	105	50	1/f	3
8	5	1	2	2	5840	1168	CL	105	50	1/f	3
9	5	1	12	12	1640	328	CL	105	50	1/f	3
10	5	1	12	12	2780	560	CL	105	50	rbs	3
11	30	15	6	6	2940	98	OL	65	70	1/f	4
12	30	15	6	6	2940	98	OL	50	100	1/f	4

Table 7.2: AHU 01 exhaust pressure: step configurations

Step	Settling time	Step length	Settling value	Step value	Number of executions
1	420	420	85	120	33
2	1200	300	80	130	5
3	1200	400	80	130	16
4	1200	900	80	130	7

of step input variables is called step configuration. Table 7.2 shows the step configurations which experiments for AHU 01 exhaust pressure used.

Out of twelve experiment runs, seven experiments were able to propose at least one PID parameter set, which leads to lower ITAE values, see figure 7.1[5]. Regarding all step experiments, 14 out of 49 proposed PID parameter sets provided a better ITAE control performance than their respective initial configurations.

In the following, experiment number eleven, “AHU01 exhaust pressure 2015-09-06 14h00", is fully represented in order to show the algorithm’s procedure and in order to visualize the results and sub-results within the algorithm’s methodology in more detail.[6]

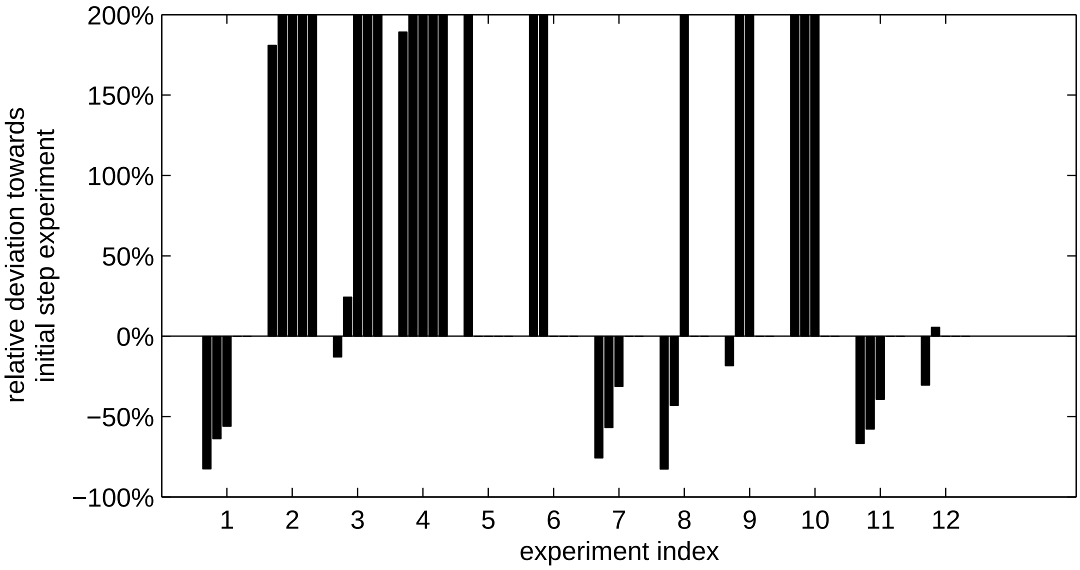

Figure 7.1: AHU 01 exhaust pressure: relative ITAE deviation for each experiment

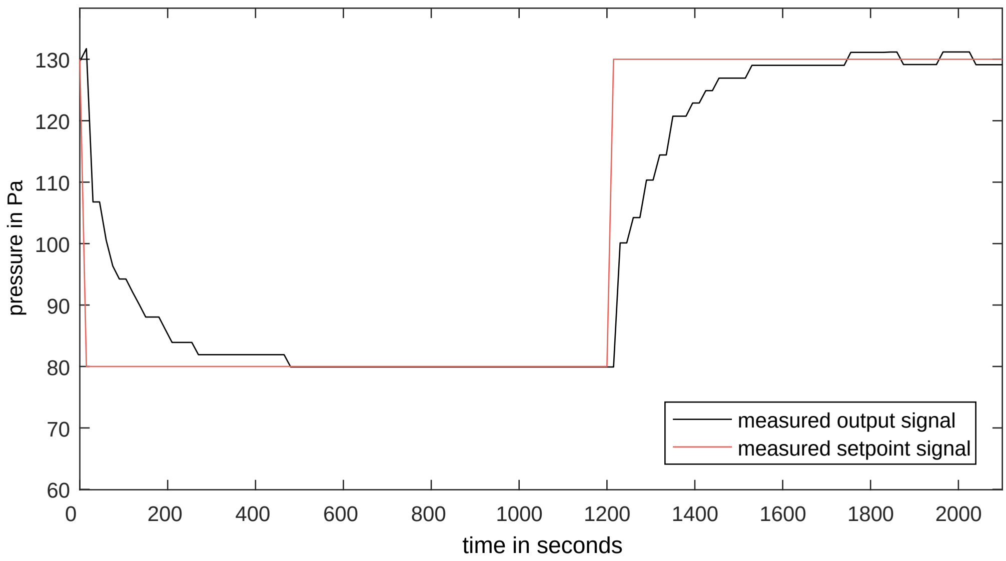

Figure 7.2: AHU01 exhaust pressure 2015-09-06 14h00: Initial closed-loop step experiment, showing the step response with the initial control parameters $(P, I) = (0.129, 38.5s)$

AHU 01 exhaust pressure - experiment 2015-09-06 14h00

For each experiment, relevant experiment configuration parameters are presented by an experiment short one-line-discription, the so-called “experiment string”. For experiment “AHU01 exhaust pressure 2015-09-06 14h00" this experiment string looks like follows:
[**STW** 30 s **STR** 15 s **MMO** 6 **MDO** 6, **IDT** 2940 **MAE** 98 **OL ER** (30 %;100 %) **1/f F**]
Starting from left, it tells that the experiments minimal write sampling time (STW) is 30 seconds and its read sampling time (STR) is 15 seconds. For the system identification it uses all models with model orders below the maximal model order (MMO) of 6 and all models with a disturbance model order below a maximal disturbance order (MDO) of 6. Its identification time (IDT) is 2940 seconds which means that the maximum amount of full range excitations (MAE) is 98. The excitation range (ER) of this open loop experiment (OL) is from 30 % to 100 % meaning the excitation signals amplitude is 70 %. This means that it sends 30 %, respectively 100 % as set point signals for the ventilator. The excitation signals frequency distribution follows the 1/f-signal-shaping method, (1/f), and the data is filtered (F) before the identification takes place.

Initial step experiment

Figure 7.2 shows the closed loop step experiment for the considered control loop with the initial control parameter, which is the result from the adaptive PID tuning method applied by JCI.

Investigating the step response in figure 7.2 provides the control quality criteria within table 7.3. The system has a rise time (RT) of 210 seconds and since it has neither overshoot (OV) nor undershoot (US). The RT equals the settling time (ST). The integral criteria are presented as well.

Table 7.3: AHU01 exhaust pressure 2015-09-06 14h00: Initial control quality indicators

RT	ST	OS	US	IAE	ISE	ITAE
210 s	210 s	0 Pa	0 Pa	338,86 Pa	7278,64 Pa^2	47,62 kPa · s

Identification Experiment

Figure 7.3 shows the identification experiment’s input signal. As it is an open loop signal, it varies the controller output, which is the setpoint signal for the ventilator, in this case from 30 % to 100 %. The frequency spectrum shows lower power towards very low frequencies compared to higher amplitudes at higher frequencies. In this case, the maximum excitation frequency is slightly above 0.016 Hz.

[5] The values for step experiments shown in figure 7.1 that exceed the y-axes limit of 200 % can be found in the online documentation. Algorithm run number two conducts 15 step experiments. The figure shows the best five results. For clarity purposes, the other ten step experiments are neglected.

[6] This extend of information is only given once within this thesis. For each mentioned experiment, the same documentation is available within the online documentation.

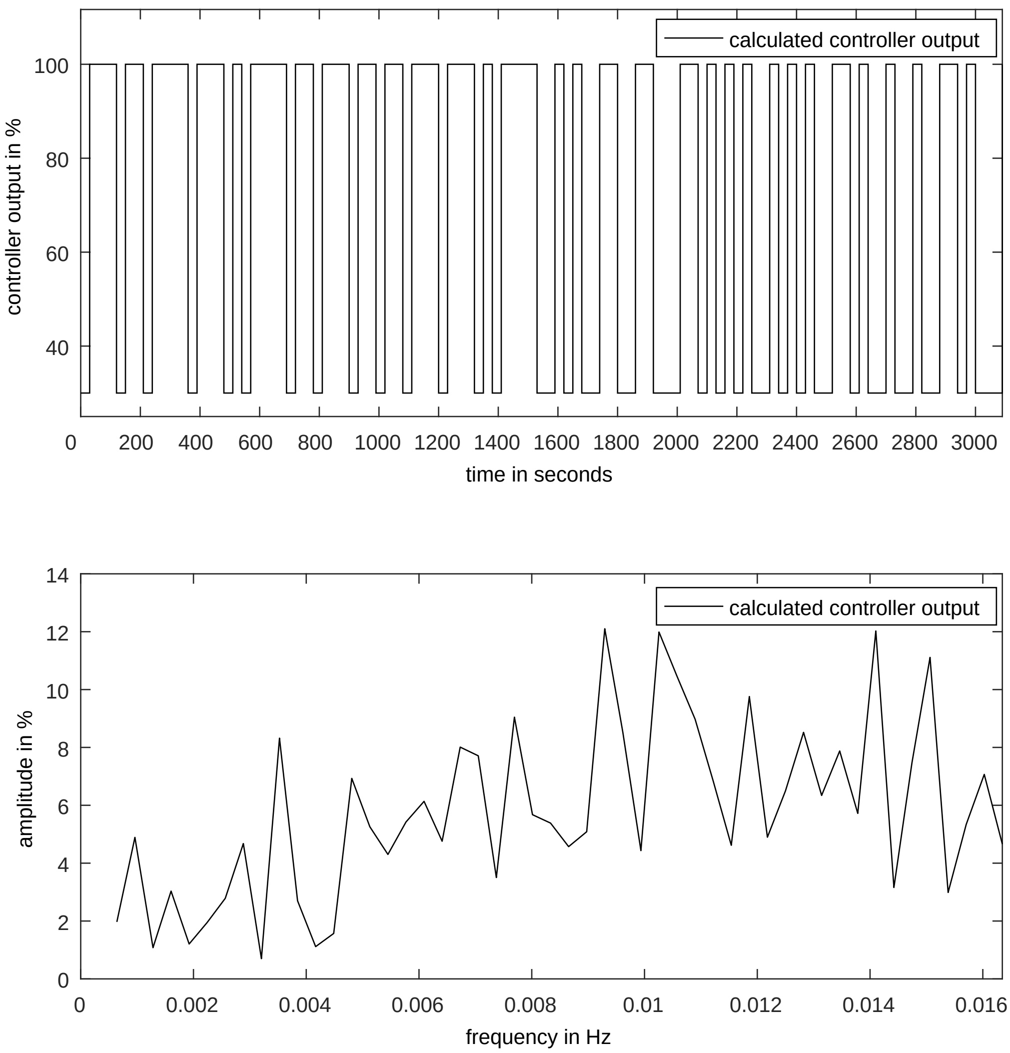

Figure 7.3: AHU01 exhaust pressure 2015-09-06 14h00: Excitation signal (1/f) and frequency spectrum

Figure 7.4 shows a direct comparison of system input (controller output respectively) and system output signal – in this case, of the ventilator set point and measured pressure.

As already mentioned within section 2.7, only system relevant frequencies of the system input and output signals should be regarded. The maximum frequency of the generated system input signal is slightly above 0.016 Hz. Still, the measured system input, which is in this open loop case equal to the controller output, spreads over a wider frequency range because of hardware processing frequen-

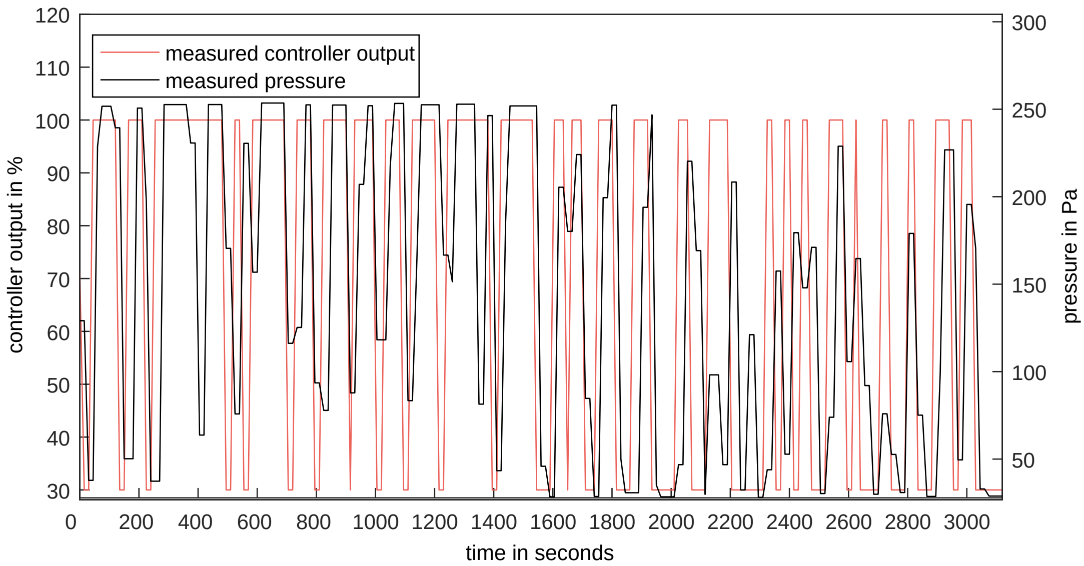

Figure 7.4: AHU01 exhaust pressure 2015-09-06 14h00: System input and system output

cies and network communication issues. These frequency ranges, since they are not important for identification of the physical system, are filterd via a low pass filter which is shown in figure 7.5.

The identification process identifies a number of models, depending on the maximum model order and the maximum disturbance order. Figure 7.6 shows the fitting of the model with the highest residual model fit, following equation 3.6 in subsection 2.7.3.

The estimated model is a discrete-time Box-Jenkins model, having a sample rate according to STR of 15 seconds and four polynomial terms of different order, see equation 7.1. Polynomial term $B(z)$ is of second, $C(z)$ of sixth, $D(z)$ of second, and $F(z)$ of fifth order, leading to the model-abbreviation “bj(2,6,5,2,d,15)”.

$$y(t) = \frac{B(z)}{F(z)}u(t) + \frac{C(z)}{D(z)}e(t)$$

$$\begin{aligned} B(z) &= 0.4118 + \frac{0.4825}{z} \\ C(z) &= 1 + \frac{1.956}{z} - \frac{0.7333}{z^2} - \frac{3.454}{z^3} - \frac{1.066}{z^4} + \frac{1.498}{z^5} + \frac{0.8002}{z^6} \\ D(z) &= 1 - \frac{1.845}{z} + \frac{0.8458}{z^2} \\ F(z) &= 1 - \frac{1.505}{z} + \frac{1.753}{z^2} - \frac{1.468}{z^3} + \frac{0.8803}{z^4} - \frac{0.2549}{z^5} \end{aligned} \tag{7.1}$$

As described in 3.4 the algorithm splits the input-output data (IO-data) used for the identification in order to perform the so called cross-validation approach. Thus, the model fit calculation takes

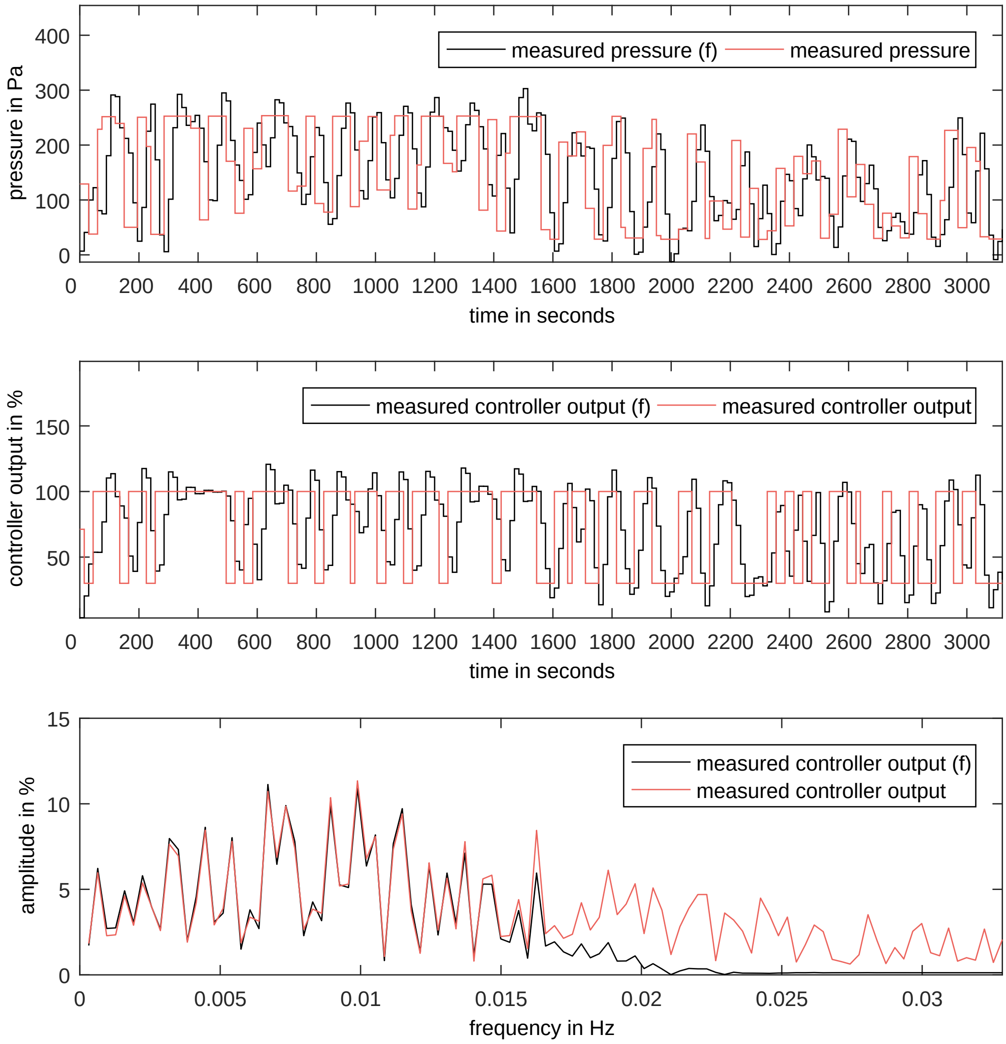

Figure 7.5: AHU01 exhaust pressure 2015-09-06 14h00: Identification data vs. filtered identifcation data (f) and the respective frequency spectra

place considering the estimation data, two thirds of the whole IO-data, and the validation data, one third of the whole IO-data. The model fit related to the estimation data (mf_{est}) equals 93.23 % while the model fit (mf) towards the evaluation data is 34.6 %.

PID-parameter calculation

The amount of estimated models is shrunk to an user-adjustable number, 150 in this case, in or-

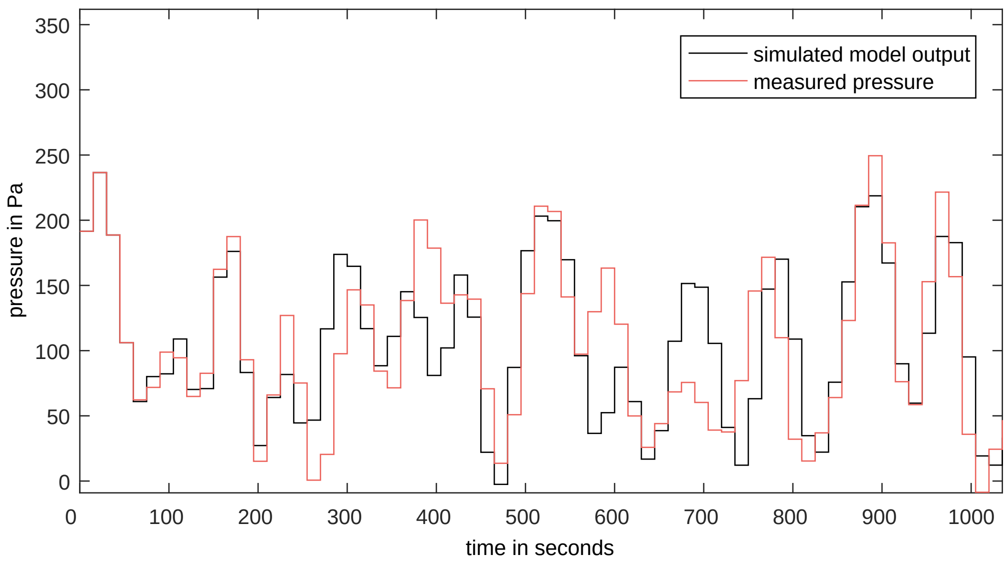

Figure 7.6: AHU01 exhaust pressure 2015-09-06 14h00: Simulated model output vs. measured system output of best fitting model, Box-Jenkins (2,6,2,5,d), model fit to validation data (mf) = 34.6%, model fit to estimation data (mf_{est}) = 90.3%

der to save computational power within the following procedures. For each of these 150 unique remaining models, all 14 classical parameter calculation methods are applied. Since the classical calculation methods demand continuous low order models, a model reduction according to the introduced rules takes place, compare subsection 2.8. In this case 2250 parameter sets (resulting from 14 calculated parameter sets and the actual parameter set times 150 estimated models) are further investigated. For each of the 2250 parameter-model-combinations the suitability for application on JCI hardware is validated, compare the JCI restrictions introduced in section 5.5. In this case, 277 parameter-model-combinations would be suitable to apply. These 277 combinations are now investigated within a simulation in SIMULINK. The simulation conducts a step experiment and calculates all before-mentioned control quality indicators. Table 7.4 provides the actual control parameters and the parameter-model-combinations which achieved the best simulative control quality in terms of ITAE.

Table 7.5 shows the achieved simulative control quality indicators per parameter-model-combination and, in addition, the model which achieves the best ITAE value using the actual control parameters.

The results of the control quality indicators are only vaguely different, resulting of nearly equal proposed control parameters.

The comparison between the step responses for bj(2,6,2,5,d) with actual parameters, with proposed parameters, calculated with the absolute value optimum method for P and I (PIBO), and the real ex-

Table 7.4: AHU01 exhaust pressure 2015-09-06 14h00: Actual and proposed PID controller parameters following Box-Jenkins (bj) models with different model and disturbance orders in combination with the absolute value optimium tuning method (PIBO)

option	K_P	T_I	T_D
actual parameters	0.129	38.500	0
bj(2,6,5,3,d)PIBO	0.146	16.047	0
bj(2,5,3,3,d)PIBO	0.146	16.046	0
bj(2,5,4,3,d)PIBO	0.146	15.958	0

Table 7.5: AHU01 exhaust pressure 2015-09-06 14h00: Simulated control quality indicators

option	**RT**	**ST**	**OS**	**US**	**IAE**	**ISE**	**ITAE**
bj(2,5,4,3,d)PIBO	135 s	135 s	0 Pa	0 Pa	212.06 Pa	6877.62 Pa^2	9.56 kPa s
bj(2,5,3,3,d)PIBO	135 s	135 s	0 Pa	0 Pa	212.74 Pa	6880.83 Pa^2	9.65 kPa s
bj(2,6,5,3,d)PIBO	135 s	135 s	0 Pa	0 Pa	212.55 Pa	6872.47 Pa^2	9.65 kPa s
actual p. bj(3,6,3,5,d)	900 s	900 s	0 Pa	0 Pa	30,73 Pa	16,80 Pa^2	15.97 kPa s

periment step response with actual parameters are shown in figure 7.7. Bj(2,6,2,5) with PIBO-tuned parameters provides a better control quality over all control quality indicators. Still, the system has no overshoot.

Table 7.6: AHU01 exhaust pressure 2015-09-06 14h00: Measured control quality indicators

option	**rise t.**	**settling t.**	**overs.**	**unders.**	**IAE**	**ISE**	**ITAE**
bj(2,6,5,3,d)	60 s	60 s	0 Pa	0 Pa	133.63 Pa	2419.71 Pa^2	15.82 kPa s
bj(2,5,3,3,d)	75 s	75 s	0 Pa	0 Pa	161.03 Pa	3850.04 Pa^2	20.13 kPa s
bj(2,5,4,3,d)	75 s	75 s	0 Pa	0 Pa	214.08 Pa	6249.83 Pa^2	28.94 kPa s
actual p.	210 s	210 s	0 Pa	0 Pa	338,86 Pa	7278,64 Pa^2	47,62 kPa s

Figure 7.9 and figure 7.8 show the step responses of the tuned PIBO parameters from the bj(2,5,3,3,d) and the bj(2,6,5,3,d) model respectively, while applied in a step experiment within the real controlled system.

As it can be seen, both parameter sets achieve a very satisfactory control performance with quick rise and settling time, no over- or undershoot, and far better integral criteria than the reference case.

In comparison to the reference control quality parameters, all three proposed parameter sets provided better control results. E.g. rise time was improved by down to −71.43 %, while IAE and ITAE have been lowed by −60.56 % and −66.79 %, see table 7.7.

This control loop tuning started on September 5^{th}, 2015 at 14:00:00 and took until 17:43:56. The experiment took in total 03:43:56, while four time 1200 seconds settling time and 900 seconds time for control quality measurements have been used in the four conducted step experiments, in total

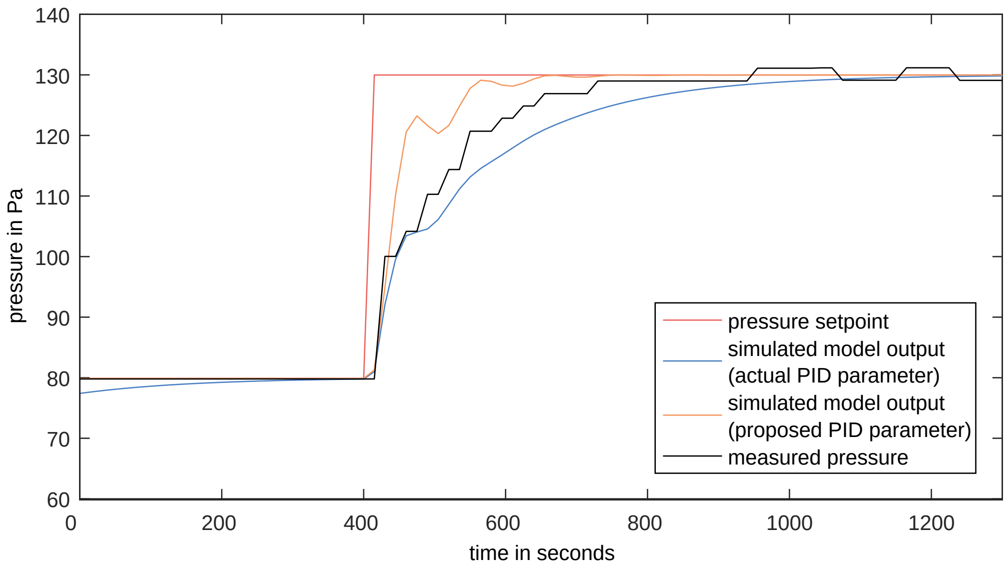

Figure 7.7: AHU01 exhaust pressure 2015-09-06 14h00: comparison between simulative steps for the bj(2,5,4,3,d)-model with actual parameters, the bj(2,5,4,3,d)-model with PIBO-tuned, i.e. proposed parameters, and the initial step experiment, i.e. with the actual parameters

Table 7.7: AHU01 exhaust pressure 2015-09-06 14h00: Relative deviation of control quality indicators

option	RT	ST	OS	US	IAE	ISE	ITAE
bj(2,6,5,3,d)PIBO	−71.43 %	−71.43 %	0	0	−60.56 %	−67.21 %	−66.79 %
bj(2,5,3,3,d)PIBO	−64.29 %	−64.29 %	0	0	−52.47 %	−47.82 %	−57.73 %
bj(2,5,4,3,d)PIBO	−64.29 %	−64.29 %	0	0	−36.82 %	−15.30 %	−39.22 %

02:20:00. 49 minutes were used for system excitation and thus information gathering. Communication, data base queries, setting experiment conditions, model estimation etc. took 44 minutes and 56 seconds.

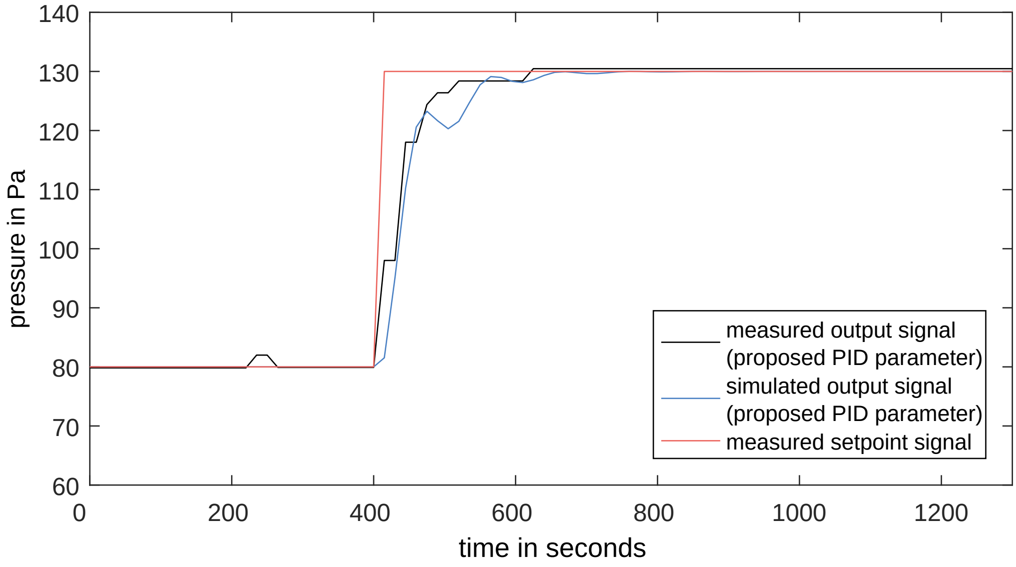

Figure 7.8: AHU01 exhaust pressure 2015-09-06 14h00: bj(2,6,5,3,d) PIBO real step comparison

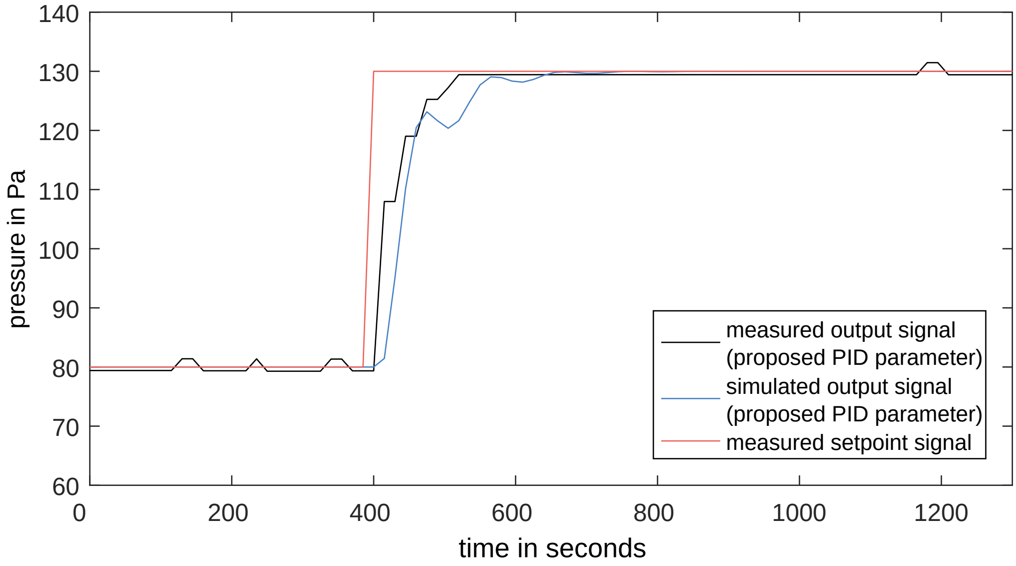

Figure 7.9: AHU01 exhaust pressure 2015-09-06 14h00: bj(2,5,3,3,d) PIBO real step comparison

AHU 01 supply pressure

The supply pressure control loop of the air handling unit 01 served for 71 experiments in total, whereas 47 experiments were conducted during code development for the automation of the proposed method. Ten experiments did not provide successful results due to various reasons, see D within the appendix. 14 successfully conducted experiments remain for analysis.

These experiments used five differently configured types of step experiments to evaluate the control quality of actual and proposed parameters, see table 7.9. During the conduction of two experiments (number eleven and number 14, see table 7.1.1) the initial step experiments with actual parameters failed. Therefore, it is not possible to relatively compare proposed parameter sets via step experiments with the experiment's initial step experiments. Also for an absolute evaluation, the integral quality criteria of the experiment 14 cannot be compared to any other step. The initial step experiment of experiment number eleven can be compared against initial step experiments of the same type from other experiments, since four further experiments used the same step experiment configuration, configuration four. Thus, the experiment is included in Figure C.7. During experiment number seven, the OPC data connection was interrupted. The identification was successful in theoretical terms but did not identify a physical system. Thus, its results are neglected here. In experiment number eight the ventilator showed a slightly different physical behavior compared with all other experiments. The reason cannot be clarified in an ex post investigation[7]. Still, the algorithm successfully proposed PID parameters and ameliorated the initial control situation.

Out of the remaining eleven experiments (including experiment number eight), seven experiments provided at least one parameter set which led to lower ITAE-values than their respective initial step response. Figure 7.10 shows the relative deviations of the step responses of each proposed parameter set towards the initial step response of the actual parameter set. While looking at figure 7.10, keep in mind that experiment eight had different physical behavior, as mentioned above.

Compare section C.2 within the appendix for further results on AHU 01 supply pressure.

AHU 04 exhaust pressure

The algorithm tried and tuned the control loop AHU 04 exhaust pressure 33 times, whereas 5 runs served code development purposes. 16 successful experiments remain for analysis, since different faults occurred twelve times, see section D within the appendix.

The 16 algorithm runs conducted 56 step experiments following eleven step types. Table 7.10 provides the most important conditions of all successful algorithm runs and table 7.11 provides configurations of all conducted step experiments.

[7] The most probable reason are maintenance workers opening and closing ventilation ducts.

Table 7.8: AHU 01 supply pressure: Experiment configurations

Exp.	STW	STR	MMO	MDO	IDT	MAE	ID	mean	ampl.	shape	Ste.
-	in s	in s	-	-	in s	-	-	in % or Pa		-	-
1	10	1	4	4	4530	453	OL	55	60	rbs	1
2	10	1	4	4	9000	900	CL	75	60	1/f	2
3	20	5	4	4	30360	1518	CL	75	60	1/f	2
4	10	1	8	8	15060	1506	CL	75	60	1/f	2
5	10	1	8	8	9360	936	CL	75	60	1/f	2
6	10	1	8	8	34560	3456	CL	75	60	1/f	2
7	90	1	2	2	2640	29.3	CL	75	60	step	3
8	30	1	2	2	2240	74.7	CL	75	60	rbs	3
9	100	1	3	1	7640	76.4	CL	70	40	1/f	4
10	200	1	2	2	2240	11.2	CL	70	40	1/f	4
11	200	5	2	2	25640	128.2	OL	50	70	1/f	4
12	5	1	2	2	5840	1168	OL	50	70	1/f	4
13	30	15	6	6	3140	104.7	OL	50	70	1/f	4
14	30	15	6	6	2940	98	OL	65	70	1/f	5

Table 7.9: AHU 01 supply pressure: step configurations

Step	Settling time$_i$	Step length	Settling value	Step value	Number of executions
-	in s	in s	in PA	in PA	-
1	300	360	60	85	3
2	360	360	60	85	27
3	100	100	60	85	5
4	1200	400	50	90	18
5	1200	900	50	90	4

Table 7.10: AHU 04 exhaust pressure: experiment configurations

Exp.	**STW**	**STR**	**MMO**	**MDO**	**IDT**	**MAE**	**ID**	**mean**	**ampl.**	**shape**	**Ste.**
-	in s	in s	-	-	in s	-	-	in % or Pa		-	-
1	10	1	3	3	5758	576	OL	60	60	rbs	1
2	10	1	3	3	6660	666	OL	60	60	1/f	2
3	10	1	3	3	11158	1116	OL	60	60	1/f	3
4	10	1	3	3	14760	1476	OL	60	60	1/f	3
5	10	1	3	2	15480	1548	OL	60	60	1/f	4
6	10	1	3	2	940	94	CL	50	50	1/f	5
7	60	1	3	2	3740	62.3	CL	50	50	step	6
8	100	1	4	0	14840	148.4	CL	35	70	rbs	7
9	200	1	2	2	2240	11.2	CL	35	70	1/f	7
10	20	1	2	2	7640	382	CL	35	65	1/f	8
11	20	1	2	2	7640	382	CL	35	65	1/f	9
12	60	15	6	6	1700	28.3	OL	35	70	1/f	10
13	60	15	6	6	1700	28.3	OL	50	100	1/f	10
14	60	15	6	6	1700	28.3	OL	50	100	1/f	10
15	30	15	6	6	2940	98	OL	80	40	rbs	11
16	30	15	6	6	2940	98	OL	80	40	rbs	11

Table 7.11: AHU 04 exhaust pressure: step configurations

Step	**Settling time$_i$**	**Step length**	**Settling value**	**Step value**	**Number of executions**
1	360	360	85	110	4
2	360	360	50	70	4
3	360	360	75	100	8
4	360	360	50	75	3
5	200	200	50	75	2
6	400	250	50	75	2
7	1200	400	0	75	7
8	1200	400	0	65	4
9	1200	400	20	65	4
10	1200	400	0	70	10
11	1200	900	30	70	8

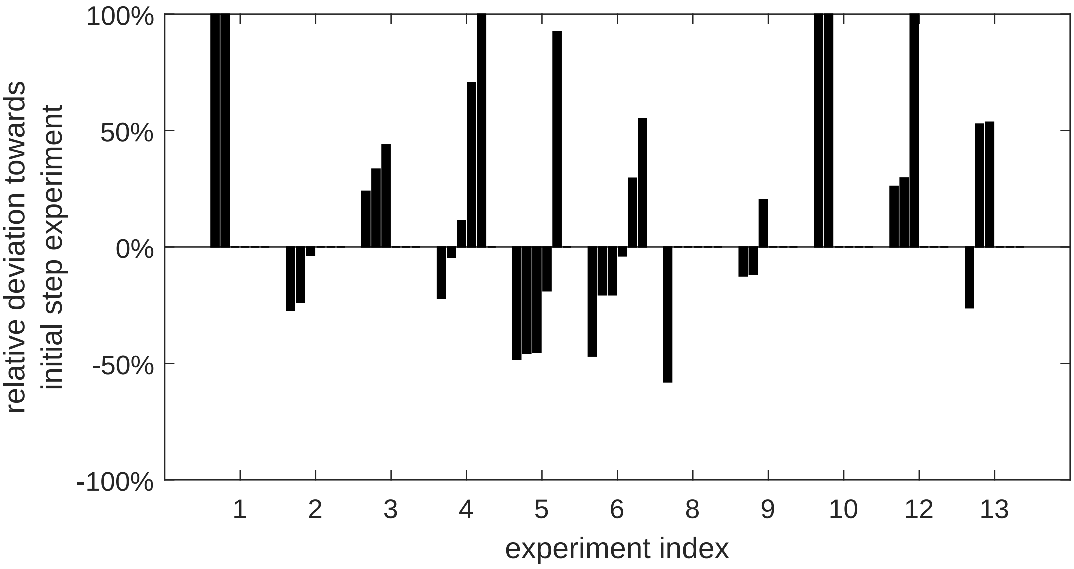

Figure 7.10: AHU 01 supply pressure: relative ITAE deviation for each experiment

The experiment analysis revealed four experiments that had different issues. Experiment number one, three, and four had differing pressure conditions in the downstream air duct system so that the ventilator did not reach the targeted step values, leading to immense, incomparable ITAE-values. In addition, experiment one had OPC-server issues during the conduction of its last step experiment. Experiment number nine had a OPC-blackout during the logging of the identification experiment's validation data, which led to bizarre results. The following results analysis neglects these four experiments. Further, two experiments used different version of the algorithm, i.e. an adaption of the ventilators operation range, consequently their results are not comparable and neglected here. Thus, ten experiments remain for analysis for the here-discussed algorithm.

Figure 7.11 shows the relative deviation of ITAE-values of each step experiment towards its initial step experiment with actual PID parameters. 23 out of 23 proposed PID parameter sets provided a better control performance. Consequently, each algorithm run proposed at least one advantageous PID parameter set.

For further results for the AHU 04 exhaust pressure control loop please refer to section C.3 within the appendix.

AHU 04 supply pressure

The supply pressure control loop of AHU 04 served for 21 experiments – four experiments for code development, nine unsuccessful experiments, please refer to D, and eight successfully conduced

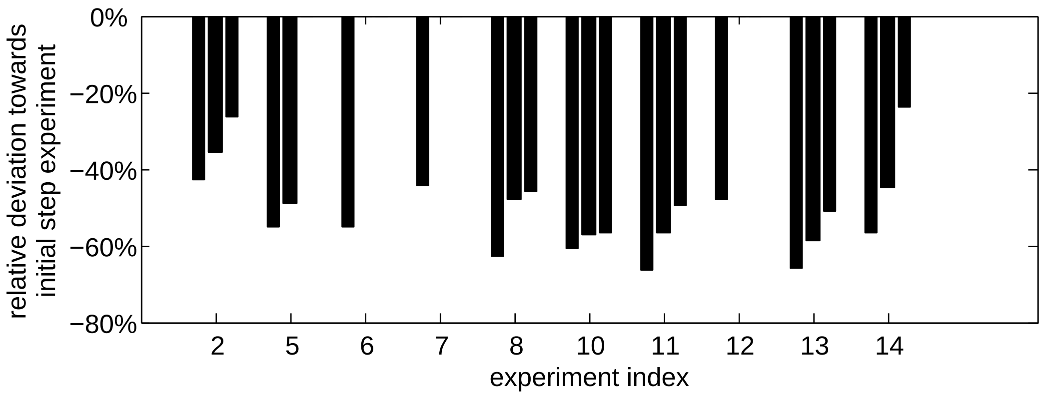

Figure 7.11: AHU 04 exhaust pressure: relative ITAE deviation for each experiment

Table 7.12: AHU 04 supply pressure: experiment configurations

Exp.	STW	STR	MMO	MDO	IDT	MAE	ID	mean	ampl.	shape	Ste.
-	in s	in s	-	-	in s	-	-	in % or Pa		-	-
1	10	1	8	8	20520	2052	CL	145	110	1/f	1
2	10	1	3	3	7200	720	OL	60	60	rbs	2
3	10	1	3	3	3900	390	OL	60	60	rbs	3
4	10	1	3	3	6660	666	OL	60	60	rbs	3
5	10	1	3	3	6660	666	OL	60	60	step	3
6	20	1	2	2	7640	382	OL	60	60	1/f	4
7	20	1	2	2	7640	382	CL	100	100	1/f	4
8	30	15	6	6	2940	98	OL	65	70	1/f	5

experiments. These eight experiments used five differently configured steps and conducted 34 step experiments. The experiment configurations and the step configurations provide table 7.12 and table 7.13 respectively[8].

Experiment number two had plant faults insofar that the ventilator did not reach the step value. Experiment number three had a malfunctioning of the pressure sensor in a way that it did measure values more than as triple as high as expected. The sensor had to be maintained after that experiment. Six experiments remain for quantitative analysis.

As figure 7.12 shows, the algorithm was able to find PID parameter sets achieving lower ITAE-values in three out of six runs. Two out of 20 investigated step responses showed an oscillating behavior, see experiment one in figure 7.12, and six proposals ameliorated the ITAE-control performance.

[8]The different step settling values and step heights within the step configurations one to three are due to differing conditions of the downstream air duct system.

Table 7.13: AHU 04 supply pressure: step configurations

Step	Settling time$_i$	Step length	Settling value	Step value	Number of executions
1	360	360	100	250	6
2	360	360	200	250	4
3	360	360	60	85	12
4	1200	400	60	85	8
5	1200	900	30	70	4

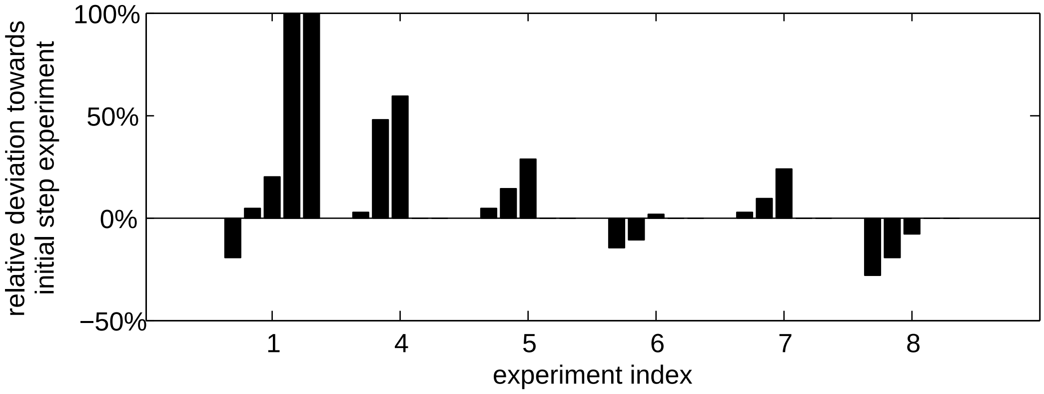

Figure 7.12: AHU 04 supply pressure: relative ITAE deviation for each experiment

7.1.2 Two-way-valve air temperature control over heat exchanger(w/a)

128 experiment focused on tuning two-way-valve air temperature over heat exchanger from water to air control loops. 49 had to be neglected due to a methodological fault[9] and again 49 had to be neglected due to operation conditions heavily disturbed by laboratory users. 16 investigated experiments provided evaluable results. Ten experiments, 63 %, ameliorated the control performance and 25 out of 50, 50 %, proposed PID-parameter sets reached advantageous control performance.

[9]Within the early experiments I made a methodological mistake which I denote as the "system-zero methodological fault". At an early stage, the algorithm worked only correctly for systems that have a system output of zero when facing a system input of zero. This does apply for e.g. pressure control but not for e.g. a cooling coil. The former algorithm identified models with de-trended input-output-data (IO-data), which is suitable for sheer parameter calculation but not for simulation and comparison of simulated step responses as this thesis proposes. For such systems, I developed a procedure to adjust the "system-zero", which is the system output at zero system input. The user can choose between setting a "system-zero" parameter, conducting a "system-zero" experiment, or just taking the minimum value of the identification data. For negatively transferring control loops this applies vice-versa. The system-zero-conditions are added or subtracted from the IO-data and re-added or re-subtracted after system simulation before the simulation step response comparisons.

Table 7.14: AHU 04 cooling: experiment configurations

Exp.	STW	STR	MMO	MDO	IDT	MAE	ID	mean	ampl.	shape	Ste.
-	in s	in s	-	-	in s	-	-	in % or °C		-	-
0	100	5	2	3	8040	80.4	CL	18	2	1/f	1
0	100	5	2	3	8040	80.4	CL	18	2	1/f	1
0	100	5	6	6	8040	80.4	CL	19	2	1/f	2
0	100	15	6	6	6840	68.4	OL	50	100	1/f	2
0	100	15	6	6	8040	80.40	CL	17	6	1/f	1

Table 7.15: AHU 04 cooling: step configurations

Step	Settling time$_i$	Step length	Settling value	Step value	Number of executions
1	1800 s	1800 s	18 °C	16 °C	12
2	1800 s	1800 s	19 °C	17 °C	8

AHU 04 water air heat exchanger for cooling

The two-way-valve water-air heat exchanger for thr supply air temperature cooling control loop "AHU 04" serves for 64 experiments. 20 here-neglegted experiments did not take into account the overall operation conditions of the AHU 04, which supplies test benches and laboratories.[10] 44 experiments used the algorithm's set-experiment-conditions functionality, see last paragraph in section 6.1. Additionally the experiment execution times were set outside the operation hours or in coordination with the test bench operators and laboratory users. Thus, for these 44 experiments, detailed information about and security of the operation conditions is available.

34 are neglected due to methodological faults. Two out of the ten remaining experiments used a different optimization strategy in order to test the algorithm's functionality to include flexible optimization functions as linear combination out of different integral criteria. The experiments where successful, but, as this changes the result's comparability, these experiments are neglected within this analysis. During the execution of the remaining eight experiment, three faults occurred, refer to D within the appendix. Finally, this chapter analyzes five experiments.

Table 7.1.2 shows the configuration of the input variable of each experiment and table 7.15 shows the experiments' step configurations. The five experiments conducted in total 20 step experiments.

Out of these 20 step experiments, 15 experiments investigated PID-parameter proposals, where ten proposals ameliorated the calculated initial ITAE-value. At least one proposal ameliorated per experiment, thus, all experiment have been successfully improving control quality.

[10] Due to its use, the operation conditions change with various impacts on the experiments. They provided some stable control loops. Still, their results are not as comparable as experiments with almost-equal operation conditions. The online documentation includes these experiments for further investigation but this thesis neglects them for analysis.

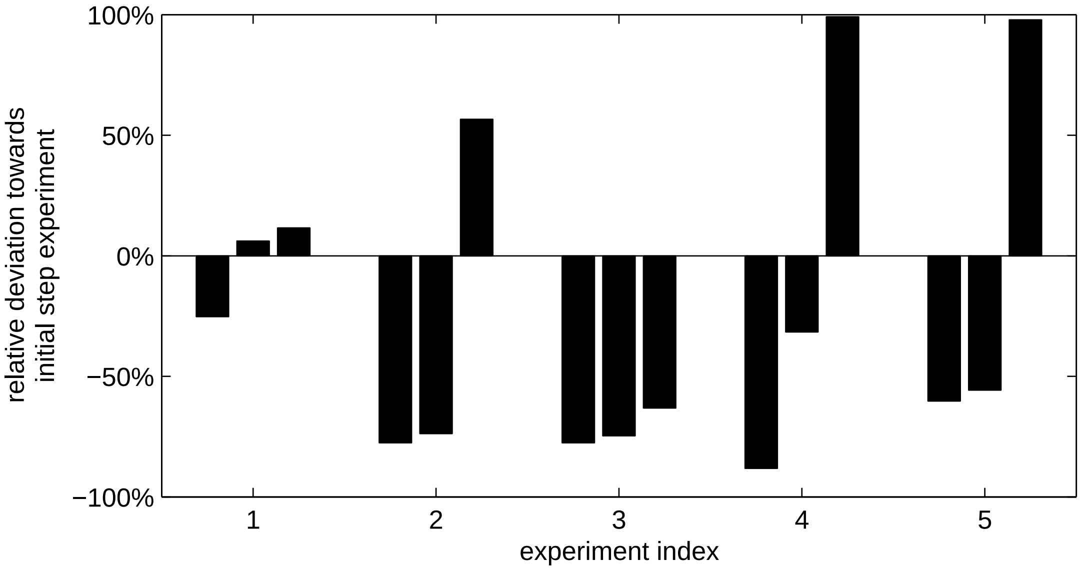

Figure 7.13: AHU 04 cooling: relative ITAE deviation for each experiment

Going deeper into detail obviates that within experiment number three, the initial step experiment was not settled before the step. This lowered ITAE value of the initial control quality evaluation, meaning the results shown underestimate the control quality of the proposals. Within experiment four, the step experiment's configuration did not match with the ambient operation conditions. The settling value was 19 °C, but it was impossible for the system to reach this value. This affects just the absolute values, the relative values are still comparable, since all faced approximately the same ambient conditions – despite step number three of experiment four, which had an OPC issue and outreaches the 100 % y-axes' limit in figure 7.13.

AHU 04 water air heat exchanger for re-heating

The two-way-valve controlled water-air heat exchanger of AHU 04 served for 37 experiments, whereas 15 experiments had uncertain operation conditions, eight experiments had methodological faults, two experiments used a different optimization function, and three algorithm runs did not finish to various reasons, see section D within the appendix. The nine remaining experiments conducted 39 step experiments using two step configurations.

During the conduction of experiment number three, a plant fault occurred insofar that no heat was provided by the supply system, compare figure C.14 within the appendix. Consequently, Figure 7.14 does not include its results.

Figure 7.14 presents the relative ITAE-value deviations of all step experiments towards their respec-

Table 7.16: AHU 04 re-heater: experiment configurations

Exp.	STW	STR	MMO	MDO	IDT	MAE	ID	mean	ampl.	shape	Ste.
-	in s	in s	-	-	in s	-	-	in % or °C		-	-
1	200	1	2	4	16340	81.7	OL	35	50	1/f	1
2	200	1	2	4	9240	46.2	OL	35	50	1/f	2
3	100	5	2	3	15240	152.4	OL	35	50	1/f	1
4	150	60	2	3	5040	33.6	OL	60	80	1/f	1
5	150	45	6	6	8040	53.6	OL	50	100	1/f	1
6	150	45	6	6	4440	29.6	OL	50	100	1/f	1
7	100	15	8	6	8040	80.4	CL	25	10	1/f	1
8	100	15	6	6	8040	80.4	CL	25	10	1/f	1
9	50	5	8	6	28440	568.8	OL	50	100	1/f	1

Table 7.17: AHU 04 re-heater: step configurations

Step	Settling time_i	Step length	Settling value	Step value	Number of executions
2	1800 s	1800 s	20 °C	24 °C	9
2	2400 s	1800 s	20 °C	24 °C	6
3	2400 s	1800 s	20 °C	25 °C	24

tive initial step experiment. 14 out of 27 experiments led to lower ITAE-values. Five out of nine experiments led to at least one advantageous configuration.

Throughout all experiments, the initial step experiments showed oscillating behavior. Only six PID-parameter proposals provided a stable control behavior. Despite sometimes ameliorating, the other proposals had oscillating behavior.

An investigation of the system characteristics yields an explanation: the control loop is able to reach temperatures between the inlet temperature, which differs due to AHU 04's operation and ambient conditions, and temperatures up to 70 °C · In contrast, the operation range, meaning the desired temperature range, is in the frame between 20 and 30 °C · Hence, the desired operation range is just a small part of the possible operation range. Further, the system has large dead times and some hysteresis. For further discussion refer to chapter 8, subsection 8.1.2.

AHU 04 water air heat exchanger for pre-heating

This air-preheating heat exchanger controlled by a two-way-valve on the water side served for 27 experiments, whereas for 14 experiment have undefined operation conditions, seven contained methodological faults. From the six remaining experiments, four did not finish, refer to section D within the appendix. Table 7.1.2 shows the two experiments, that remain for analysis. These

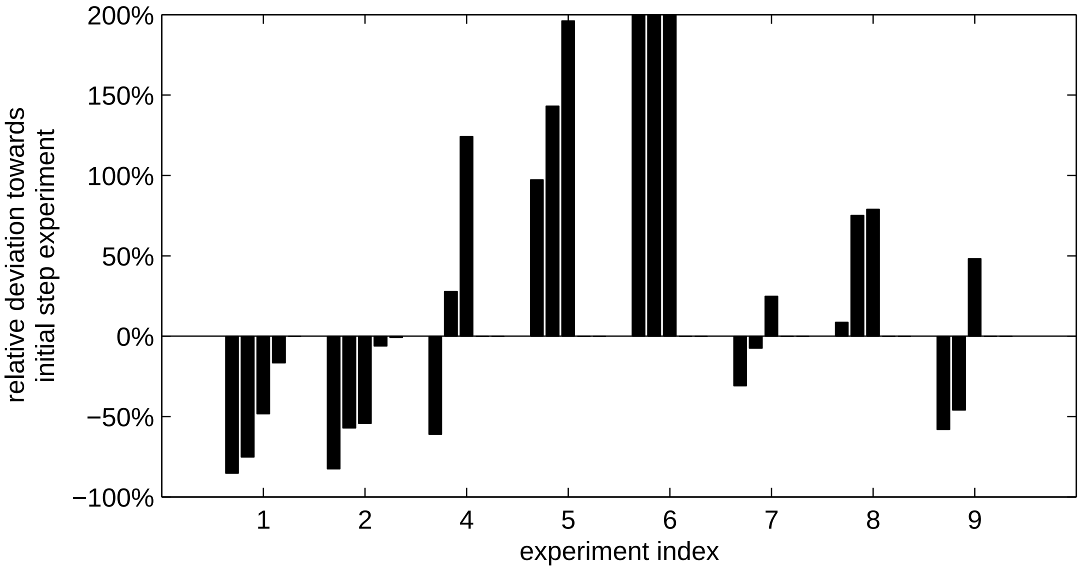

Figure 7.14: AHU 04 re-heater: relative ITAE deviation for each experiment

Table 7.18: AHU 04 pre-heater: experiment configurations

Exp.	STW	STR	MMO	MDO	IDT	MAE	ID	mean	ampl.	shape	Ste.
-	in s	in s	-	-	in s	-	-	in % or °C		-	-
1	150	45	6	6	5040	33.6	OL	50	100	1/f	1
2	150	45	6	6	8040	53.6	OL	50	100	1/f	1

experiments conducted eight steps with one step configuration, which is exactly the same as step configuration three for the re-heater, please refer to table 7.17.

This system has the same issue towards control-ability[11] as AHU 04's re-heater, but, in contrast to the re-heater, initial control parameters that yield far lower ITEA-values. With the given configurations, the algorithm provided not one single PID-configration that hat stable operation conditions, neither it ameliorated the control performance. Six out of six proposed parameter sets had higher ITAE-values. Two out of two runs did not improve the control loop.

7.1.3 Two-way-valve supply temperature control over heat exchanger (w/w)

Two-way heat exchanger H061 heating

This two-way-valve controls the supply temperature for a heating system hydraulically decoupled via a water-water (w/w) heat exchanger. It served for 20 algorithm runs. During nine runs, the algo-

[11] For further discussion of the issue on control-ability refer to chapter 8, subsection 8.1.2.

Table 7.19: H061 heating: experiment configurations

Exp.	STW	STR	MMO	MDO	IDT	MAE	ID	mean	ampl.	shape	Ste.
-	in s	in s	-	-	in s	-	-	in % or °C		-	-
1	300	60	6	6	8040	26.8	OL	42.5	75	1/f	1
2	100	15	6	6	6840	68.40	CL	25	8	1/f	2
3	100	15	8	3	6840	68.40	CL	27	8	1/f	3

Table 7.20: H061 heating: step configurations

Step	Settling time$_i$	Step length	Settling value	Step value	Number of executions
1	1200 s	1200 s	22 °C	24 °C	4
2	1800 s	1800 s	23 °C	25 °C	4
3	1800 s	1800 s	26 °C	29 °C	6

rithm had methodological faults. Thereafter, nine experiment did not provide comparable results. These nine experiments have been excluded. Further, eight experiment runs did not finish due to various faults, refer to section D within the appendix. Finally, three experiments using three step configurations remain for analysis.

Experiment number one and experiment number two are not quantitively compareable due to configurations of the step experiments, for more details please refer to C.6 on page 147 within the appendix.

Experiment number three, "H061 Supply Temp Heating 2015-09-16 11h45" lead to comparable results: compared to the initial step response, the algorithm provided immense amelioration of the ITAE value between -90.23 % and -77.39 %.

Depending on the step configuration and in the case of comparable results (one out of three investigated runs), the algorithm led to very high performance amelioration. Five out of five PID-parameter proposals provided advantageous control quality.

7.1.4 Three-way-valve temperature control

The algorithm tuned two different three-way-valve control loops in 14 runs, whereby four experiments are evaluable. Three of them, 75 %, were successful in terms of improving ITAE control performance. Eight out of twelve proposals, 67 % reached lower ITAE values that their respective evaluation reference.

Table 7.21: H061 cooling: experiment configurations

Exp.	STW	STR	MMO	MDO	IDT	MAE	ID	mean	ampl.	shape	Ste.
-	in s	in s	-	-	in s	-	-	in %		-	-
1	300	60	6	6	8580	26.8	OL	45	45	1/f	1
2	200	15	6	6	7740	38.7	OL	55	90	1/f	2

Table 7.22: H061 cooling: step configurations

Step	Settling time$_i$	Step length	Settling value	Step value	Number of executions
1	1200 s	1200 s	22 °C	18 °C	4
2	1800 s	1800 s	21 °C	18 °C	4

Three-way-valve H061 cooling

This temperature-controlling three-way-valve served for five algorithm runs and for various experiments for a first proof of concept within a manual conduction of control tuning with classical control tuning rules, compare Fütterer et al. [2014]. In five algorithm runs, three runs did not finished and two remain for quantitative analysis.

Fütterer et al. [2014] showed that these kinds of systems are improvable by manual tuning, applying classical control heuristics. Further, that the integral criteria suffer significance within these relatively heavy-disturbed systems[12], since e.g. ITAE-values are very dependent on disturbances. This makes an visual investigation of step responses necessary.

Experiment number one, "H061 Supply Temp Cooling 2015-09-07 12h10", having a system-zero manually set to 25 °C , provided two out of three times lower ITAE-values. The best step experiment improved the ITAE value by -84.20 % with an aggressive but stable control behavior. The other two PID-parameter sets provided oscillations during their step experiments.

Experiment number two, "H061 SupplyTempCooling 2015-09-10 11h00", having a measured system-zero with 900 s measurement time at 22. °C , provided sluggish control performance within all three proposed PID-parameter sets.

Within two experiments, one experiment provided better control performance. Within six PID-parameter proposals, two provided lower ITAE-values.

[12]In the scope of this thesis, the disturbance impact is considered high or heavy, when the disturbance impact on the system output is larger than or equal to 50 % of the regular system input's impact on the system output. A light disturbance has impacts below 5 %.

Table 7.23: K08Y02 cooling: experiment configurations

Exp.	STW	STR	MMO	MDO	IDT	MAE	ID	mean	ampl.	shape	Ste.
-	in s	in s	-	-	in s	-	-	in %		-	-
1	60	15	6	6	2640	44	OL	50	100	1/f	1
2	300	60	6	6	8040	26,8	OL	50	100	1/f	2

Table 7.24: K08Y02 cooling: step configurations

Step	Settling time$_i$	Step length	Settling value	Step value	Number of executions
1	1200 s	1200 s	14.5 °C	12.5 °C	4
2	1800 s	1800 s	14.5 °C	12.5 °C	4

Three-way-valve K08Y02

The cooling supply temperature controlling valve K08Y02 served for nine experiments in total. Four had methodological faults, three did not finish, see D, fault documentation within the appendix, and two experiments remain for quantitative analysis. The before-mentioned aspect of heavy-disturbances also account for this control loop, which makes a visual investigation of the step responses necessary. Please refer to section C.4 within the appendix for further results and figures.

On an ITAE basis, both experiments led to amelioration from -21.05 % up to -54.92 %. All step experiments had better control quality than the initial steps and, accordingly, both experiments led to better control behavior.

7.1.5 Room temperature control

The algorithm tried and tuned five room temperature control systems. All rooms had plant faults insofar as the controlling devices were not to able influence the rooms' temperature. No room model was identified. In order to visualize that control behavior, figure C.15 and figure C.16 within the appendix show step responses, one of the EBC laboratory and another of the FCN CIP pool.

As the figures show, there is no relatable influence by the set point towards the room temperature, these systems have to be considered as plant faults. Thus, they are not tune-able by this algorithm and, further, not PID-controllable. This accounts for all investigated rooms within the demonstration bench. Consequently, these systems are not included within the following result summary and the overall algorithm evaluation but discussed in section 8.1.2.

The algorithm was not able to tune any out of five investigated systems.

Table 7.25: Aggregated results

system type	evaluable experiments	successful experiments		proposals	ameliorating proposals	
AHU air pressure	39	27	69 %	127	60	47 %
three-way-valve flow temperature	4	3	75 %	12	8	67 %
two-way-valve air temperature	16	10	63 %	50	24	48 %
two-way-valve flow temperature over heat exchanger	1	1	100 %	5	5	100 %
Aggregation	69	41	68 %	194	97	50 %

7.2 Tuning results summary

The proposed method ran 396 times in seven different types of control loops using 14 different controlled systems. 89 runs were conducted in order to ameliorate the method as well as the implemented code. Since user interacted with control loops, especially for control loops within AHU 04, the operation conditions became unclear which made the results not reliably evaluable[13]. 49 experiments had to be neglected due to this reason. Another 62 algorithm runs included methodological faults and seven were used to test the possibilities to variate the optimization function. These variations led to different results, e.g. shorter rise times or no overshoots depending on the weights of the optimization function. Within this result presentation, these runs are neglected for comparability reasons. Finally, 86 algorithm runs aborted due to various reasons, see D within the appendix.

I investigated 103 algorithm runs in detail, as described in the previous section 7.1, out of which 89 experiments were quantitatively evaluable. 20 algorithm runs investigated different communication infrastructures, as presented in the following chapter, see section 7.3. As conducted within the standard communication infrastructure, 69 algorithm run are quantitatively comparable.

As table 7.25 shows, the algorithm worked successful for three way-valve flow temperature (75 %), air pressure loops (69 %), and two-way-valve air temperature loops (63 %). In total, out of 69 experiments, 41, 68 % were successful.

[13]The user interaction was mainly changing pressure and, consequently, flow conditions in downstream air duct systems while connecting and disconnecting test benches in laboratories.

7.3 Results of the communication infrastructure variation

In the following, the results of the variation of the communication infrastructure are presented. For all control systems within the communication infrastructure study, it has to be regarded that these systems were not auto-tuned by the JCI PRAC algortihm but the JCI standard parameters have been used[14].

7.3.1 Three-way-valve volume flow control - user-added monitoring

Three-way-valve volume flow control H061 Y01

The inlet-volume-flow-controlling three-way-valve H061 Y01 served for 20 experiments, whereas eleven experiment failed for different reasons and nine experiments remain for analysis[15]. The nine experiment used six different step configurations and conducted 36 step experiments, which are presented in table C.5 and table C.6, both attached to the appendix. Experiment number three had OPC issues and is neglected in the following.

The results are severe: First, for shorter settling times and step lengths, the initial control loop did not settle. For experiment number six, it cannot be evaluated whether the initial step settles during the step length. Consequently, both times were again extended, see step configuration 5 and 6. Within experiment number 7, the initial step experiment showed oscillations, within 8 the system showed no reaction, and, within 9, the experiment overshoots, undershoots and maybe rests with an permanent deviation or remains oscillating. Thus, the experiments' time configurations were still to short.

For experiments 6, 7, 8, and 9, all 13 proposed parameter sets showed strong oscillating behavior. For experiments 1 to 5, the control behavior cannot be evaluated due to too short step lengths.

Out of nine experiment, no experiment was identified that ameliorated the control behavior. Further, no reliable-stable PID-parameter configuration is identifiable.

[14]For controlled systems having standard communication infrastructure presented in the previous sections, the reference cases were three-month-auto-tuned PID parameters. The infrastructure was varied and implemented within the real-life demonstration building. Still, its BES needs to fulfill the e.g. comfort needs at any time, this there was no time for conducting auto-tuning. Nevertheless, using PID standard parameters is a common approach amongst practitiones, refer to Fütterer et al. [2015].

[15]Experiments one to six used a different optimization function. Nevertheless, the results are analyzed, since other system-specific characteristics overcompensates the impact of the slightly different optimization function.

7.3.2 Two-way-valve volume flow control - user-added monitoring

Two-way-valve volume flow control H061 Y02

Conducted experiment conditions and steps are presented in tables C.7 and C.8 within the appendix, see page 150. The results are as severe as for control loop H061 Y02. Likewise, for shorter settling times and step lengths the initial step experiment did not settle. For step configurations 4 and 6, they were oscillating during settling at the settling value and during settling at the step value. Moreover, for experiments 1 to 7, the control behavior cannot be reliably described due to wrong step configurations. For experiments 8 to 12, no experiment configuration found any stable PID-parameter configuration.

None of the 39 conducted step experiments provided usable configurations, non of the twelve experiment runs provided an amelioration of the initial control performance.

7.3.3 Two-way-valve volume flow control - BACnet 3rd party control integration

Two control loops with this specification are investigated for tuning within 23 experiments that provided eight evaluable results. 50 %, four out of eight experiments improved the control performance. Seven out of 28 proposals were advantageous.

Two-way-valve volume flow control Z022 S0020

This two-way-valve volume flow control loop served for ten experiments, whereas two experiments used a different optimization function and one experiment did not finish. Thus, seven experiments conducting 29 step experiments with three different step configurations remain for analysis. Experiment and step configuration are presented within table C.9 and C.10, both attached to the appendix, see page 150.

Compared to the volume flow control systems H061 Y01 and H061 Y02 the observed control quality for Z022 S0020 is more suitable for investigation. Figure 7.15 shows the relative deviations of ITAE for each PID-parameter proposal compared to the respective initial step experiment.

Experiment 1 has an initial step experiment that shows a sluggish behavior with deviation. All proposed parameters for this system have oscillating step responses. Experiment 2 is neglected within the figure, since all step responses for proposed parameters failed insofar as no volume flow was recorded. The settling of initial step experiment was oscillating, the step itself was stable but had deviation. Experiment number 3 had an initial step experiment that was sluggish with deviation. The steps for proposals were all stable after a few oscillations but showed deviations. Still, an amelioration of control quality can be stated. Experiment 4 showed an very sluggish initial step experiment

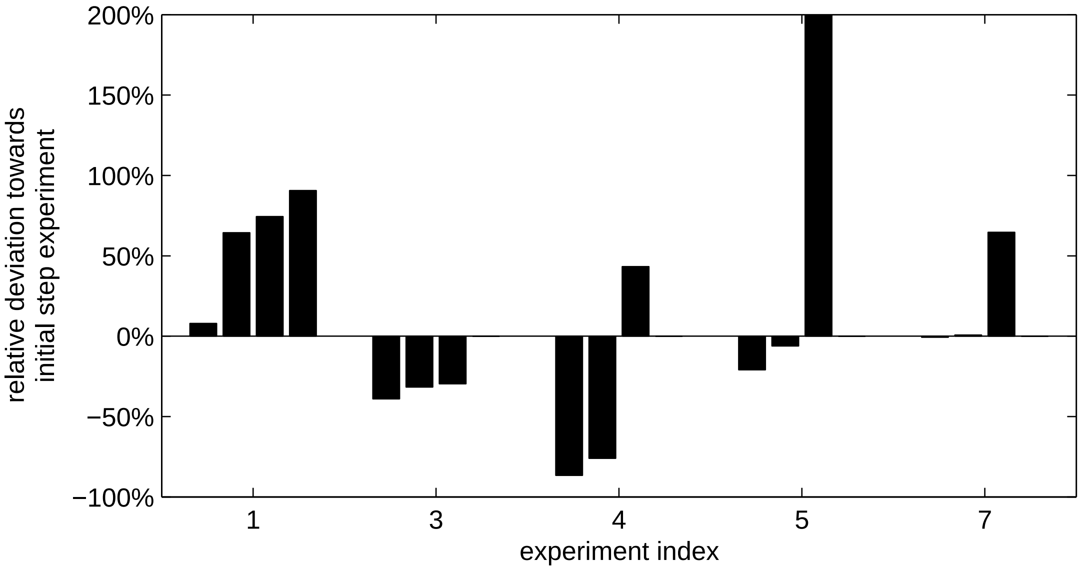

Figure 7.15: Z022S0020 Volume flow: relative ITAE deviation for each experiment

with strong deviation. Two proposals behaved clearly advantageous but still oscillating. The other proposal showed no volume flow. Within experiment 5, the initial step experiment had a sluggish settling and an oscillating step. Two better and one worse control proposals were identified. Experiment 6 had an initial step experiment which was oscillating towards settling and during its step. Unfortunately all proposed parameters failed or had plant faults. Experiment 7's initial step experiment was oscillating during settling and stable but strong deviating during the step, its proposals oscillated during settling but provided two times a stable with slightly no quantitative difference regarding the ITAE-value and one time first stable and then then oscillating behavior.

Considering this, five out of 22 proposed PID-parameter sets are considered as advantageous. The algorithm was able to ameliorate the control behavior of this control loop in three out of seven experiments.

Two-way-valve volume flow control Z022 S0021

13 experiments tried to tune this control loop. Two of them had a different optimization function and eight algorithm runs did not finished due to OPC-problems, refer to section D. Experiment and step configuration are presented within table C.11 and C.12, both attached to the appendix, see page 151.

Due to the heavy OPC-problems with certain data points the data basis is rare and various experiments are missing. Still, and as the control system's structure is exactly the same, the results indicate

Table 7.26: Aggregated results

system type	evaluable experiments	successful experiments		proposals	ameliorating proposals	
three-way-valve volume flow control com inf 1	9	0	0	36	0	0
two-way-valve volume flow control com inf 1	12	0	0	39	0	0
two-way-valve volume flow control com inf 2	8	4	50 %	28	7	25 %
Aggregation	29	4	14 %	103	7	7 %

the same behavior as that of Z022 S0021. Experiment one had a very sluggish initial step experiment, while one experiment for proposed PID-parameters oscillated permanently and the other two oscillated during settling but reached stability at the step value. Experiment number two had a stable and non-deviating step experiment. The algorithm degraded this control performance with all three proposals, as all of them were oscillation during settling and at the settling value. Still, two out of three reached stable conditions at the step value.

One out of two experiments was able to ameliorate the initial situation. Two out of six proposed parameter sets provided better control behavior.

7.3.4 Summary of results of communication infrastructure variation

In total, out of 29 experiments, four, 14 % were successful, see table 7.26. The algorithm achieved worse results using communication infrastructure one, user-added monitoring system, in comparison to communmication infrastructure two, BACnet 3^{rd} party control, refer to section 8.1.6 on page 113 for further discussion.

8 Discussion

8.1 General issues

8.1.1 When to tune

The first question is when to tune a control loop. Of course every tuning should be conducted during an operation-like system status. An optimal tuning is only possible during full operation. Still, it is not possible to tune every control loop during real, every-day operation, since e.g. thermal comfort and other system services as well as system conditions that may affect the system operation do change during tuning. The algorithm's user has to find a trade-off between maintaining desired services and optimal tuning conditions. The first best solution would be a tuning during the taking-into-operation-phase of a building. Second best solution would be to tune during full operation even though services would be affected. Thereby, users play an important role, as they can make identification impossible due to overruling identification signals as happened in AHU 04 re-heater experiment number four, refer to figure C.14 within the appendix on page 153.

8.1.2 Control-ability

The algorithm only achieves satisfying results, if the system is generally PID-control-able. This does not apply to all PID-control loops as the results show. A system is not PID-control-able, if the system does have any plant faults, e.g. like being out of order due to a device malfunctioning and if the control loop is unable to reach given set points. This low control authority occurred e.g. in room temperature control loops in the demonstration building, e.g. refer to figure C.15 on page 154. Hysteresis occurs in various building control loops, which affected the control loops' behavior. Further, the question if hysteretic control loops should be PID controlled is valid. Further, large dead time negatively influence the achieved control quality, as e.g. the experiments for the AHU 04 re-heater indicate, refer subsection 7.1.2 on page 101. Finally, the communication architecture (e.g. elements of a control loop distributed over different BACnet-devices or further external systems, as the previously introduced user-added monitoring system) affects the PID-control-ability and, thus, the success of the proposed tuning algorithm, please refer to the unsuccessful experiments under control infrastructure one in table 7.25 on page 106.

Based on the results of the demonstration case, there is a need for control fault detection. Therefore, I implemented and successfully tested the control fault detection algorithm proposed by Salsbury [1999]. Due to the thesis' scope I did not implement it in the final algorithm which has to be regarded before turning the proposal into a product.

8.1.3 Disturbances

The experiments unveiled that the two different types of disturbances, physical disturbances, such as oscillating system supply temperatures, changing ambient conditions, etc., and system-caused disturbances, such as sensor oscillations, communication noise, ICT-system-inherent time lags, etc. should be handled with different approaches. Experiments were successful when handling the physical disturbance as a disturbance to be identified in the system identification with disturbance-respecting model structures, and, using a filter for system-caused disturbances. In general, system-caused disturbances have higher frequencies, which makes filtering an efficient method to deal with them.

Moreover, an algorithm user has to investigate and evaluate the influence of physical disturbances towards superior control and towards the supply system, since this might change the whole system operation and thus the experiment conditions. E.g. a falling ambient temperature can switch the supplying system's operation mode, where the supply temperature changes from a stable value to an oscillating behavior. Further, the user has to consider the controlled systems' supervisory control level, that may enable and disable controllers due to disturbances.

Operating ranges of a controlled system depend on external conditions, especially for long-lasting experiments, e.g. the outside air temperature. It is not safely possible to predict external conditions for the entire duration of the experiment; the fact that the start time of the experiments' setup is not the same as the start time for the experiments enforces this challenge. This is a quite common situation since the experiment's execution normally takes place outside of building's operation times. If not predictable, a solution for control influencing disturbance handling is switching to open loop.

Within the simulation study, the algorithm itself proved that it is capable of dealing with different kinds of disturbances, either by using low-pass filtering or by increasing model orders.

8.1.4 Operation mode change due to set point signal

While shaping an excitation signal within a certain set point range, the limits of the aimed operation mode can be reached. A deactivation of the investigated control loop could follow. Therefore, the values for amplitude of the set point signal have to be chosen with respect to the limits of the supervisory operation mode in order to prevent such a deactivation of the controller during the experiment.

8.1.5 Data security

Data security becomes more and more relevant in recent times. I experienced this by trying and implementing monitoring systems within BACS and by convincing ICT-staff to approve the connection of building automation networks (BAN) to the internet.

This algorithm is designed to be operated with higher computational power than available in state-of-the-art programmable logic controllers. Thus, it needs either a cloud infrastructure and a BAN connected to the internet or an industrial computer attached to the BAN. The algorithm would work in both cases, while a cloud-based solution is the preferred alternative due to the scalability of computational resources.

8.1.6 Communication infrastructures

The algorithm did not propose any PID-paremeter sets that ameliorated the control performance of systems under communication infrastructure with user-added monitoring. That indicates, that the additional time offsets are too big for the used approach. The algorithm is not able to tune theses systems. Thus, when retrofit sensor equipment is to be used for control system extension as a direct integration into PID-control loops with an automated tuning using the proposed algorithm, it is crucial to minimize these time offsets and the additional measurement noise.

For an external BACnet component control infrastructure the results are ambiguous. Thus, it is worth trying to auto-tune such control systems with the proposed method. Nevertheless, a manual result verification remains necessary.

When putting the results into a larger scope, it is vaguely to conclude, that fast control loops should be directly controlled within their native control environment. Direct fast cloud control or further thinkable innovative control approaches and strategies, like e.g. agent based control, might need high-performance communication.

8.2 Configuring the algorithm

Having the above-mentioned issues considered, the algorithm's configuration is the most important influencing factor for the tuning results. At the same time it is the most complex issue, since the algorithm has, as mentioned before, 614432 possible input variations.

8.2.1 Shaping the excitation signal

As already mentioned in the section on system identification, compare section 2.7, the shaping of the excitation signal has enormous influence on the controlled system's identification. From theory, it was derived that power and exciation times should be as high as possible, which was easy to accomplish for the signal's power. Still, identification experiments' time remains a trade-off.

In general, the excitation signal can produce controlled system outputs that focus more on the system's transition states or that focus more on the system's steady states at the set operation ranges. This accounts likewise for open and closed loop excitation. A transition-focused excitation signal leads to an identified system model, that under-estimates the process gain but has more precision within the transition ranges. The consequence is an aggressively tuned control loop.

Likewise, a more steady-state focused excitation leads to a robustly tuned control loop. Different algorithm inputs as writing sampling time, the operation ranges in closed and open loop, and the signal type, shape this excitation signal. Considering the experimental results and in line with the simulative study, the tuning proposals are better if the excitation signal is well distributed over transition and steady states.

Within the recent literature and as described in section 2.7, multi-identification-experiments should be done for system identification needs that exceed three decades of time constants. In general, the considered controlled systems do not have such broad frequency ranges of interest. Despite of the latter and since results shows satisfying identification results in terms of the identification for control methodology, there is no need for multiple identification experiments among the considered controlled systems.

8.2.2 Sampling time write

The sampling time write defines the minimal allowed time between two single changes in the excitation signal. The plants' states should be equally distributed to guarantee an identification that does neither under nor overestimate the system's gains. If the sampling time is shorter than the major time constant of the physical controlled system, it is likely that the transition states will be overestimated. Good results indicate, as a rule of thumb, that the sampling time write should be between two and five times the mayor time constant.

8.2.3 Relative and absolute identification time

The length of the identification signal is another signal-shaping dimension. It basically aggravates imbalances towards transition or steady information due to the fact that it extends the identification data vectors while weight to one direction is not affected. Derived from the experimental and simulation results, I propose to use the theoretic maximum amount of excitation, which is the identification time divided by the sampling time write. As a rule of thumb, its value should be at least 30. Going beyond that did not significantly improve the identification results.

8.2.4 Open loop mode vs. closed loop mode

The results indicate, that closed loop excitation signals achieve better results than open loop excitation signals. Thus, a conclusion is that open loop should only be used when the system is not stable, e.g. for initial tuning. Unfortunately, this is not always possible. An initially far too conservatively, sluggishly tuned controller is a reason to switch to open-loop experiments, even if the system is stable with this controller. In this case, the controller then prohibits a sufficient excitation of the system and therefore the identification method fails. The algorithm is not able to detect such situations automatically. Hence, the user has to detect it in the resulting plots and restart the algorithm with an open-loop identification experiment. A further challenge provides the issue that, when the algorithm executes the identification experiment in closed-loop mode, it may be difficult to find appropriate values for the setup of the set point signal, since the inherent controller processes the excitation signal and the consequences are not immediately obvious. Even further, if there are disturbances and a complex supervisory control, it can be worth switching to open loop experiments.

8.2.5 Operation ranges

In general, a system has a physically available operation range and an operation range of interest for the operation of the overall system. It is possible to adjust the limits of the excitation signal over the whole (for open loop systems) or even beyond (for closed loop systems) the physical operation range of a controlled system. If chosen in such a way, the algorithm provides parameters that achieve acceptable performance over the whole operation range. If the excitation limits lie in the operation-relevant range, the algorithm provides robust performance within this operation range but may get unstable when exceeding this range. The proper choice thus depends on the user's preferences.

8.2.6 Signal types

The algorithm offers a $1/f$ frequency-shaped signal, a random binary signal (RBS) and a signal with exactly defined steps. The experimental results as well as the simulation results clearly show the superiority of the $1/f$ signal. Thus, the user should only use other signals on special purpose.

8.2.7 Shaping the identification data

After having shaped the excitation signal, the algorithm offers the possibility to process the gathered controlled system output data, the identification data, by adjusting the sampling time read and adding a low-pass filter. The input “sampling time read” defines the time between two recordings of a data point. The lower the sampling time read, the more data and the more information is available. The question is whether this additional information is improving the identification process or not. And that again depends on the relevance of information towards the physical system with respect to its mayor time constants. The information on all possible disturbances, especially white-noise-like disturbances, rises with smaller sampling-time-read-values. The results slightly indicate, that with lower sampling time read better results are achieved, which makes sense, if a filter is used that cuts off high frequencies. The main thought for setting up the sampling time read is that as many information as possible should be gathered. A suitable filter should then remove the irrelevant information in that way that high frequencies and non-physical disturbances disappear from the identification data while system inherent frequencies and physical-disturbance-caused frequencies remain. With sampling time reads towards zero, the amount of identification data goes infinite and so does computation time needed for identification. Within state-of-the-art BACS’, the minimum of sampling time read is always limited. In my case the minimum is one second.

The results show that within the practical algorithm application the minimum sampling time read of one second provides best results with an acceptable computation time. Thus, the algorithm should be set up with a small sampling time read and a low pass filter in a suitable range, which might be around four times the highest occurring system frequency.

Not all state-of-the-art buildings provide one-second-sampled monitoring data. The results with sampling time read at 15 seconds or even higher showed control quality improvements as well. Thus, the alogrithm would be suitable for system with less precise monitoring systems, too.

8.2.8 Model orders

The algorithm’s PID-parameter tuning rules base on low-order models. Thus, the algorithm reduces the model order. On the one hand, high model orders’ advantage is that they meet disturbances and noise with some frequencies, which are then neglected during the model order reduction. On the other hand, the real system behavior can be identified as part of higher orders, meaning that the system gain of the reduced model might not meet the the real system gain.

The experimental results do not indicate a clear correlation between model orders and results. Due to computational power limitation, the maximum model order used is twelve. Experiments with model order twelve were only rarely successful. Most experiments had model orders of six. Model orders of two together with a high maximal amount of excitation alternations provide generally better results than small model orders with short identification times, which lead to poor results. Contrarily, the simulation study provided the best results with model order of five and eight, compare figure 4.6 on page 57. Taking the computational effort into account a suggestion to algorithm users would be to use a model order of five together with filtering.

8.2.9 Model types and number of considered models

Depending on the input-output-data characteristics and in particular depending on the varying inherent time constants, different models lead to better identification results for different controlled systems. The algorithm faces this issue with the fact that it identifies a large number of models depending on the model orders and the disturbance orders. For the PID-parameter-calculation, the algorithm considers only an user-adjusted amount of models which it ranks using the model fit criteria. Derived from result observations it is to conclude that the more models are available, the better results are produced, but the higher is the computational effort. Amelioration approaches lie in the fact that the model fit is not the perfect criteria, as argued in section 3.4. One the one hand, there are other advantageous criteria which need higher calculation efforts, as spectral and frequency analysis. On the other hand, further research should derive a correlation between suitability of models and controlled systems, in order to use only suitable model types for the considered controlled system and thus be able to consider more relevant models. As a start, the simulation study yielded a ranking of model types for each type of controlled system but more research is necessary.

8.2.10 Choosing the control quality cost function

The algorithm's user is able to adjust the quality function so that the algorithm follows the user's preferences. E.g. for energy intensive control loops, setting a limit for the overshooting height OS can prevent too costly overshoots. Within the general scope of this thesis, I propose using ITAE as argued in section 3.2 as control quality optimization criteria. Further work can focus on an optimal combination of quality criteria for each type of control loop. The simulation study showed that no other control quality indicator was as successful as the ITAE criterion.

9 Conclusion

I developed and demonstrated an extended PID auto-tuning algorithm for HVAC systems and building energy systems using the advances in computational power in recent years that is easily applicable to all state-of-the-art building energy management systems and building automation and control systems through the use of cloud-based services and standardized communication protocols. I conducted a simulation study to investigate the main characteristics of the proposed algorithm. Its real-life demonstration took place in a multifunctional office building during full operation. I extended the building's building automation and control system with a server infrastructure as well as with a monitoring and interface system in order to enable this research.

The major contributions of this thesis are an innovative PID tuning algorithm, its general configuration suggestions for application within different types of control loops and its demonstration. Its applicability is proved and demonstrated within a simulaton study and real-life experiments.

The results for a classical real-life building automation system and different classically PID-controlled loops, show an amelioration of the tuned systems' control performance in 68 % of the algorithm's applications. The application of the algorithm leads to control quality improvements of up to 90 %, accounting for both, simulation and field study, following the integral time-weighted absolute error criterion, ITEA and in comparison to a state-of-the-art adaptive auto-tuning method.

In order to investigate the applicability of alternative control infrastructures as they might occur in future cloud-based building control systems, I implemented and tuned control loops with such control infrastructures. Their tuning was far less successful, indicating that data resolution and transmission times are important and should be regarded in future applications.

Moreover, I proposed and demonstrated a technical structure for cloud-based services for building operation optimization wtih PID control loop tuning as an use case. Finally yet importantly, I developed a demonstration bench for control research as well as a simulation framework for the same purpose.

The method, by its nature, is limited towards systems that are PID-controllable and it is limited towards plant faults. Even if the evaluation criteria are adjusted under means of robust tuning, the long-term behavior can deteriorate. Thus, the proposed method can either be periodically repeated or an adaptive extension should be integrated which would enhance the long-term control quality.

As a research perspective, the algorithm should be applied to various systems using the proposed standard configurations in order to gather data from various buildings in order to provide a standard configuration catalog for standard PID control loop types. Further, the algorithm offers many possibilities for variations within its methodological approach, e.g. application of further tuning rules, including high-order-model-based tuning rules, of physical models, of different model estimation techniques, of further excitation signals, and many more. As a further research perspective the algorithm can be combined or enhanced with adaptive approaches.

The algorithm should be offered as a cloud-based, platform-based service product in order to provide an easy taking-into-operation of HVAC systems, to provide a standardized certification and evaluation method of PID control loops in buildings, and to ameliorate performance of PID control loops in existing buildings.

Bibliography

Abel, D. (2009). *Umdruck zur Vorlesung Regelungstechnik und Ergänzungen (Höhere Regelungstechnik) - Lecture notes towards automatic control*. Verlagshaus Mainz, Aachen, 33. aufl edition.

Afram, A. and Janabi-Sharifi, F. (2014). Theory and applications of hvac control systems – a review of model predictive control (mpc). *Building and Environment*, 72:343–355.

Agüero, J. C., Goodwin, G. C., and Van Den Hof, Paul M.J. (2011). A virtual closed loop method for closed loop identification. *Automatica*, 47(8):1626–1637.

Anderson, M., Buehner, M., Young, P., Hittle, D., Anderson, C., Tu, J., and Hodgson, D. (2007). An experimental system for advanced heating, ventilating and air conditioning (hvac) control. *Energy and Buildings*, 39(2):136–147.

ASHRAE (2012). Bacnet: A data communication protocol for building automation and control networks.

Åström, K. J. (1980). Maximum likelihood and prediction error methods. *Automatica*, 16(5):551–574.

Åström, K. J. and Hägglund, T. (1995). *PID controllers: [theory, design, and tuning]*. Instrument Society of America, Research Triangle Park, NC, 2. ed edition.

Åström, K. J. and Hägglund, T. (2006). *Advanced PID control*. ISA-The Instrumentation, Systems, and Automation Society, Research Triangle Park, NC.

Åström, K. J., Hägglund, T., Hang, C. C., and Ho, W. K. (1993). Automatic tuning and adaptation for pid controllers - a survey. *Control Engineering Practice*, 1(4):699–714.

Bai, J., Wang, S., and Zhang, X. (2008). Development of an adaptive smith predictor-based self-tuning pi controller for an hvac system in a test room. *Energy and Buildings*, 40(12):2244–2252.

Bai, J. and Zhang, X. (2007). A new adaptive pi controller and its application in hvac systems. *Energy Conversion and Management*, 48(4):1043–1054.

Balow, J. (2012). *Systeme der Gebäudeautomation: Ein Handbuch zum Planen, Errichten, Nutzen ; mit CD-ROM*. Grundlagen beraten + planen. cci Dialog, Karlsruhe, 1. aufl. edition.

Bennett, S. (1996). A brief history of automatic control. *IEEE Control Systems Magazine*, 16(3):17–25.

Bertil, T., Mohsen, S.-M., and Fahlén, P. (2005). Feed-forward in temperature control of buildings. *Energy and Buildings*, 37(7):755–761.

Bi, Q., Cai, W.-J., Wang, Q.-G., Hang, C.-C., Eng-Lock Lee, Sun, Y., Liu, K.-D., Zhang, Y., and Zou, B. (2000). Advanced controller auto-tuning and its application in hvac systems. *Control Engineering Practice*, 8(6):633–644.

Bombois, X., Scorletti, G., Gevers, M., Van den Hof, P.M.J., and Hildebrand, R. (2006). Least costly identification experiment for control. *Automatica*, 42(10):1651–1662.

Brandt, S. G. (1986). Adaptive control implementation issues. In ASHRAE, editor, *ASHRAE Trans.; (United States)*, volume 92:2B. American Society of Heating, Refrigerating and Air-Conditioning Engineers.

Butterworth, S. (1930). On the theory of filter amplifiers. *Wireless Engineer*, 7.

Chen, J., Lian, Z., Tan, L., Zhu, W., and Zhang, W. (2011). Modeling and experimental research on ground-source heat pump in operation by neural network. In *2011 International Conference on Computer Distributed Control and Intelligent Environmental Monitoring (CDCIEM)*, pages 459–462.

Chien, Hrones, and Reswick (1952). On the automatic control of the generalized passive systems. *Trans. Assoc. Soc. Mech. Eng.*

Constantin, A., Fütterer, J., Streblow, R., Müller, D., and Rovas, D. (2012). Simulation assisted adaption of a model based control parameter fine-tuning methodology for a nonresidential buildings within a complex energy system. In *Proceedings of the International Symposium in Sustainable Energy in Buildings and Urban Areas.*

Copeland, B. R., Julien, R. H., and Foley, M. W. (2010). Proportional-integral-derivative lambda-tuning for integrating processes with deadtime. *IET Control Theory & Applications*, 4(3):425–436.

Dexter, A. L., Geng, G., and Haves, P. (1990). The application of self-tuning pid control to hvac systems. In *Control in Building Energy Management Systems, IEE Colloquium on*, page 4/1.

DIN German Institute for Standardization (2007-11). Firmenneutrale datenkommunikation für die gebäudeautomation und gebäudemanagement - gebäudedatennetzprotokoll.

Dounis, A. I. and Caraiscos, C. (2009). Advanced control systems engineering for energy and comfort management in a building environment—a review. *Renewable and Sustainable Energy Reviews*, 13(6-7):1246–1261.

Erbe, H.-H., K., E., and I., T. (2006). Control performance assessment for building automation systems. In *Energy Saving Control*, IFAC proceedings volumes, pages 7–18. IFAC, Elsevier.

European Committee for Standardization (12.2008). Control for heating, ventilating and air-conditioning applications — electronic individual zone control equipment.

Felsmann, C. and Knabe, G. (2002). Test von reglern für fußbodenheizungen. *HLH. Heizung, Lüftung/Klima, Haustechnik*, 53; Jg. 2002(8):75–82.

Forssell, U. (1999). *Closed-loop identification: Methods, theory, and applications*, volume 566 of *Linköping studies in science and technology Dissertation*. Univ, Linköping.

Forssell, U. and Ljung, L. (1999). Closed-loop identification revisited. *Automatica*, 35(7):1215–1241.

Fuchs, M., Constantin, A., Lauster, M., Remmen, P., Streblow, R., and Müller, D. (2015). Structuring the building performance modelica library aixlib for open collaborative development. In *Proceedings of the 14th International Conference of the International Building Performance Simulation Association*.

Fütterer, J. (2014). A practical view on building automation systems: Interview protocol; unpublished.

Fütterer, J. and Constantin, A. (2014). *Energy concept for the E.ON ERC main building*, volume 4,9 of *E.ON Energy Research Center Series*. E.ON Energy Research Center, Aachen.

Fütterer, J., Constantin, A., Schmidt, M., Streblow, R., and Müller, D. (2013). Monitoring technique, evaluation methodology and results for a multifunctional building with geothermal energy. In *CISBAT 2013 Proceedings Vol. II - Cleantech for Smart Cities and Buildings*, volume 2, pages 751–756. EPFL Solar Energy and Building Physics Laboratory (Lausanne, Switzerland).

Futterer, J., Constantin, A., Schmidt, M., Streblow, R., Muller, D., and Kosmatopoulos, E. (2013). A multifunctional demonstration bench for advanced control research in buildings—monitoring, control, and interface system. In *Industrial Electronics Society, IECON 2013 - 39th Annual Conference of the IEEE*, pages 5696–5701.

Fütterer, J., Huber, M., and Müller, D. (2015). Practical use of building automation systems–a survey among practitioners.

Futterer, J., Kraus, P. J. E., Schmidt, M., and Muller, D. (2015). Demonstration of an easy-to-apply, automated control tuning method for typical pid control loops in building energy systems. In *2015 IEEE 10th Conference on Industrial Electronics and Applications (ICIEA)*, pages 2069–2075.

Fütterer, J., Stinner, F., and Müller, D. (2016). Simulation-based assessment of an easy-to-apply, automated control tuning method for typical pid control loops in building energy systems. In *Proceedings of ECOS 2016 - The 29th international conference on efficiency, cost, optimization, simulation and environmental impact of energy systems*.

Fütterer, J. P., Henn, S., Schmidt, M., and Mueller, D. (2014). Pid control loop tuning for three-port mixing valves within building energy distribution systems—application and assessment of different tuning methods under real operation conditions. In *Proceedings of ECOS 2014 - The 27th* *international conference on efficiency, cost, optimization, simulation and environmental impact of energy systems.*

Ghiaus, C., Chicinas, A., and Inard, C. (2007). Grey-box identification of air-handling unit elements. *Control Engineering Practice*, 15(4):421–433.

Ginestet, S. and Marchio, D. (2010). Control tuning of a simplified vav system: Methodology and impact on energy consumption and iaq. *Energy and Buildings*, 42(8):1205–1214.

Goodwin, G. C., Agüero, J. C., Welsh, J. S., Yuz, J. I., Adams, G. J., and Rojas, C. R. (2008). Robust identification of process models from plant data. *Journal of Process Control*, 18(9):810–820.

Gu, X., Li, H., Zhao, L., and Wang, H. (2008). Adaptive pid control of indoor air quality for an air-conditioned room. In *Intelligent Computation Technology and Automation (ICICTA), 2008 International Conference on*, volume 1, pages 289–293.

Henze, G., Kalz, D., Felsmann, C., and Knabe, G. (2004). Impact of forecasting accuracy on predictive optimal control of active and passive building thermal storage inventory. *HVAC&R Research*, 10(2):153–178.

Homod, R. Z., Mohamed Sahari, Khairul Salleh, Almurib, H. A., and Nagi, F. H. (2012a). Rlf and ts fuzzy model identification of indoor thermal comfort based on pmv/ppd. *Building and Environment*, 49:141–153.

Homod, R. Z., Sahari, Khairul Salleh Mohamed, Almurib, H. A., and Nagi, F. H. (2011). Double cooling coil model for non-linear hvac system using rlf method. *Energy and Buildings*, 43(9):2043–2054.

Homod, R. Z., Sahari, Khairul Salleh Mohamed, Almurib, H. A., and Nagi, F. H. (2012b). Gradient auto-tuned takagi–sugeno fuzzy forward control of a hvac system using predicted mean vote index. *Energy and Buildings*, 49:254–267.

Huang, G. (2011). Model predictive control of vav zone thermal systems concerning bi-linearity and gain nonlinearity. *Control Engineering Practice*, 19(7):700–710.

Huang, W. and Lam, H. N. (1997). Using genetic algorithms to optimize controller parameters for hvac systems. *Energy and Buildings*, 26(3):277–282.

Hücker, J. R. (2000). *Selbsteinstellende und prädiktive Kompaktregler*, volume 855 of *Fortschritt-Berichte VDI Reihe 8, Meß-, Steuerungs- und Regelungstechnik*. VDI-Verl., Düsseldorf, als ms. gedr edition.

Jetté, I., Zaheer-uddin, M., and Fazio, P. (1998). Pi-control of dual duct systems: manual tuning and control loop interaction. *Energy Conversion and Management*, 39(14):1471–1482.

Jian Liu, Wen-Jian Cai, and Gui-Qing Zhang (2009). Design and application of handheld auto-tuning pid instrument used in hvac. In *2009 4th IEEE Conference on Industrial Electronics and Applications (ICIEA)*, pages 1695–1698.

Karimi, A. and Doré Landau, I. (1998). Comparison of the closed-loop identification methods in terms of the bias distribution. *Systems & Control Letters*, 34(4):159–167.

Kiam Heong Ang, Chong, G., and Yun Li (2005). Pid control system analysis, design, and technology. *IEEE Transactions on Control Systems Technology*, 13(4):559–576.

Kraus, P. J. E. (Sep 2014). *Design of an automated tool to optimize the control quality of typical control loops in building energy systems.* Master thesis, RWTH Aachen, Aachen.

Kumar, M. and Kar, I. N. (2009). Non-linear hvac computations using least square support vector machines. *Energy Conversion and Management*, 50(6):1411–1418.

Kusiak, A., Li, M., and Zhang, Z. (2010). A data-driven approach for steam load prediction in buildings. *Applied Energy*, 87(3):925–933.

Kusiak, A. and Xu, G. (2012). Modeling and optimization of hvac systems using a dynamic neural network. *Energy*, 42(1):241–250.

Lahrech, R., Gruber, P., Riederer, P., Tessier, P., and Visier, J. (2002). Development of a testing method for control hvac systems by emulation. *Energy and Buildings*, 34(9):909–916.

Lin, J.-L. and Yeh, T.-J. (2007). Modeling, identification and control of air-conditioning systems. *International Journal of Refrigeration*, 30(2):209–220.

Liu, J., Zhou, H., Zhou, X., Cao, Y., and Zhao, H. (2011). Automative air conditioning system control - a survey. In *2011 International Conference on Electronic & Mechanical Engineering and Information Technology (EMEIT 2011)*, pages 3408–3412, Piscataway, NJ, USA. IEEE.

Lixing, D., Jinhu, L., Xuemei, L., and Lanlan, L. (2010). Support vector regression and ant colony optimization for hvac cooling load prediction. In *2010 International Symposium on Computer, Communication, Control and Automation (3CA)*, pages 537–541.

Ljung, L. (1999). *System identification: Theory for the user.* Prentice Hall information and system sciences series. Prentice-Hall, Upper Saddle River, NJ, 2. aufl. 11. print edition.

Ljung, L. (2002). Prediction error estimation methods. *Circuits, Systems, and Signal Processing*, 21(1):11–21.

MacArthur, J. W. and Zhan, C. (2007). A practical global multi-stage method for fully automated closed-loop identification of industrial processes. *Journal of Process Control*, 17(10):770–786.

Mahnke, W., Leitner, S.-H., and Damm, M. (2009). *OPC unified architecture.* Springer-Verlag, Berlin and Heidelberg.

Michalski, A., Fütterer, J., and Rothe, A. (2014). Exergetisch optimierte betriebsführung der wärme- und kälteversorgung eines gebäudes unter nutzung eines dynamischen regelungssystems und flexibler einbindung eines vollständig überwachten erdsondenfeldes. In Projektträger Jülich, editor, *Energieinnovationen in Neubau und Sanierung*. Forschungszentrum Jülich GmbH, Jülich.

Mirinejad, H., Welch, K. C., and Spicer, L. (2012). A review of intelligent control techniques in hvac systems. In *2012 IEEE Energytech*, pages 1–5.

Modelica Association (2015). Modelica - a unified object-oriented language for systems modeling: Version 3.3 revision 1.

Nagaraj, B. and Murugananth, N. (2010). A comparative study of pid controller tuning using ga, ep, pso and aco. In *2010 IEEE International Conference on Communication Control and Computing Technologies (ICCCCT)*, pages 305–313.

Naidu, D. S. and Rieger, C. (2011a). Advanced control strategies for heating, ventilation, air-conditioning, and refrigeration systems—an overview: Part i: Hard control. *HVAC&R Research*, 17(1):2–21.

Naidu, D. S. and Rieger, C. (2011b). Advanced control strategies for hvac&r systems—an overview: Part ii: Soft and fusion control. *HVAC&R Research*, 17(2):144–158.

Nassif, N. (2014). Modeling and optimization of hvac systems using artificial neural network and genetic algorithm. *Building Simulation*, 7(3):237–245.

Nassif, N., Moujaes, S., and Zaheeruddin, M. (2008). Self-tuning dynamic models of hvac system components. *Energy and Buildings*, 40(9):1709–1720.

Nesler, C. (1986). Adaptive control of thermal processes in buildings. *IEEE Control Systems Magazine*, 6(4):9–13.

Ovaska, S. J., VanLandingham, H. F., and Kamiya, A. (2002). Fusion of soft computing and hard computing in industrial applications: An overview. *IEEE Transactions on Systems, Man and Cybernetics, Part C (Applications and Reviews)*, 32(2):72–79.

Pinnella, M. J., Wechselberger, E., Hittle, D. C., and Pedersen, C. O. (1986). Self-tuning digital integral control. In ASHRAE, editor, *ASHRAE Trans.; (United States)*, volume 92:2B. ASHRAE.

Qu, G. and Zaheeruddin, M. (2004). Real-time tuning of pi controllers in hvac systems. *International Journal of Energy Research*, 28(15):1313–1327.

Rehrl, J. and Horn, M. (2009). Supply air temperature control in an industrial hvac pilot plant based on smith predictor and inward approach. In *2009 International Conference on Computational Intelligence, Modelling and Simulation*, pages 220–225.

Rojas, C. R., Welsh, J. S., and Goodwin, G. C. (2007). A receding horizon algorithm to generate binary signals with a prescribed autocovariance. In *2007 American Control Conference*, pages 122–127.

Salsbury, T. I. (1999). A practical algorithm for diagnosing control loop problems. *Energy and Buildings*, 29(3):217–227.

Salsbury, T. I. (2002). A new pulse modulation adaptive controller (pmac) applied to hvac systems. *Control Engineering Practice*, 10(12):1357–1370.

Salsbury, T. I. and Diamond, R. C. (2001). Fault detection in hvac systems using model-based feedforward control. *Energy and Buildings*, 33(4):403–415.

Schild, T., Futterer, J., Sangi, R., Streblow, R., and Muller, D. (2015). System of systems theory as a new perspective on building control. In *23th Mediterranean Conference on Control and Automation (MED)*, pages 783–788.

Seem, J. E. (1998). A new pattern recognition adaptive controller with application to hvac systems. *Automatica*, 34(8):969–982.

Skogestad, S. (2003). Simple analytic rules for model reduction and pid controller tuning. *Journal of Process Control*, 13(4):291–309.

Song, W. S., Hong, S. H., and Park, T. J. (2007). The effects of service delays on a bacnet-based hvac control system. *Control Engineering Practice*, 15(2):209–217.

Soyguder, S. and Alli, H. (2009). Predicting of fan speed for energy saving in hvac system based on adaptive network based fuzzy inference system. *Expert Systems with Applications*, 36(4):8631–8638.

Soyguder, S., Karakose, M., and Alli, H. (2009). Design and simulation of self-tuning pid-type fuzzy adaptive control for an expert hvac system. *Expert Systems with Applications*, 36(3):4566–4573.

Van Den Hof, Paul M.J. and Schrama, R. J. (1995). Identification and control: Closed-loop issues. *Automatica*, 31(12):1751–1770.

VanDoren, V. (2013). Fundamentals of lambda tuning: Understanding a particularly conservative pid controller design technique.

Waide, P., Ure, J., Karagianni, N., Smith, G., and Borbass, B. (2014). The scope for energy and co2 savings in the eu through the use of building automation technology.

Wallenborg, A. O. (1992). A new self-tuning controller for hvac systems. *ASHRAE Transactions*, 1992(98):19–25.

Wang, S. and Ma, Z. (2008). Supervisory and optimal control of building hvac systems: A review. *HVAC&R Research*, 14(1):3–32.

Warwick, K. and Rees, D. (1988). *Industrial digital control systems*, volume 37 of *IEE control engineering series*. P. Peregrinus on behalf of the Institution of Electrical Engineers, London, comprehensively revised edition edition.

Wemhoff, A. P. (2012). Calibration of hvac equipment pid coefficients for energy conservation. *Energy and Buildings*, 45:60–66.

Wenge, L., Deyuan, L., Siyuan, C., Shaoming, L., Xiangwei, Z., and Linhai, Z. (2010). Research on pid control parameters tuning based on election-survey optimization algorithm. In *2010 International Conference on Computing, Control and Industrial Engineering*, pages 323–326.

Wetter, M., Fuchs, M., Grozman, P., Helsen, L., Jorissen, F., Lauster, M., Müller, D., Nytsch-Geusen, C., Picard, D., Sahlin, P., and Thorade, M. (2015). Iea ebc annex 60 modelica library: An international collaboration to develop a free open-source model library for buildings and community energy systems. In *Proceedings of the 14th International Conference of the International Building Performance Simulation Association*.

Wetter, M., Zuo, W., Nouidui, T. S., and Pang, X. (2014). Modelica buildings library. *Journal of Building Performance Simulation*, 7(4):253–270.

Ya-Gang Wang, Zhi-Gang Shi, and Wen-Jian Cai (25-27 June 2001). Pid autotuner and its application in hvac systems. In *American Control Conference*, pages 2192–2196.

Yiu, C.-m. J. (2008). *Statistical modelling and forecasting schemes for air-conditioning system*. Phd thesis, The Hong Kong Polytechnic University, Hong Kong.

Zhou, J. Q. and Claridge, D. E. (2012). Pi tuning and robustness analysis for air handler discharge air temperature control. *Energy and Buildings*, 44:1–6.

Ziegler, J. G. and Nichols, N. B. (1942). Optimum settings for automatic controllers. *Transactions of ASME*, 64:759–768.

Appendix

A Appendix towards theory

Table A.1: Parameter calculation for PID controller

tuning rule	process model	K_P	T_I	T_D
ZN	PT_1T_d	$\frac{1.2}{k}\frac{T_1}{\theta}$	$2\,\theta$	$0.5\,\theta$
LT	PT_1T_d	$\frac{1}{k}\frac{\theta}{\theta+2\lambda}$	$T_1+0.5\,\theta$	$\frac{T_1\theta}{\theta+2T_1}$
AO	PT_2	$\left(1+\frac{T_2}{T_1}\right)\frac{T_1}{2\,k\,T_\Sigma}$	T_1+T_2	$\frac{T_1T_2}{T_1+T_2}$
SO	PT_2	$\frac{T_1T_2}{8kT_\Sigma^2}$	$16\,T_\Sigma$	$4\,T_\Sigma$
SIMC	PT_2T_d	$\left(1+\frac{T_2}{min(T_1,8\,\theta)}\right)\frac{1}{k}\frac{T_1}{2\,\theta}$	$min(T_1,8\,\theta)+T_2$	$\frac{min(T_1,8\,\theta)\;T_2}{min(T_1,8\,\theta)+T_2}$

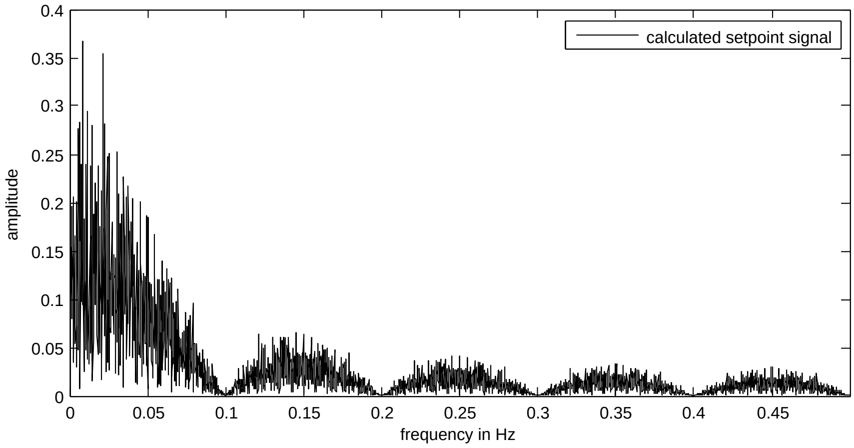

Figure A.1: Explanatory frequency spectrum of the random binary signal (RBS) excitation signal

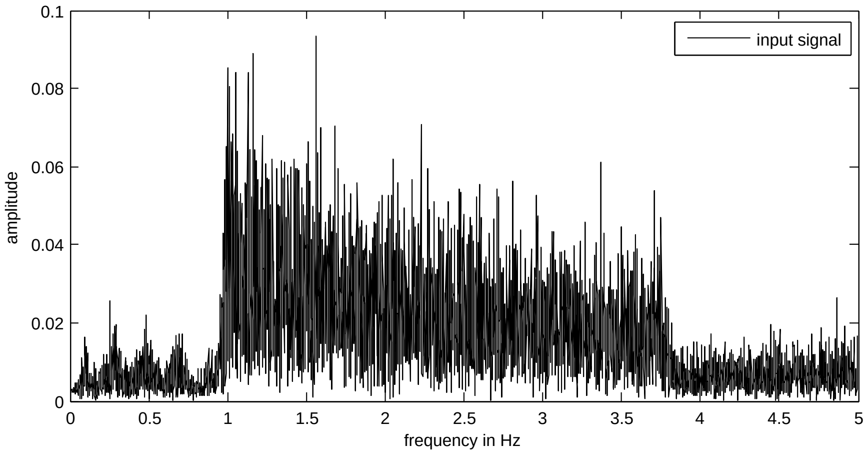

Figure A.2: Explanatory frequency spectrum of the $1/f$ excitation signal

A.1 Estimation algorithm

The whole following section is cited from Kraus [2014], a masters thesis which I supervised.

See figure A.3 for an overview of the setup and the signals considered in an estimation method. Here, ε is the prediction error that is explained in detail below.

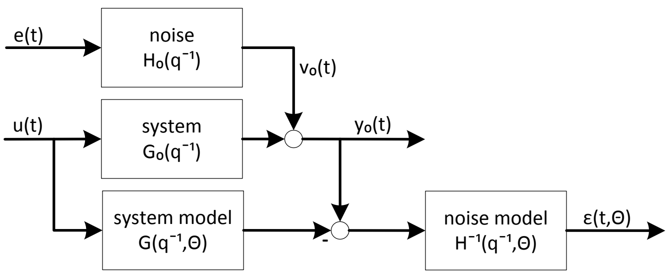

Figure A.3: prediction error

Consider a system as defined as in :

$$y(t) = G(q^{-1})u(t) + v(t) \tag{A.1}$$

$$v(t) = H(q^{-1})e(t) \tag{A.2}$$

The first equation can be rewritten as

$$y(t) = G(q^{-1})u(t) + \left[H(q^{-1}) - 1\right] e(t) + e(t) \tag{A.3}$$

When

$$e(t) = H^{-1}(q^{-1})\left[y(t) - G(q^{-1})u(t)\right] \tag{A.4}$$

is set into the equation above, that becomes

$$y(t) = G(q^{-1})u(t) + \left[H(q^{-1}) - 1\right] H^{-1}(q^{-1})\left[y(t) - G(q^{-1})u(t)\right] + e(t) \tag{A.5}$$

and can be transformed into

$$y(t) = H^{-1}(q^{-1})G(q^{-1})u(t) + \left[1 - H^{-1}(q^{-1})\right] y(t) + e(t) \tag{A.6}$$

Under the assumption that $H(q^{-1})$ is proper, monic and has a stable inverse, the following equation holds

$$\frac{1}{H(q^{-1})} = 1 + d_1 q^{-1} + d_2 q^{-2} + d_3 q^{-3} + \ldots \tag{A.7}$$

where $\{d_i\}$ is a sequence which tends to 0. Consequential the expression

$$H^{-1}(q^{-1})G(q^{-1})u(t) + \left[1 - H^{-1}(q^{-1})\right] y(t) \tag{A.8}$$

is completely determined by $G(q^{-1})$,$H(q^{-1})$ and by past observations $y(t-1)$ and $u(t-1)$. The above expression is known as the one-step-ahead predictor of $y(t)$ and defined as

$$\hat{y}(t|t-1) = H^{-1}(q^{-1})G(q^{-1})u(t) + \left[1 - H^{-1}(q^{-1})\right] y(t) \tag{A.9}$$

so that follows

$$y(t) = \hat{y}(t|t-1) + e(t) \tag{A.10}$$

with $\hat{y}(t|t-1)$ as the known and $e(t)$ as the unknown part of the output signal at the time $t-1$. Finally the one-step-ahead prediction error can be defined as

$$\varepsilon(t) := \hat{y}(t|t-1) - y(t) \tag{A.11}$$

$$\varepsilon(t) = H^{-1}(q^{-1})\left[y(t) - G(q^{-1})u(t)\right] \tag{A.12}$$

The prediction error can only be calculated a posteriori and represents that part of the system output signal $y(t)$ that could not have been predicted one step before. In case of comparing the prediction of the model output with the measured output of the true system, the equations can be written more precisely to

$$\varepsilon(t,\theta) := \hat{y}(t|t-1,\theta) - y_0(t) \tag{A.13}$$

$$\varepsilon(t,\theta) = H^{-1}(q^{-1},\theta)\left[y_0(t) - G(q^{-1},\theta)u(t)\right] \tag{A.14}$$

If the model is identical to the true system ($G(q^{-1},\theta) = G_0(q^{-1})$ and $H(q^{-1},\theta) = H_0(q^{-1})$) the prediction error becomes equal to the model output error, which is equal to the noise signal.

$$\varepsilon(t) = e(t) \tag{A.15}$$

This is an important result for the model validation, which is discussed in the next section. For further details see e.g. [Forssell and Ljung, 1999].

The scalar-valued function, which is minimized in the algorithm, is also called the identification criterion. The most frequently applied criterion function is a quadratic function on the prediction error $\varepsilon(t,\theta)$:

$$V_N(\theta, Z^N) = \frac{1}{N}\sum_{t=1}^{N} \varepsilon(t,\theta)^2 \tag{A.16}$$

where Z^N is the data vector of the length N. This criterion is known as the "last squares criterion". The estimated parameter vector that minimizes the criterion is defined by

$$\hat{\theta} = \arg\min_{\theta \epsilon \Theta} V_N(\theta, Z^N) \tag{A.17}$$

The prediction error method provides the possibility to filter the prediction error with a linear stable filter $L(q^{-1})$ before it is used in the identification criterion. As the following equations show, filtering the prediction error is identical to changing the noise model or to filtering the measured input and output data if $G(q^{-1},\theta)$ and $H(q^{-1},\theta)$ are scalar transfer functions.

$$\varepsilon_F(t,\theta) = L(q^{-1})\varepsilon(t,\theta) \tag{A.18}$$

$$= L(q^{-1})H^{-1}(q^{-1},\theta)\left[y(t) - G(q^{-1},\theta)u(t)\right] \tag{A.19}$$

$$= H^{-1}(q^{-1},\theta)\left[L(q^{-1})y(t) - G(q^{-1},\theta)L(q^{-1})u(t)\right] \tag{A.20}$$

By filtering the data it is possible to shape the relative importance of specific frequency ranges in the criterion function. When the algorithm is applied on closed-loop data the controller in the loop already provides an implicit filtering effect [Karimi and Doré Landau, 1998].

The prediction error method allows arbitrary model parametrizations. However, the interesting parameters must have a clear effect on the output prediction to archive a small variance. If the true model of the dynamic system is within the model set the PEM provides optimal asymptotic accuracy. If this is not the case the bias distribution can still be explained and effected. The estimation algorithm relies on iterative search methods - except for the linear regression case e.g. if an ARX model structure is used - and therefore the global minimum can not be guaranteed [Ljung, 1999]. This underlines the importance of good start conditions. The exact predictor would be calculated with the Kalman-filter including non-zero initial states. Normally an approximation of the optimal predictor is used assuming zero initial states or they are calculated based on an initial model [MacArthur and Zhan, 2007].

In the case of identification for control the attention in the estimation methods is directed away from the identifiability and accuracy towards the possibility of shaping the bias distribution to archive control-relevant model approximations [Forssell and Ljung, 1999].

B Further descriptive figures for controlled systems used for experiments

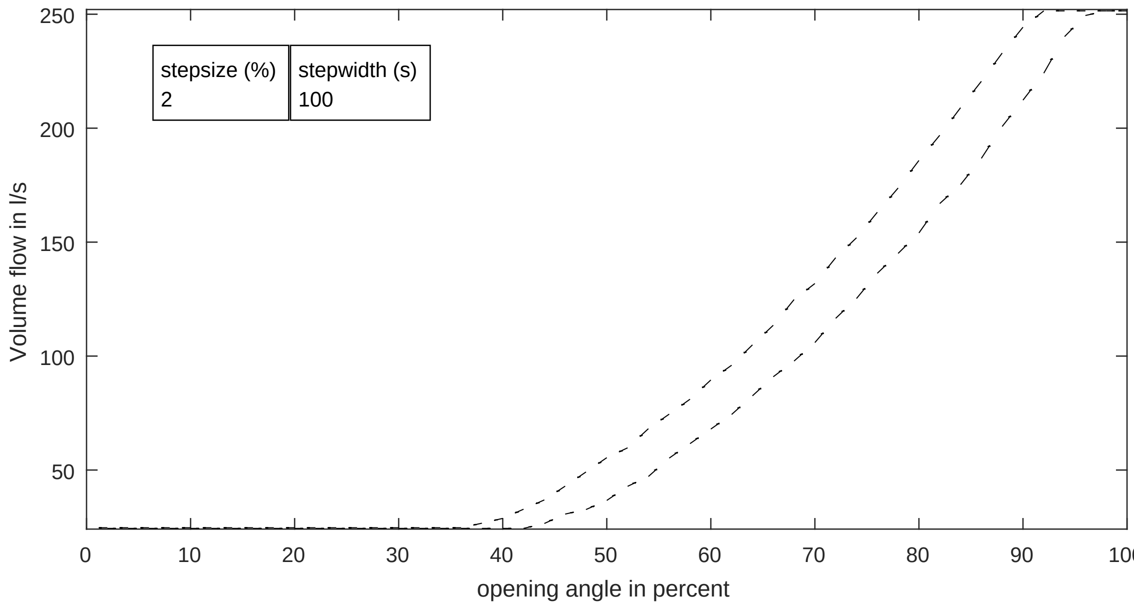

Figure B.1: AHU01 exhaust pressure 2015-09-01: AHU01 exhaust pressure operation range assessment

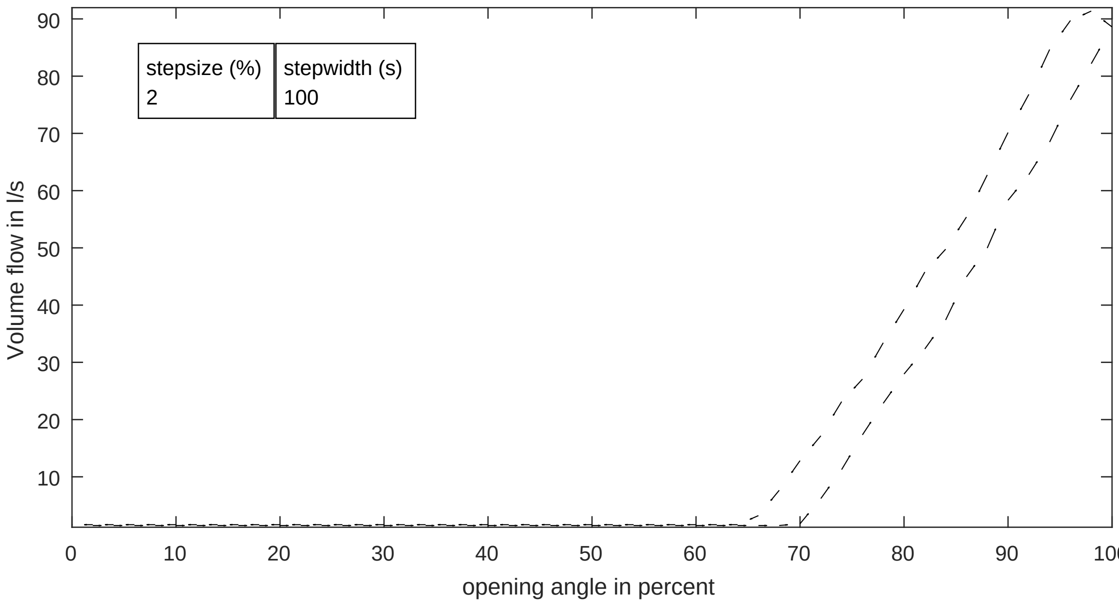

Figure B.2: AHU04 exhaust pressure 2015-09-01: AHU04 exhaust pressure operation range assessment

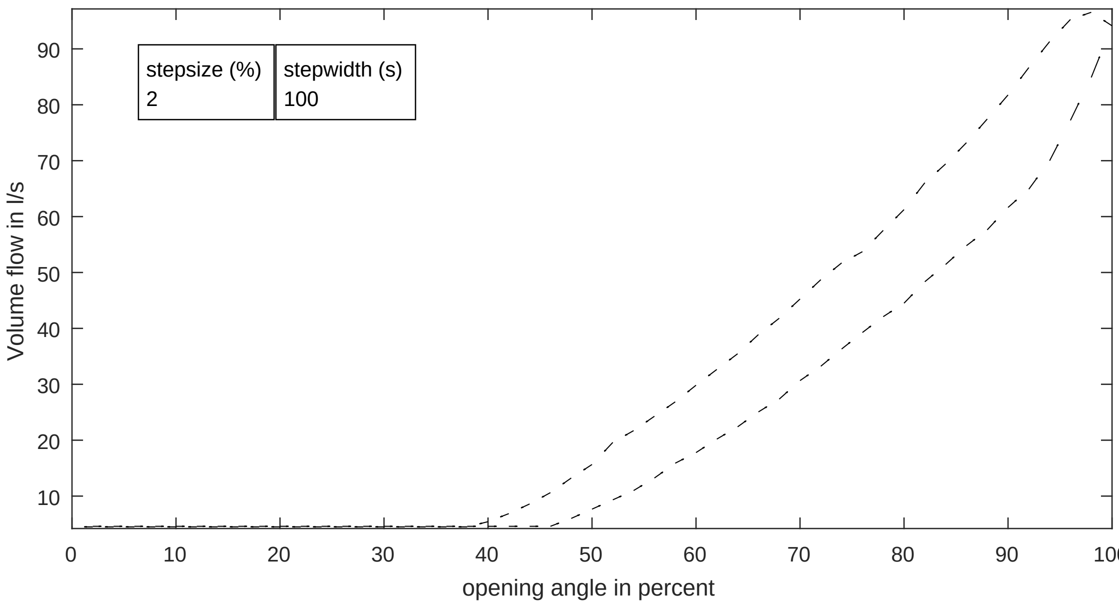

Figure B.3: AHU04 supply pressure 2015-09-01: AHU04 supply pressure operation range assessment

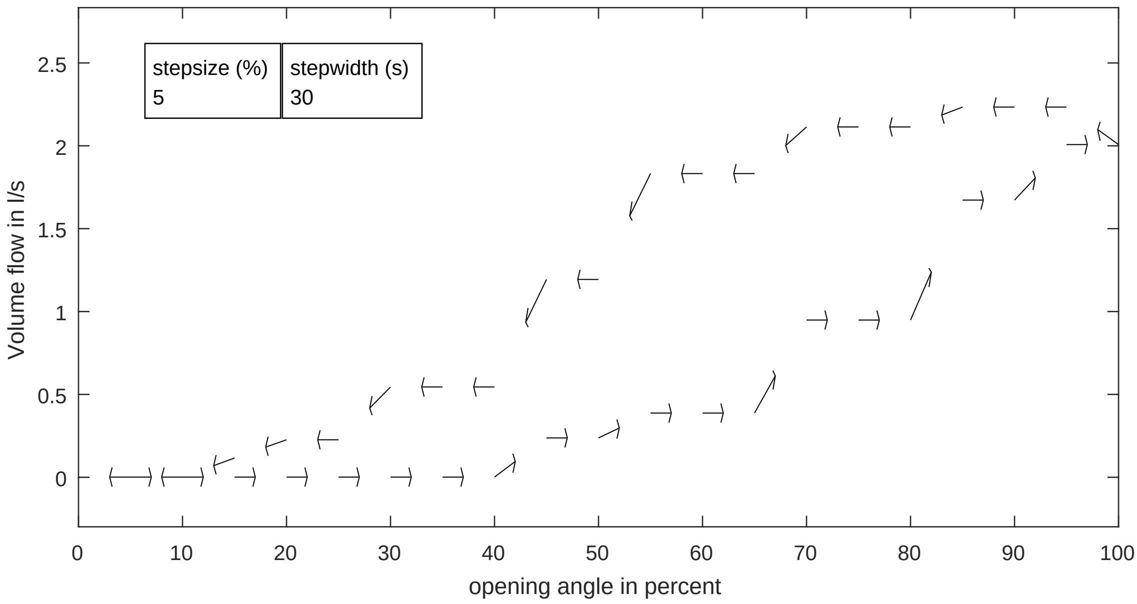

Figure B.4: Three-way-valve H061Y02 volume flow 2015-07-20: Three-way-valve volume flow operation range assessment

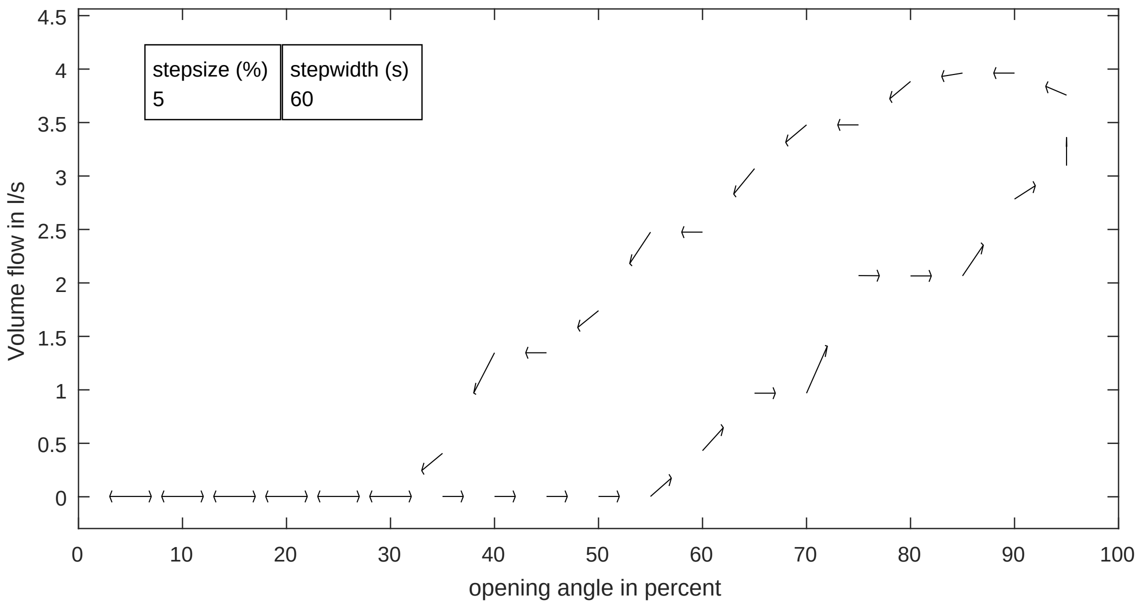

Figure B.5: Three-way-valve K08Y02 2015-07-17: Three-way-valve volume flow operation range assessment

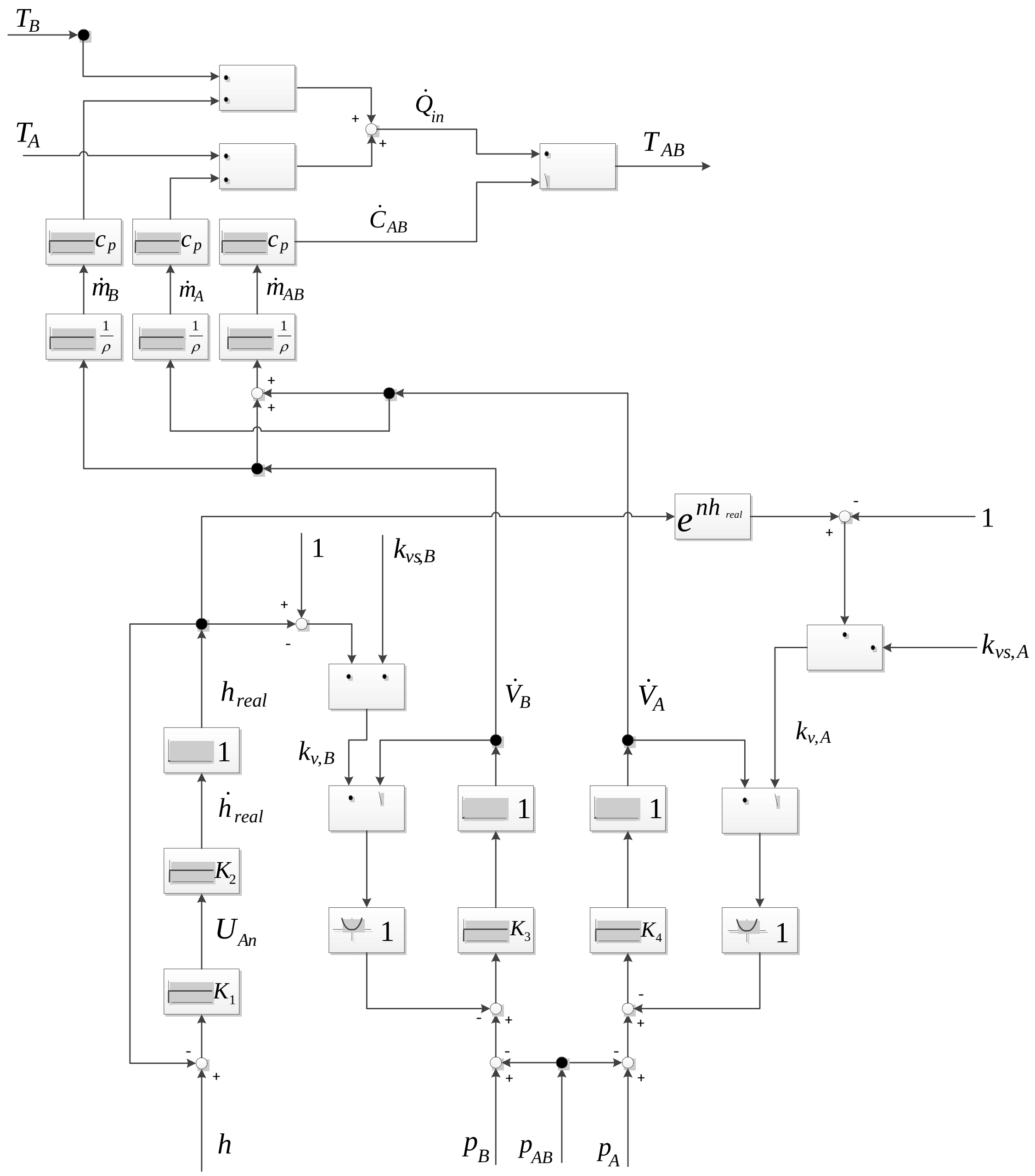

Figure B.6: Functional diagram for supply temperature control via three-way-valve volume flow modulation - for a detailed discussion please refer to Fütterer et al. [2014]

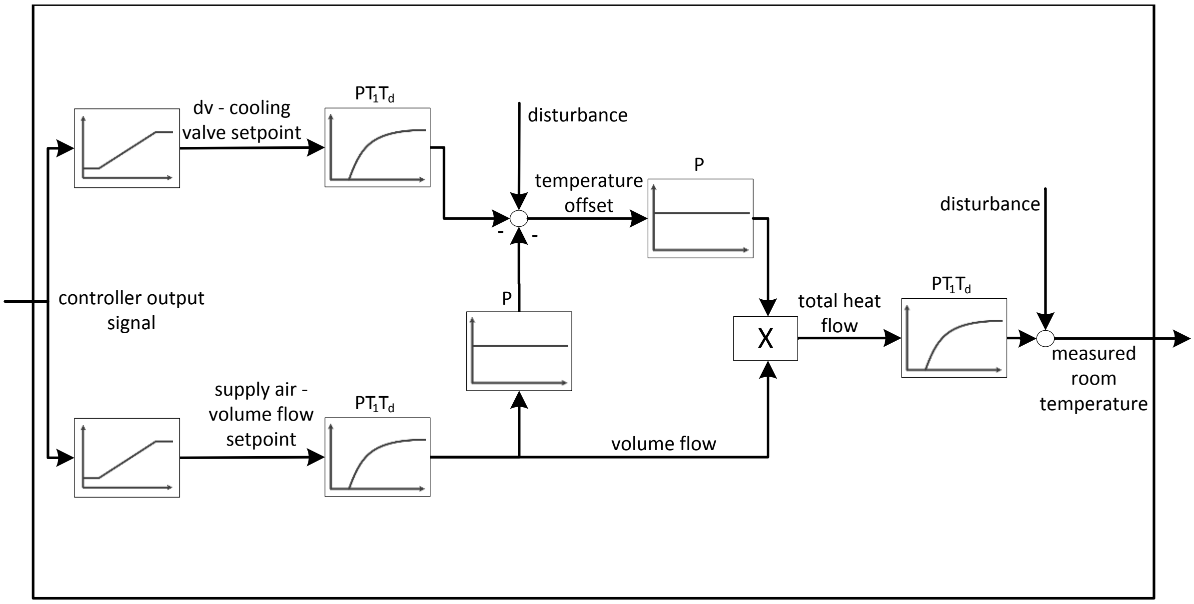

Figure B.7: Functional chart for the room temperature control via displacement ventialtion as found in staff facilities and conference rooms

C Further results

C.1 Furhter results towards AHU 01 exhaust pressure

This chapter takes a look at the influence of, first, the operation's range adaption, second, the model orders and types for system model and disturbance model, third, long and short excitation times having low and high excitation frequencies.

Within the experiment number twelve, "AHU 01 Exhaust Pressure 150907 02h10" [**STW** 30 **STR** 15 **MMO** 6 **MDO** 6 **IDT** 2294 **MAE** 98 **OL ER** (0;100 %) **1/f F**], which differs from the previous experiment by using the full technically available operation range instead of an adjusted operation range within the open loop excitation, the algorithm is able to achieve advancements of control quality indicators, too. The absolute values and the relative deviation in comparison to the initial control quality provides table C.1. Sorted by ITAE, these results cannot compete against the previous bj(2,6,5,3)PIBO configuration.

Table C.1: AHU01 exhaust pressure 2015-09-06 02h10: Absolute control quality indicators and relative deviation of control quality indicators (experiment number 12)

option	RT	ST	OS	US	IAE	ISE	ITAE
bj(3,4,4,6,d)PISIMC	90 s	90 s	0	0	160,53 Pa	3500.80 Pa^2	20.00 kPa s
	−57.14 %	−57.14 %	0	0	−52.62 %	−52.55 %	−58.01 %
bj(3,4,4,6,d)PIBO	90 s	90 s	0	0	215,39 Pa	4847,58 Pa^2	30.28 kPa s
	−57.14 %	−57.14 %	0	0	−36.43 %	−34.30 %	−36.42 %

Various further conducted experiments showed comparable results for this controlled system. In the following, experiments with varied input parameters are presented.

Four times [**MMO** 12 **MDO** 12]-experiments were executed. Two of those experiments with STW of 150 where aborted due to computational capacity during the model estimation and during the Skogestad model order reduction respectively. Nevertheless, two experiments, having both a STW of 5, were successfully conducted.

The experiment number ten, "AHU 01 Exhaust Pressure 150825 22h00", [**STW** 5 **STR** 1 **MMO** 12 **MDO** 12 **IDT** 2800 **MAE** 560 **CL rbs F full OR**], has a random binary signal (RBS) excitation in closed loop (CL) mode and was not able to achieve superior control performance in comparison to the reference case.

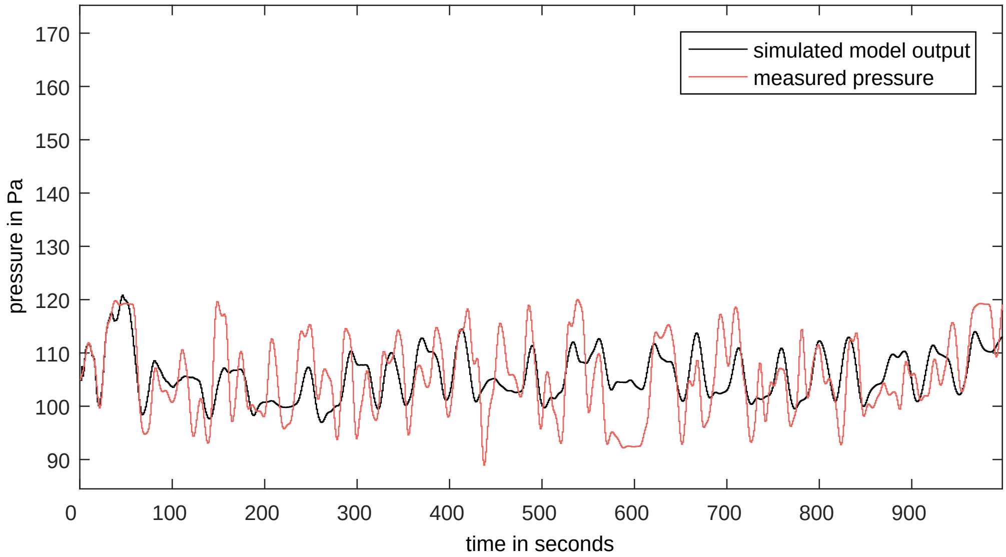

Figure C.1: AHU01 exhaust pressure 2015-08-25 22h00: Simulated model output vs. measured system output of best fitting model, bj(5,11,11,11,d), mf = %, model fit to estimation data (mf_{est}) = % (experiment number 10)

Figure C.1 shows the fit of the best fitting model for experiment ten, in this case a bj(5,11,11,11,d)-model. It is obvious that the simulated model output does not meet the peaks of the measured pressure. The model seems to represent the system in a damped way.

Best simulative control qualities were gathers by Box-Jenkins models and the Zigler-Nichols control tuning rule. Table C.2 provides an overview of the calculated control parameter sets.

Table C.2: AHU01 exhaust pressure 2015-08-25 22h00: Actual and proposed PID controller parameters(experiment number 10)

	K_P	T_I	T_D
actual parameters	0.129	38.500	0
bj(7,11,8,10,d)PIZN	0.872	16.996	0
bj(5,12,11,11,d)PIZN	12.685	16.400	0
bj(4,9,9,6,d)PIZN	30.683	14,745	0

Within figure C.2 this experiment's step response comparison of the bj(7,11,8,10,d)PIZN-combination is shown. On a simulation basis, a stable behavior is achieved, yet the simulated system is not able to meet the set point. In contrast, the real system starts to oscillate, showing a non-stable behavior.

The experiment number 9, "AHU 01 Exhaust Pressure 150824 15h10", [**STW** 5 **STR** 1 **MMO** 12 **MDO** 12 **IDT** 1640 + full ID **MAE** 328 **CL 1/f F**] gained slightly better results. Still, it shows the same aforemen-

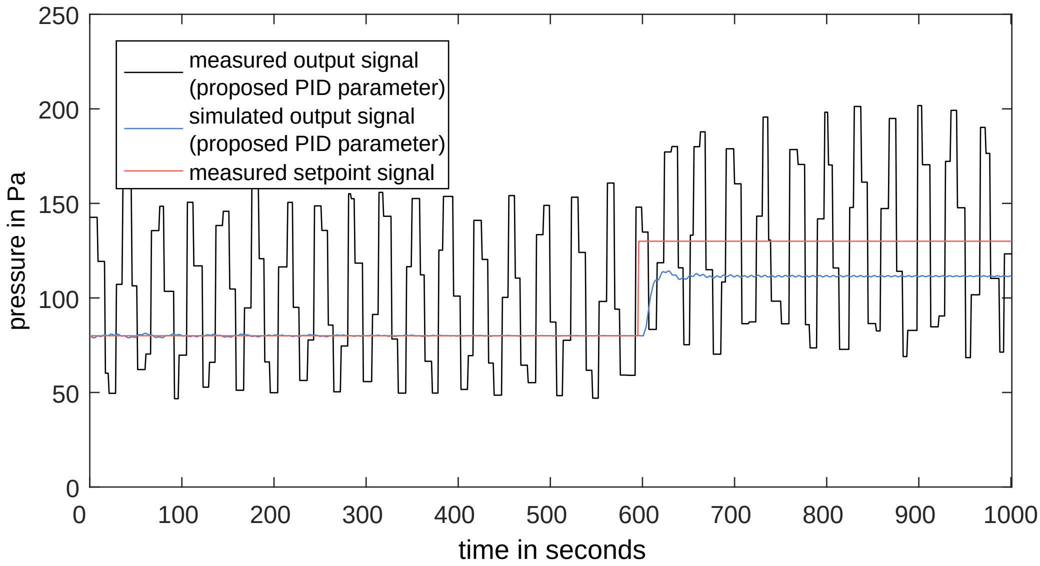

Figure C.2: AHU01 exhaust pressure 2015-08-25 22h00: bj(7,11,8,10,d) PIZN step comparison (experiment number 10)

tioned characteristics, i.e. underestimation of the real system's transfer gain, and, thus, a tendency towards too aggressive tuning, and, thus, oscillating control behavior. It achieved one stable but aggressively tuned, over- and undershooting parameter set, with a proportional gain, K_P, of 0.148 and an integral time, T_I, of 3.787 seconds. Table C.3 presents its control quality indicators. Its step comparison is presented in figure C.3. This parameter set leads to a short rise time and a short settling time, which outmatches all before-mentioned parameter sets. Still, the price is over- and undershooting behavior and higher integral criteria values.

Table C.3: AHU01 exhaust pressure 2015-08-24 15h10: Absolute control quality indicators and relative deviation of control quality indicators (experiment number 9)

option	RT	ST	OS	US	IAE	ISE	ITAE
bj(4,9,9,7;13;d;1)	16 s	54 s	29.78 PA	−18.23 PA	1985.47 Pa	50688.88 Pa^2	139.42 kPa s
PISIMC	−57.14 %	−57.14 %	0	0	485.97 %	586.97 %	192.80 %

The closed-loop experiment, experiment number eight, "AHU 01 Exhaust Pressure 15-08-22 07h00" [**STW** 5 **STR** 1 **MMO** 2 **MDO** 2 **IDT** 5840 **MAE** 1168 **CL ER** (80;130 Pa) **1/f F**] has a very high excitation frequency, a low maximum model order and disturbance order, and a moderate identification time. Thus, due to the high frequency, the maximum amount of excitation is quite high.

The results are comparable to experiment number ten, "AHU01 exhaust pressure 2015-08-25 22h00", i.e. underestimation of the real system's transfer gain, and, thus, a tendency towards too aggressive

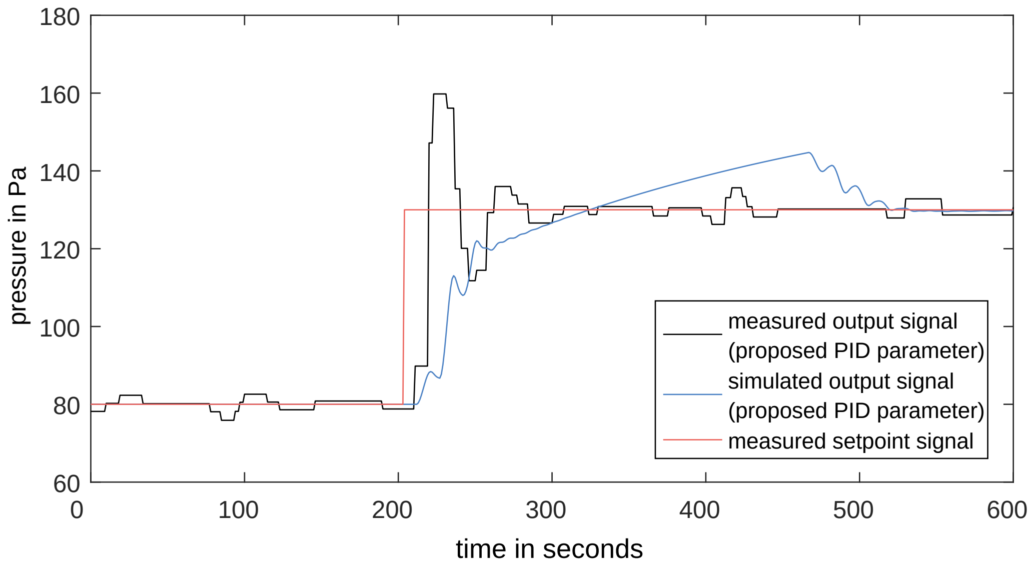

Figure C.3: AHU01 exhaust pressure 2015-08-24 15h10: bj(4,9,9,7;13;d;1) PSSIMC step comparison (experiment number 9)

tuning, and, thus, oscillating control behavior.

The closed-loop experiment number seven, "AHU 01 Exhaust Pressure 15-08-21 21h05" [**STW** 200 **STR** 5 **MMO** 2 **MDO** 2 **IDT** 25640 **MAE** 128,2 **CL ER** (80;130 %) **1/f F1**] combines a low model order with a high STW and, therefore, a low excitation frequency. Its best fitting model is an armax(2,1,0;18,d)-model, having one second order polynomial term and one first order polynomial term but a zero order, thus, a non-existing error term, see table 3.1 in chapter 3. Its fit is represented in figure C.4. The estimation of the real system's transfer gain is better compared to the higher frequency excitation experiments, as peaks as the simulation meets peaks and valleys. The from an armax(2,1,2;18,d,5)-model PIZN-derived control parameters, even if negative[1], provide the best ITAE control performance throughout all AHU 01 exhaust pressure experiments. The step experiment for this combination is shown in figure C.5[2].

The experiment number three, "AHU 01 Exhaust Pressure 2015-03-25 18h30", [**STW** 10 **STR** 1 **MMO** 4 **MDO** 4 **IDT** 1440 **MAE** 144 **CL ER** (52,5;117,5 %) **rbs F**] provided the worst results of all AHU 01 Exhaust Pressure experiments.

[1] How the JCI PID algorithm handles negative control parameters exactly stays unclear, as no detailed documentation is available. Still, negative values are accepted as input parameters to the JCI controller. Negative parameters can obviously provide acceptable control performance.

[2] Since the proposed PID parameters are negative, the simulation is constant with a value of 0 and not shown in the figure.

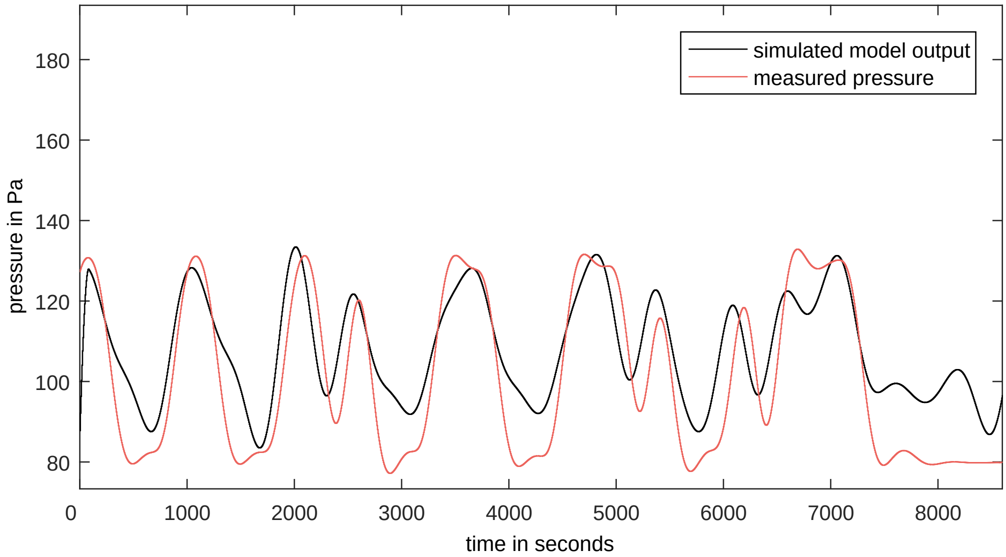

Figure C.4: AHU01 exhaust pressure 2015-08-21 21h05: Simulated model output vs. measured system output of best fitting model, armax(2,1,0;18;d), mf = 39.4%, model fit to estimation data (mf_{est}) = 99.85% (experiment number 7)

C.2 Furhter results towards AHU 01 supply pressure

Step configuration one was only used for one initial step experiments and two step experiments for proposed parameters within experiment one. Thus, the absolute values of these three steps cannot be compared against other step experiments. As figure 7.10 indicates, experiment one's proposed PID parameters had ITAE results multiple times higher than the initial parameters. This is a consequence of oscillating control behavior of the proposed parameter sets.

Step configuration two was used for 27 step experiments. The mean value of all five reference steps was 75 kPAs. The best reference step reached a value of 46 KPas whereas the highest ITAE value

Table C.4: AHU01 exhaust pressure 2015-08-21 21h05: Absolute control quality indicators and relative deviation of control quality indicators (experiment number 7)

option	RS	ST	OS	US	IAE	ISE	ITAE
armax(2,1,2;18;d)	60 s	60 s	0 PA	0 PA	311.95 Pa	8288.13 Pa^2	9.53 kPa s
PIZN	−71.43 %	−71.43 %	0	0	−7.93 %	12.33 %	−79.99 %
armax(2,1,1;18,d)	85 s	85 s	0 PA	0 PA	356.52 Pa	8161.14 Pa^2	17.01 kPa s
PILrobust	−59.52 %	−59.52 %	0	0	5.21 %	10.60 %	−64.29 %
armax(2,1,1;18;d)	105 s	105 s	0 PA	0 PA	424.59 Pa	8219.93 Pa^2	27.04 kPa s
PIZN	−59.52 %	−59.52 %	0	0	5.21 %	10.60 %	−64.29 %

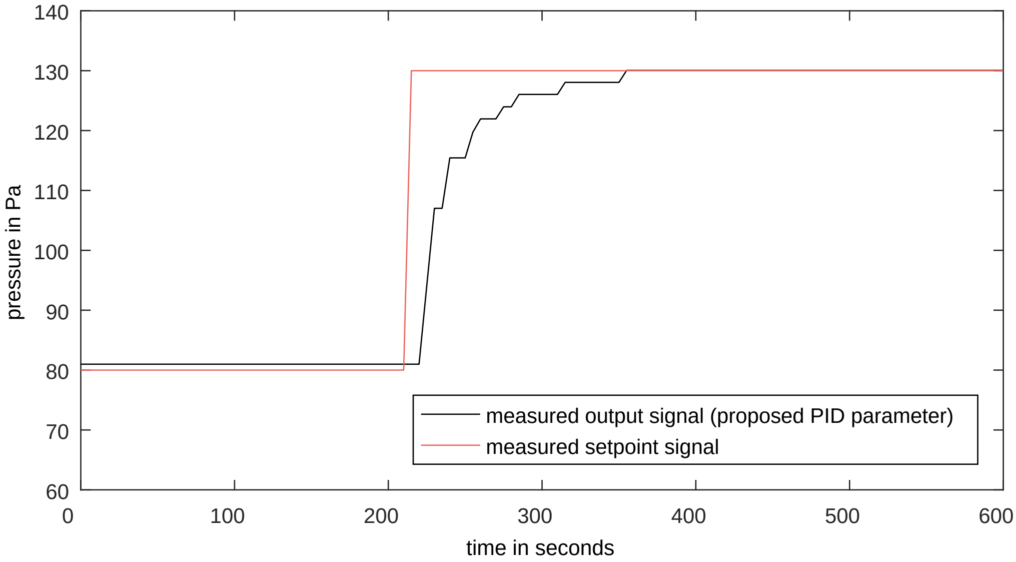

Figure C.5: AHU01 exhaust pressure 2015-08-21 21h05: armax(2,1,2;89;d) PIZN step (experiment number 7)

was 104 kPAs. Experiment number six proposed three parameter sets that provided ITAE-values below the best reference value. Throughout experiments using step configuration number two, 15 proposed parameter sets achieved values under the reference mean value. Seven parameter sets provided higher ITAEs as the mean reference.

Step number three was used for experiment number seven and eight, which both had issues, as mentioned above.

Step number four was used in 18 step experiments, whereas one initial step experiment failed. Figure C.7 shows the 17 remaining absolute ITAE results. The mean value of the four initial step experiments is again 75 kPAs. Three proposed parameter sets achieved lower ITAE-values than the mean value, two showed more or less the mean value, whereas eight showed higher values. PID configurations (12,2), (10,2), and (11,4) showed an oscillating control behavior. Thus, ITEA values are vary high an out of the y-axes limits within figure C.7. The best parameter set, (13,2), reached an ITAE-value of 37035 kPa s.

Step number five is neglected, since it was only used in experiment number 14, whose initial step experiment failed.

The lowest absolute ITAE value within step type 2 has experiment number 6, “AHU 01 supply pressure 2015-06-15 18h00‘” [**STW** 10 **STR** 1 **MMO** 8 **MDO** 8 **IDT** 34560 **MAE** 3456 **CL ER** (45;105 PA) **1/f F**] within step experiment number 2, a bj(1,5,3,3;1;d)-PIBO-combination, which is shown in figure C.8. The lowest absolute ITAE value within step type 4 reached experiment number 13, “AHU 01 supply

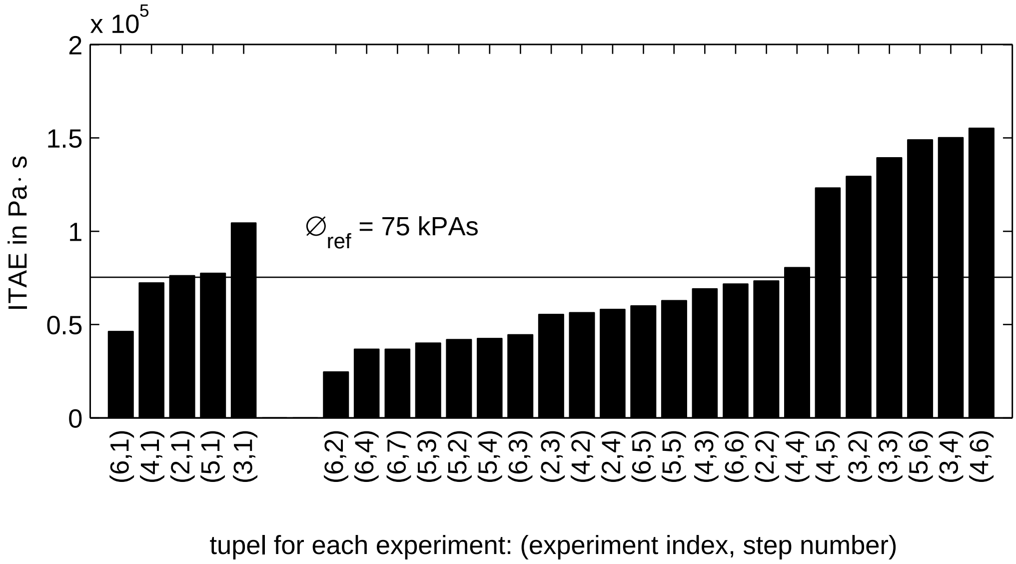

Figure C.6: AHU 01 supply pressure: ITAEs of step experiments under step configuration 2: left, actual parameters; right, proposed parameters.

pressure 2015-08-29 10h00" [**STW** 30 **STR** 15 **MMO** 6 **MDO** 6 **IDT** 3140 **MAE** 104,7 **OL ER** (15;85 %) **1/f F**] within step experiment number 2, a bj(1,3,2,2;0;d)-PIBO-combination, which is shown in figure C.9.

Experiment number 8, "AHU 01 Supply Pressure 2015-08-05 11h25" [**STW** 30 **STR** 1 **MMO** 2 **MDO** 2 **IDT** 2240 **MAE** 74,7 **CL ER** (45;105 PA) **rbs F**], reached the best fitting value towards the validation data. Its simulated model output is drawn versus the measured system output in figure C.10.

In summary, 17 step experiments out of 35 proposed PID parameter sets provided relatively better results than their initial step experiment. Seven out of eleven algorithm executions provided better ITAE control quality.

C.3 Further results towards AHU 04 exhaust pressure

In order to provide an haptic example, Figure C.11 visualize a comparison of the actual step response, its simulation with actual parameters, the simulated step response with proposed parameters and the measured step response with proposed parameters for the second step of experiment eleven. The step configuration is of type.

When comparing the identification data and the BJ(1,2,3,2;1,d)-model data – which is not shown here – it becomes obvious that the model slightly overestimates the system's dominant time constant and slightly underestimates the system's gain. This explains that the simulated step responses,

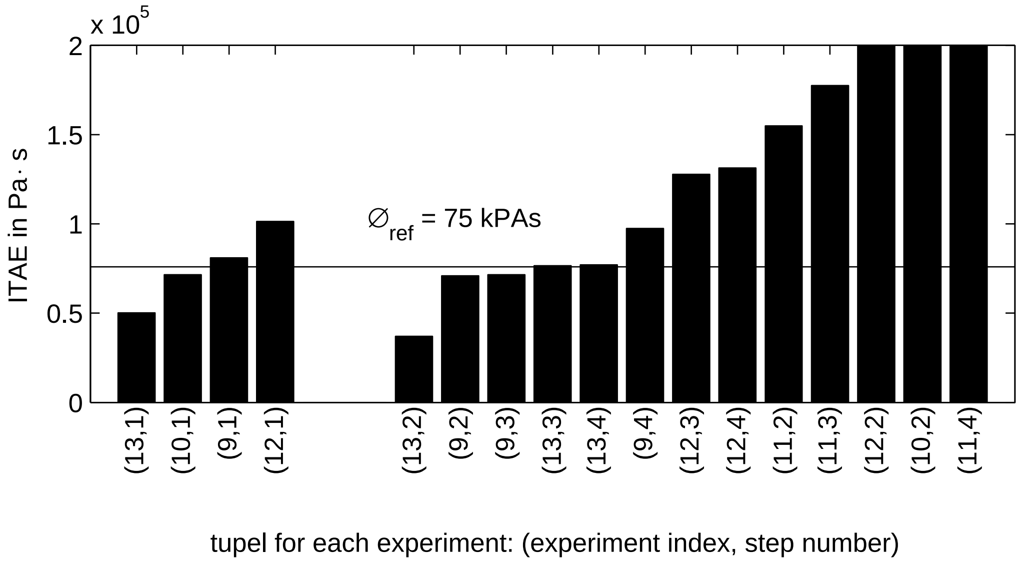

Figure C.7: AHU 01 supply pressure: ITAEs of step experiments under step configuration 4: left, actual parameters; right, proposed parameters.

both, with actual and initial parameters, are reluctant and behind their respective real step responses. The real step reaches very low ITAE-values with the normal lambda-tuning heuristic and its behavior is close to the simulated step.

C.4 Further results towards Three-way-valve K08Y02

Assuming an uniformly distributed occur of disturbances, the probability of each occur is equal during each step experiment. For a large number of step experiments, the consideration of integral criteria recovers as a valid evaluation instrument. For this reason, the final result summary includes all ITEA values of heavily-disturbed systems.

When investigating experiment number one, “K08 Y02 Supply Temp 2015-09-07 09h20”, it becomes obvious, that the initial step response, which figure C.12 shows, is heavily disturbed about 5 minutes after the step. Still, the control system with initial parameters is on the one hand not able to cope with the disturbance itself, on the other hand not able to counteract the permanent deviation.

Figure C.13 shows the tfest(2,5,5;1,3,3;d)-PISIMC-PID-Parameter proposal’s step response, which provided a control amelioration via decreasing the ITAE-value by -48.42 %. A disturbance occurred during the step, but, still, this control configuration is able to attain lower deviation at the end of the experiment. The other two suggested PID-parameter sets performed partly oscillating, but both achieved stable control behavior towards the end of their respective step experiment.

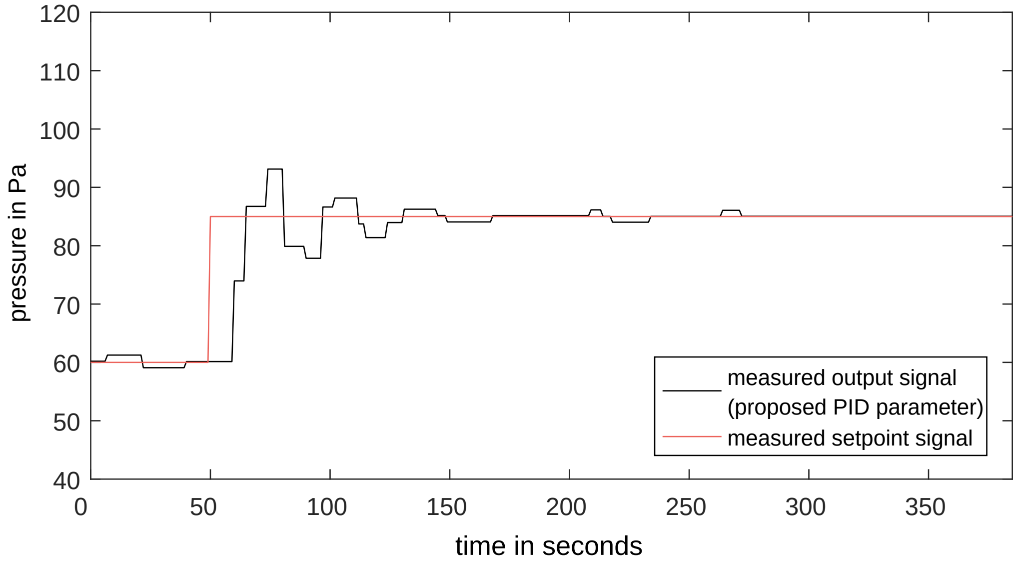

Figure C.8: AHU 01 supply pressure 2015-06-15 18h00: bj(1,5,3,3;1;d)PIBO step experiment, step type 2, experiment number 6, step number 2

Experiment number two, “K08 Y02 Supply Temp 2015-09-08 11h50 ”, reached slightly better control performance but had the same issues. By visual investigation becomes obvious, that its control behaviour is slightly more aggressive than that of experiment one, which may be explained by the excitation signal, refer to subsection 8.2.1.

Finally, both experiment provided more aggressive, but still better performing control loop configurations from an ITAE perspective. Six out of six proposals ameliorated the control performance.

C.5 Further results towards AHU04 re-heater

See figure C.14.

C.6 Further results towards two-way heat exchanger H061 heating

Experiment number one, “H061 Supply Temp Heating 2015-09-07 03h00”, using step configuration one, provided PID-parameter sets that have not been evaluated correctly due to not properly configured step experiments. The system’s return temperature was as high as the step value, i.e. 24 °C · The consequences are, first, the system was not able to settle at 22 °C , second, the system perfectly reached the step value for all three step experiment while the controller output was zero, meaning

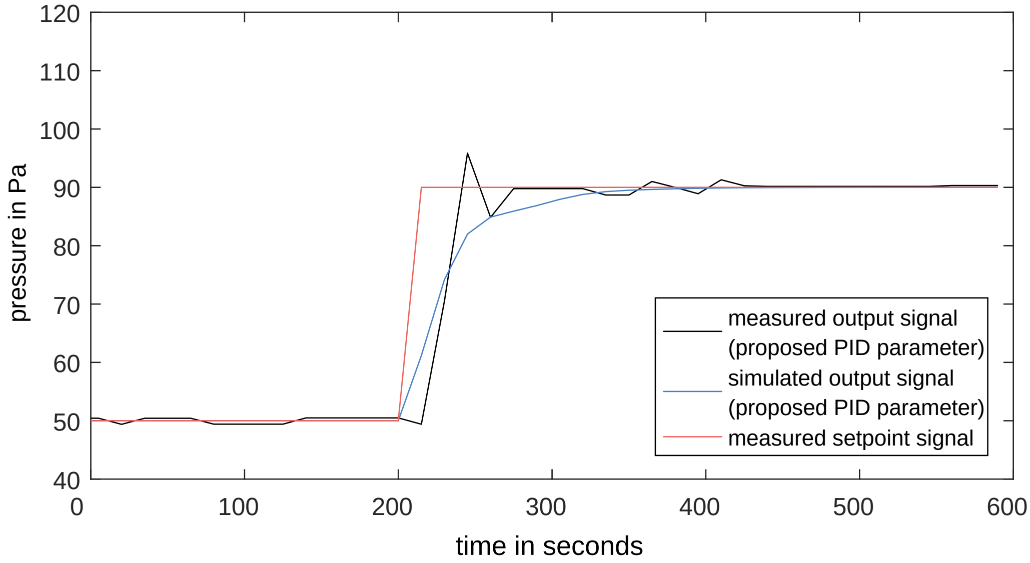

Figure C.9: AHU 01 supply pressure 2015-08-29 10h00: bj(1,3,2,2;0;d)PIBO step comparison, step type 4, experiment number 13, step number 2

the heating valve was closed, and third, the evaluation provided very low ITAE-values. As the algorithm regards disturbances within the identification, the time-varying system return temperature does not deteriorate the identification but still it defines the lowest reachable temperature point of the system. Therefore, the step configuration for the next experiment has higher settling and step temperatures.

When comparing the initial step to the three steps with proposed parameters, the control performance is advantageous insofar as, within the initial step experiment, the system's temperature increased after the step, due to valve opening, while within the proposed parameter's step experiment, the system closed the valve and the temperature matched the step value. This means that the algorithm ameliorated the control performance but a fair quantitative comparison between the three proposals is not possible.

Within experiment number two, "H061 Supply Temp Heating 2015-09-10 20h00", this new step configuration two lead to very low opening angles during the proposed step experiments. The system was not able to find stable operating conditions. Still, the step configuration's temperatures are too low, the system did not settle. A fair quantitative comparison is still not possible.

C.7 Further results towards room temperature control

See figures C.15 and C.16.

C.8 Experiment configurations towards communication infrastructure variation

See tables C.5 and C.6 for experiment and step configurations of the three-way-valve volume flow control H061 Y01.

See tables C.7 and C.8 for experiment and step configurations of the two-way-valve volume flow control H061 Y02.

See tables C.9 and C.10 for experiment and step configurations of the two-way-valve volume flow control Z022 S0020.

See tables C.11 and C.12, for experiment and step configurations of the two-way-valve volume flow control Z022 S0021.

Table C.5: H061 Y01 volume flow: experiment configurations

Exp.	**STW**	**STR**	**MMO**	**MDO**	**IDT**	**MAE**	**ID**	**mean**	**ampl.**	**shape**	**Ste.**
-	in s	in s	-	-	in s	-	-	in %		-	-
1	30	1	3	0	11640	388	CL	1	1	rbs	1
2	100	1	3	0	14440	144.4	CL	1	1	rbs	2
3	200	1	3	0	13640	68.2	CL	1	1	rbs	3
4	200	1	3	0	18040	90.2	CL	1	1	rbs	2
5	200	1	3	0	21640	108.2	CL	1	1	rbs	2
6	100	1	3	0	9240	92.4	CL	1	1	rbs	4
7	200	1	3	2	24720	123.6	CL	1	1	1/f	5
8	60	45	6	6	2640	44	OL	42.5	85	1/f	6
9	300	15	6	6	9840	32.8	OL	42.5	85	step	6

Table C.6: H061 Y01 volume flow: step configurations

Step	**Settling time$_i$**	**Step length**	**Settling value**	**Step value**	**Number of executions**
1	300	300	0 l/s	1 l/s	1
2	400	400	0 l/s	1 l/s	14
3	500	500	0 l/s	1 l/s	4
4	600	600	0.1 l/s	1 l/s	4
5	1200	1200	0.2 l/s	1 l/s	5
6	1200	1200	0.4 l/s	1.2 l/s	8

Table C.7: H061 Y02 volume flow: experiment configurations

Exp.	STW	STR	MMO	MDO	IDT	MAE	ID	mean	ampl.	shape	Ste.
-	in s	in s	-	-	in s	-	-	in %		-	-
1	30	1	3	0	4440	148	CL	1	1	rbs	1
2	30	1	3	0	839	28	CL	1	1	rbs	1
3	30	1	3	0	11640	388	CL	1	1	rbs	1
4	30	1	3	0	11640	388	CL	1	1	rbs	1
5	100	1	3	0	14440	144.4	CL	1	1	rbs	2
6	200	1	3	0	18040	90.2	CL	1	1	rbs	2
7	200	1	3	0	18040	90.2	CL	1	1	rbs	2
8	100	1	3	0	16440	164.4	CL	1	1	rbs	3
9	200	1	3	2	12720	63.6	CL	1	1	1/f	4
10	400	1	3	2	8040	20.1	CL	1	1	1/f	5
11	60	45	6	6	2640	44	OL	55	90	1/f	5
12	300	15	6	6	6960	23.2	OL	55	90	step	5

Table C.8: H061 Y02 volume flow: step configurations

Step	Settling time$_i$	Step length	Settling value	Step value	Number of executions
1	300	300	0 l/s	1 l/s	17
2	400	400	0 l/s	1 l/s	13
3	600	600	0.1 l/s	1 l/s	4
4	1200	1200	0.2 l/s	1 l/s	5
5	1200	1200	0.4 l/s	1.2 l/s	12

Table C.9: Z022 S0020 volume flow: experiment configurations

Exp.	STW	STR	MMO	MDO	IDT	MAE	ID	mean	ampl.	shape	Ste.
-	in s	in s	-	-	in s	-	-	in % or l/s		-	-
1	200	1	3	2	30600	153	CL	5	2	1/f	1
2	400	1	3	2	10440	26.1	CL	5.5	1.5	1/f	2
3	20	1	2	2	10440	522	OL	50	80	1/f	2
4	4	1	8	8	6840	1710	OL	50	80	1/f	2
5	60	45	2	2	2640	44	OL	50	100	1/f	3
6	90	30	2	2	4140	46	OL	50	100	1/f	3
7	90	30	6	6	4440	49.3	OL	50	100	rbs	3

Table C.10: Z022 S0020 Volume flow: step configurations

Step	Settling time$_i$	Step length	Settling value	Step value	Number of executions
1	600	600	3 l/min	6 l/min	5
2	900	900	4 l/min	7 l/min	12
3	1200	1200	4 l/min	7 l/min	12

Table C.11: Z022 S0021 volume flow: experiment configurations

Exp.	STW	STR	MMO	MDO	IDT	MAE	ID	mean	ampl.	shape	Ste.
-	in s	in s	-	-	in s	-	-	in %		-	-
6	90	30	6	6	2640	26.3	OL	50	100	1/f	1
7	90	30	6	6	4440	49.3	OL	50	100	rbs	1

Table C.12: Z022 S0021 Volume flow: step configurations

Step	Settling time$_i$	Step length	Settling value	Step value	Number of executions
1	1200	1200	4 l/min	7 l/min	8

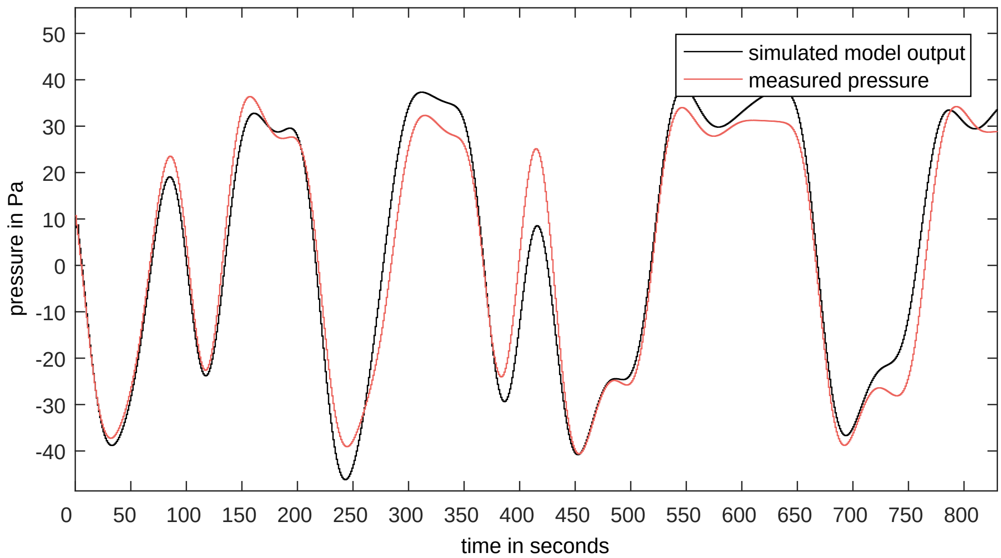

Figure C.10: AHU 01 supply pressure 2015-08-05 11h25: Filtred simulated model output vs. filtred measured system output of best fitting model, bj(1,2,2,2;3;d), mf = 77.13 %, mf_{est}= 99.93 %

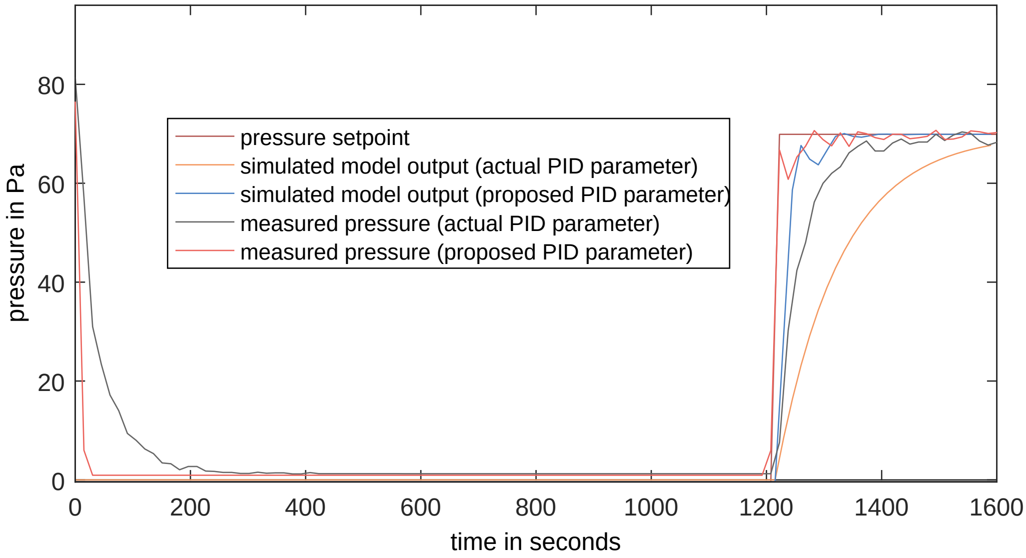

Figure C.11: AHU 04 exhaust pressure 2015-08-31 12h30: Composite steps for BJ(1,2,3,2;1,d)-PILnormal, $ITAE_{initial}$ = 175268 PA s, $ITAE_{new}$ = 59674 PA s, rel.dev = -65.95 %, (experiment 13, step 2, step type 10)

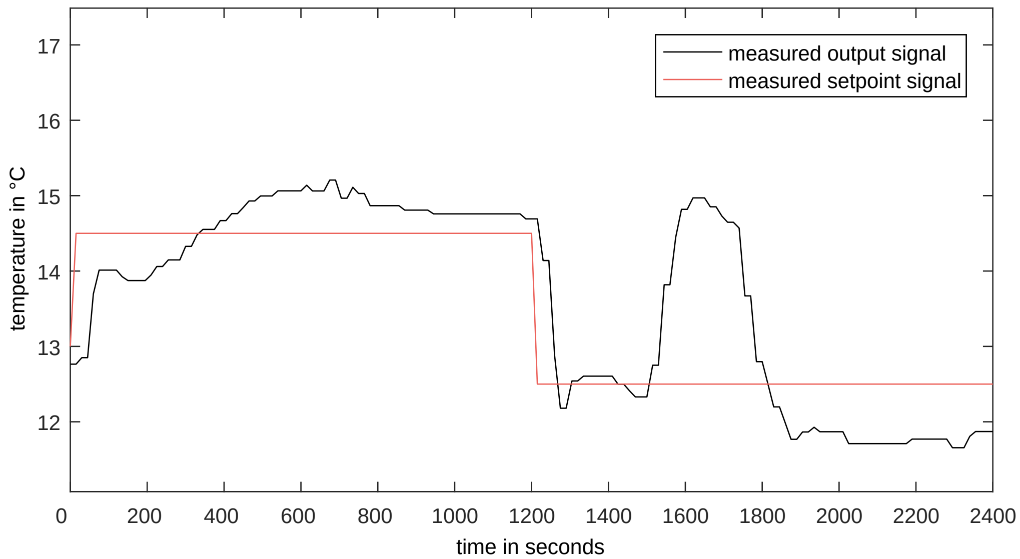

Figure C.12: K08 Y02 Supply Temp 2015-09-07 09h20: initial closed-loop step experiment (experiment number 1, step number 1, step type 1)

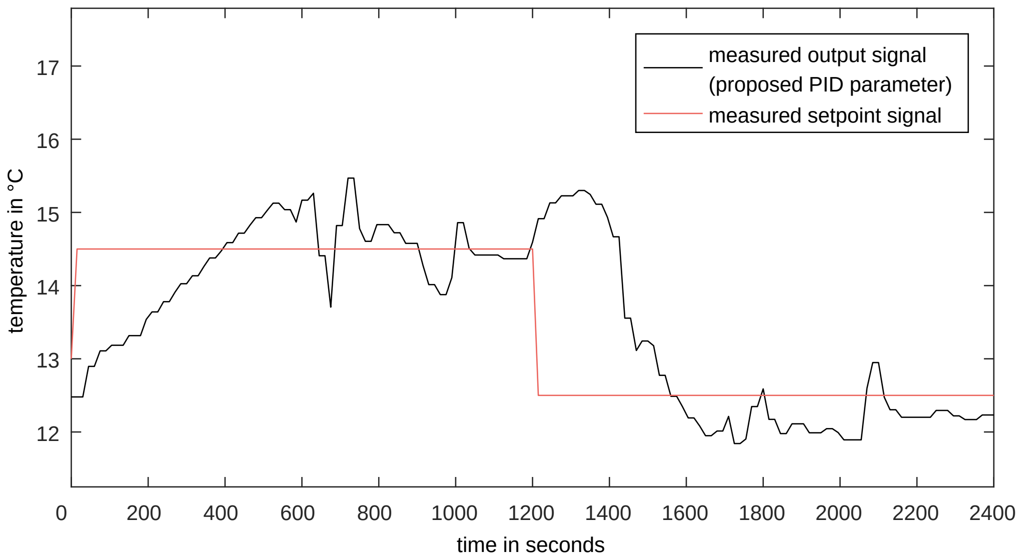

Figure C.13: K08 Y02 Supply Temp 2015-09-07 09h20: tfest(2,5,5;1,3,3;d)PISIMC step (experiment number 1, step number 2, step type 1)

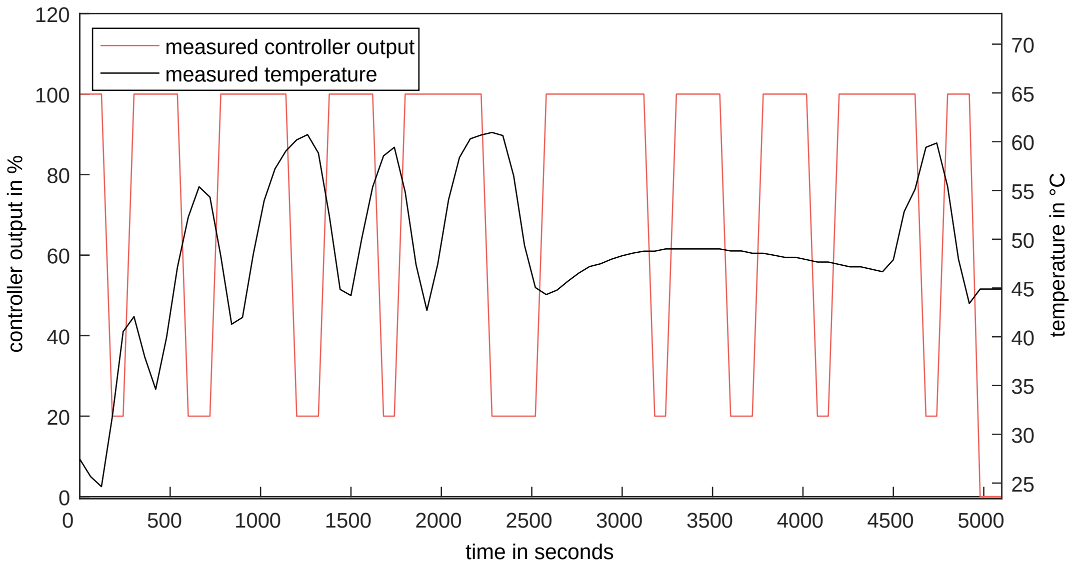

Figure C.14: AHU04 re-heater 2015-09-01 08h45: System input and system output in order to illustrate a plant fault after 2500 seconds

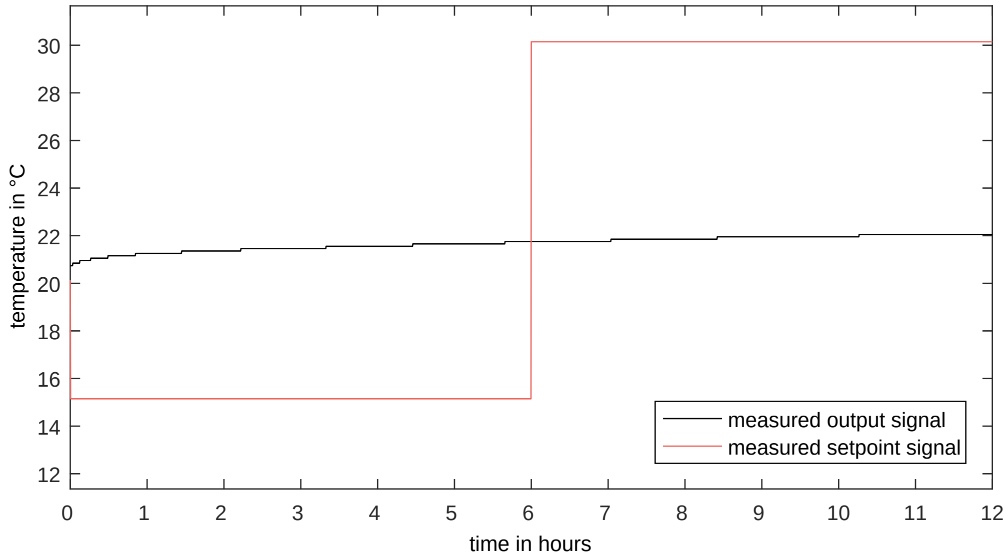

Figure C.15: EBC lab room temperature: initial step experiment

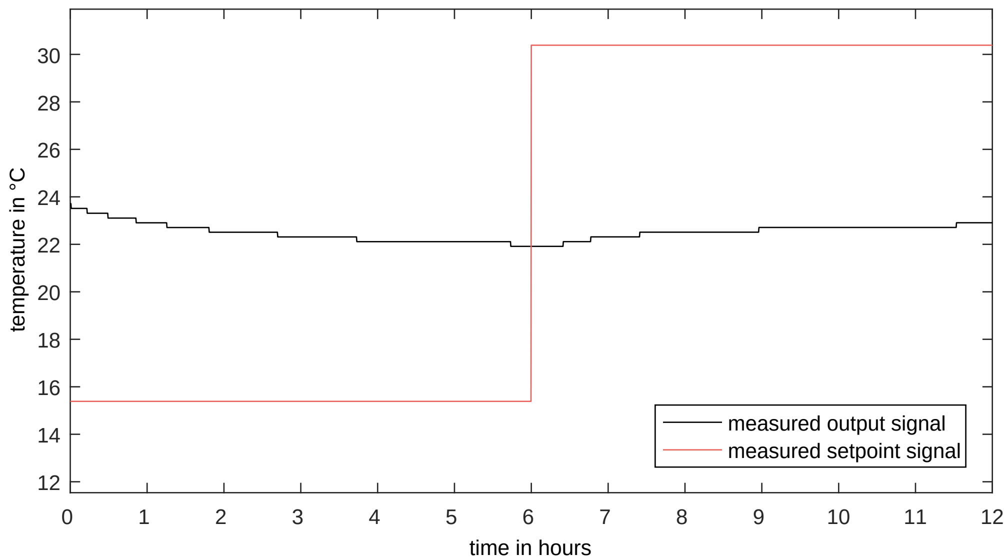

Figure C.16: FCN CIP pool room temperature: initial step experiment

D Fault documentation

I investigated 396 algorithm runs, out of which 86 runs were unsuccessful insofar as the algorithm aborted during its conduction. Table D.1 presents an overview of these faults.

Bugs in the developed code were the most frequent reason. In most cases these bugs were fixed immediately.

Second frequent reason were system faults within the OPC server architecture. During an OPC fault, measurement data is lacking and commands are not processed by the BACS, due to which the algorithm aborts. In some cases, OPC faults persisted only for several minutes and the algorithm continued, e.g. occuring during a step experiment, during settling time or step time. In such a case, only a visual analysis or an analysis of the quantitative abnormality/irregularity can identify the fault. Table D.1 includes identified OPC faults that did not lead to abortions.

During the experiment setup, data points have to be included in the TCP-OPC-interface. Typographical mistakes occurred twelve times during the configuration engineering for the interface.

After nine abortions due to a wrong configuration of the experiments' starting and ending time, meaning e.g. not enough time for all experiments or scheduled experiment that lie in the past, the algorithm's code got more features. Now it adapts starting and end times automatically regarding other experiment that involve the same system.

Seven abortions were due to the method. I.e. one endless loop during an identification experiment for "H061 heating", two times endless loops in "AHU 01 Exhaust Pressure"-experiments due to model order estimation at a model order of twelve. Two times, in "AHU 01 Exhaust Pressure" and "AHU 01 Supply Pressure", also at model orders of twelve, the Skogestad model order reduction algorithm got stuck in endless loops. Finally, the PEM-identification-method was not capable of finding models for "Z022 S0020 volume flow 2015-08-21 21h10" and "Z022 S0021 volume flow 2015-09-07 06h30".

If a plant does not react to a command whose communication is successful, it is sometimes not possible to identify whether a plant fault occurred or the data logging system had an outage. Four errors are traced back to this circumstance.

In three cases, the log file generator ended the log file before logging the reason for the abortion. Even further analyzes did not identify the reason for these abortions.

Table D.1: Reasons for occurred algorithm abortions

fault	frequency	percentage
code bugs	30	35 %
OPC errors	16	19 %
TCP-OPC-interface configuration	12	14 %
wrong configuration of experiment time	9	10 %
abortions due to method	7	8 %
plant or logging faults	4	5 %
no information on fault	3	3 %
wrong experiment configuration	2	2 %
MATLAB license manager fault	1	1 %
plant fault	1	1 %
TCP communication fault	1	1 %
sum	86	100 %

With one occurence each, the algorithm aborted due to missing connectivity to the MATLAB license server, which was due to an outage at the license server, one plant fault, and one disruption in the TCP communication between the algorithm and the TCP-OPC-interface.

E System identification in a continuous time domain

Besides the 396 investigated algorithm runs, the algorithm conducted 187 experiments with a continuous time system identification, fitting state space models and transfer functions. This led to immense computational effort and algorithm crashes. Due to the scope of this thesis I do not elaborate on continuous time system identification and due to the time available for this thesis, I did not try to find robust input parameters and experiment conditions for continuous time. If needed, future work might focus on continuous time system identification.

F Online Documentation

The online documentation is available under:
https://rwth-aachen.sciebo.de/index.php/s/4j5CEA0XvxUIjSP

For questions and further discussion, please contact Johannes Fütterer, johannes.fuetterer@rwth-aachen.de.

G List of own publications and pending patents

The following lists represent publications and pending patents untill March 31st 2017.

G.1 Publications

- Fütterer, Johannes; Constantin, Ana; Müller, Dirk (2011): An energy concept for multifunctional buildings with geothermal energy and photovoltaic. In: CISBAT 2011: cleantech for sustainable buildings; from nano to urban scale; proceedings; 14-16 September 2011, EPFL, Lausanne, Switzerland. - Vol. 1-2. Online available:
https://publications.rwth-aachen.de/record/123708
- Constantin, Ana; Fütterer, Johannes; Müller, Dirk; Rovas, Dimitrios; Kontes, Giorgos (2012): Implementierung einer modelbasierten prädiktiven Regelung für ein Nichtwohngebäude mit komplexem Energiekonzept. Simulationsergebnisse. In: Proceedings of the 4th German-Austrian IBPSA Conference: September 26 - 28, 2012, Berlin University of the Arts, S. 311–315. Online availabe: https://publications.rwth-aachen.de/record/120163
- Constantin, Ana; Fütterer, Johannes; Streblow, Rita; Müller, Dirk; Rovas, Dimitrios; Kontes, Giorgos (2012): Simulation assisted adaption of a model based control parameter fine-tuning methodology for a nonresidential building with a complex energy system. In: Proceedings of the International Symposium in Sustainable Energy in Buildings and Urban Areas: 14 - 20 October, 2012, Kusadasi, Turkey. Online avaiable:
https://publications.rwth-aachen.de/record/120164
- Fütterer, Johannes; Constantin, Ana; Streblow, Rita (2012): Concept and Energy Management in the new E.ON ERC Main Building. In: Proceedings of the International Symposium in Sustainable Energy in Buildings and Urban Areas: 14 - 20 October, 2012, Kusadasi, Turkey. Online available: https://publications.rwth-aachen.de/record/206949
- Constantin, Ana; Fütterer, Johannes Peter; Streblow, Rita; Müller, Dirk; Kontes, Giorgos; Rovas, Dimitrios (2013): Simulation Assisted Implementation of a Model Based Control Parameter Fine-tuning Methodology for a Nonresidential Building with a Complex Energy System. In: Proceedings of BS2013: 13th Conference of International Building Performance Simulation

Association, Chambéry, France, 26 - 28 August 2013. International Building Performance Simulation Association, S. 1869–1876. Online available:
https://publications.rwth-aachen.de/record/227284

- Fütterer, Johannes; Constantin, Ana; Schmidt, Martin; Streblow, Rita; Müller, Dirk; Kosmatopoulos, Elias (2013): A multifunctional demonstration bench for advanced control research in buildings. Monitoring, control, and interface system. In: IECON 2013: 39th annual conference of the IEEE Industrial Electronics Society; Vienna, Austria, 10 - 13 November 2013. Piscataway, NJ: IEEE, S. 5694–5699. Online available:
https://publications.rwth-aachen.de/record/225062

- Fütterer, Johannes Peter; Constantin, Ana; Schmidt, Martin; Streblow, Rita; Müller, Dirk (2013): Monitoring technique, evaluation methodology and results for a multifunctional building with geothermal energy. In: CISBAT 2013 - Cleantech for Smart Cities & Buildings - From Nano to Urban Scale, Lausanne, Switzerland, 4-6 September 2013 / Scartezzini, Jean-Louis. - Vol. 2. Cleantech for Smart Cities & Buildings, S. 751–756. Online available:
https://publications.rwth-aachen.de/record/228323

- Fütterer, Johannes (2014): Regelungseinstellung in der Gebäudetechnik. Methoden und Herausforderungen. In: 16. Hermann-Rietschel-Colloquium 2014 : 09.-14. März 2014, Hirschegg. 16. Hermann-Rietschel-Colloquium 2014, Hirschegg (Austria), 9 Mar 2014 - 15 Mar 2014. München: DIV Deutscher Industrieverlag GmbH, S. 107–109. Online available:
https://publications.rwth-aachen.de/record/464555

- Fütterer, Johannes; Constantin, Ana (2014): Energy concept for the E.ON ERC main building. Aachen (E.ON Energy Research Center Series). Online available: https://publications.rwth-aachen.de/record/443118

- Fütterer, Johannes; Henn, Sarah; Schmidt, Martin; Müller, Dirk (2014): PID control loop tuning for three-port mixing valves within building energy distribution systems. Application and assessment of different tuning methods under real operation conditions. In: Proceedings of ECOS 2014 - The 27th International Conference on Efficiency, Cost, Optimization, Simulation and Environmental Impact of Energy Systems: June 15-19, 2014, Turku, Finland. Aachen: Publikationsserver der RWTH Aachen University, 15 S. Online available:
https://publications.rwth-aachen.de/record/443329

- Fütterer, Johannes; Rothe, Andreas; Müller, Dirk (2014): Dynamisierung und Regelung eines Erdsondenfeldes. In: HLH : Lüftung, Klima, Heizung, Sanitär, Gebäudetechnik 65 (11), S. 21–24. Online available: https://publications.rwth-aachen.de/record/445438

- Fütterer, Johannes; Schmidt, Martin; Müller, Dirk (2014): Modus- und speicherbasierte Regelung eines Wärmepumpensystems mit Geothermiefeld. In: DKV-Tagung, Deutscher Kälte- und

Klimatechnischer Verein (DKV) e.V. Online available:
https://publications.rwth-aachen.de/record/460695

- Michalski, Alexander; Fütterer, Johannes; Rothe, Andreas (2014): Exergetisch optimierte Betriebsführung der Wärme- und Kälteversorgung eines Gebäudes unter Nutzung eines dynamischen Regelungssystems und flexibler Einbindung eines vollständig überwachten Erdwärmesondenfeldes. In: Energieinnovationen in Neubau und Sanierung: Neues aus der Forschung für mehr Energieeffizienz, Raumkomfort, Wirtschaftlichkeit und Nachhaltigkeit; 20.- 21. März 2014; Essen, Zeche Zollverein. Essen: EnOB, S. 63–67. Online available: https://publications.rwth-aachen.de/record/443424
- Fütterer, Johannes Peter; Kraus, Philipp J. E.; Schmidt, Martin; Müller, Dirk (2015): Demonstration of an easy-to-apply, automated control tuning method for typical PID control loops in building energy systems. In: 2015 IEEE 10th Conference on Industrial Electronics and Applications (ICIEA 2015): Auckland, New Zealand, 15 - 17 June 2015. Piscataway, NJ: IEEE, S. 2069–2075. Online available: https://publications.rwth-aachen.de/record/564164
- Baranski, Marc; Sangi, Roozbeh; Fütterer, Johannes Peter; Müller, Dirk; Sayadi, Saeed; Tsatsaronis, George; Morosuk, Tatiana (2016): Verwendung exergiebasierter Methoden für die Entwicklung eines neuartigen Regelungsansatzes in der Lüftungs- und Klimatechnik. In: TGA-Kongress 2016, Berlin (Germany), 14 - 15 Apr 2016, 21 Folien. Online available: https://publications.rwth-aachen.de/record/670876
- Bode, Gerrit Thorben; Fütterer, Johannes Peter; Müller, Dirk (2016): Ein Demonstrator für innovative Technologien und Konzepte. In: TGA-Kongress 2016, Berlin (Germany), 14 - 15 Apr 2016, 19 Folien. Online available: https://publications.rwth-aachen.de/record/660706
- Schild, Thomas; Futterer, J.; Sangi, R.; Streblow, R.; Müller, D. (2015): System of Systems theory as a new perspective on building control. In: 2015 23rd Mediterranean Conference on Control and Automation (MED 2015): Torremolinos (Malaga, Spain) 16 Jun 2015 - 19 Jun 2015. Piscataway, NJ: IEEE, S. 783–788. Online available: https://publications.rwth-aachen.de/record/539087
- Baranski, Marc; Sangi, Roozbeh; Fütterer, Johannes Peter; Müller, Dirk (2016): An Algorithm for Stepwise Exergy-based Model Predictive Control of Building HVAC Supply Chains. In: ECOS 2016: proceedings of the 29th International Conference on Efficiency, Cost, Optimisation, Simulation and Environmental Impact of Energy Systems, June 19. - 23. 2016, Portorož, Slovenia. Online available: https://publications.rwth-aachen.de/record/670875
- Fütterer, Johannes Peter; Bode, Gerrit Thorben; Müller, Dirk (2016): Mode and storage load based control of a complex building system with a geothermal field. In: ECOS 2016: proceedings of the 29th International Conference on Efficiency, Cost, Optimisation, Simulation and

Environmental Impact of Energy Systems, June 19. - 23. 2016, Portorož, Slovenia. Online available: https://publications.rwth-aachen.de/record/668222

- Fütterer, Johannes Peter, Stinner Florian, Müller Dirk (2016) Simulation-based assessment of an easy-to-apply, automated control tuning method for typical PID control loops in building energy systems. In: ECOS 2016: proceedings of the 29th International Conference on Efficiency, Cost, Optimisation, Simulation and Environmental Impact of Energy Systems, June 19. - 23. 2016, Portorož, Slovenia. Online available: https://publications.rwth-aachen.de/record/687197
- Sangi, Roozbeh; Schild, Thomas; Daum, Magnus; Fütterer, Johannes; Streblow, Rita; Müller, Dirk et al. (2016): Simulation-based implementation and evaluation of a system of systems optimization algorithm in a building control system. In: 24th Mediterranean Conference on Control & Automation, Athens (Greece), 21 Jun 2016 - 24 Jun 2016. Online available: https://publications.rwth-aachen.de/record/660090

G.2 Patents pending

- DE 102015102676.7. Verfahren zur Regelung von kühl- und/oder heiztechnischen Anlagen für umschlossene Gesamtobjekte. Erfinder: Huber, Max; Fütterer, Johannes Peter, Müller, Dirk. 25.02.2015
- DE 102016212208.8. System zur automatisierten Analyse und Optimierung von Gebäudeautomationssystemen. Erfinder: Fütterer, Johannes Peter; Müller, Dirk. 05.07.2016

E.ON ERC Band 1
Streblow, R.
Thermal Sensation and Comfort Model for Inhomogeneous Indoor Environments
1. Auflage 2011
ISBN 978-3-942789-00-4

E.ON ERC Band 2
Naderi, A.
Multi-phase, multi-species reactive transport modeling as a tool for system analysis in geological carbon dioxide storage
1. Auflage 2011
ISBN 978-3-942789-01-1

E.ON ERC Band 3
Westner, G.
Four Essays related to Energy Economic Aspects of Combined Heat and Power Generation
1. Auflage 2012
ISBN 978-3-942789-02-8

E.ON ERC Band 4
Lohwasser, R.
Impact of Carbon Capture and Storage (CCS) on the European Electricity Market
1. Auflage 2012
ISBN 978-3-942789-03-5

E.ON ERC Band 5
Dick, C.
Multi-Resonant Converters as Photovoltaic Module-Integrated Maximum Power Point Tracker
1. Auflage 2012
ISBN 978-3-942789-04-2

E.ON ERC Band 6
Lenke, R.
A Contribution to the Design of Isolated DC-DC Converters for Utility Applications
1. Auflage 2012
ISBN 978-3-942789-05-9

E.ON ERC Band 7
Brännström, F.
Einsatz hybrider RANS-LES-Turbulenzmodelle in der Fahrzeugklimatisierung
1. Auflage 2012
ISBN 978-3-942789-06-6

E.ON ERC Band 8
Bragard, M.
The Integrated Emitter Turn-Off Thyristor - An Innovative MOS-Gated High-Power Device
1. Auflage 2012
ISBN 978-3-942789-07-3

E.ON ERC Band 9
Hoh, A.
Exergiebasierte Bewertung gebäudetechnischer Anlagen
1. Auflage 2013
ISBN 978-3-942789-08-0

E.ON ERC Band 10
Köllensperger, P.
The Internally Commutated Thyristor - Concept, Design and Application
1. Auflage 2013
ISBN 978-3-942789-09-7

E.ON ERC Band 11
Achtnicht, M.
Essays on Consumer Choices Relevant to Climate Change: Stated Preference Evidence from Germany
1. Auflage 2013
ISBN 978-3-942789-10-3

E.ON ERC Band 12
Panašková, J.
Olfaktorische Bewertung von Emissionen aus Bauprodukten
1. Auflage 2013
ISBN 978-3-942789-11-0

E.ON ERC Band 13
Vogt, C.
Optimization of Geothermal Energy Reservoir Modeling using Advanced Numerical Tools for Stochastic Parameter Estimation and Quantifying Uncertainties
1. Auflage 2013
ISBN 978-3-942789-12-7

E.ON ERC Band 14
Benigni, A.
Latency exploitation for parallelization of power systems simulation
1. Auflage 2013
ISBN 978-3-942789-13-4

E.ON ERC Band 15
Butschen, T.
Dual-ICT – A Clever Way to Unite Conduction and Switching Optimized Properties in a Single Wafer
1. Auflage 2013
ISBN 978-3-942789-14-1

E.ON ERC Band 16
Li, W.
Fault Detection and Protection inMedium Voltage DC Shipboard Power Systems
1. Auflage 2013
ISBN 978-3-942789-15-8

E.ON ERC Band 17
Shen, J.
Modeling Methodologies for Analysis and Synthesis of Controls and Modulation Schemes for High-Power Converters with Low Pulse Ratios
1. Auflage 2014
ISBN 978-3-942789-16-5

E.ON ERC Band 18
Flieger, B.
Innenraummodellierung einer Fahrzeugkabine
in der Programmiersprache Modelica
1. Auflage 2014
ISBN 978-3-942789-17-2

E.ON ERC Band 19
Liu, J.
Measurement System and Technique for Future Active Distribution Grids
1. Auflage 2014
ISBN 978-3-942789-18-9

E.ON ERC Band 20
Kandzia, C.
Experimentelle Untersuchung der Strömungsstrukturen in einer Mischlüftung
1. Auflage 2014
ISBN 978-3-942789-19-6

E.ON ERC Band 21
Thomas, S.
A Medium-Voltage Multi-Level DC/DC Converter with High Voltage Transformation Ratio
1. Auflage 2014
ISBN 978-3-942789-20-2

E.ON ERC Band 22
Tang, J.
Probabilistic Analysis and Stability Assessment for Power Systems with Integration of Wind Generation and Synchrophasor Measurement
1. Auflage 2014
ISBN 978-3-942789-21-9

E.ON ERC Band 23
Sorda, G.
The Diffusion of Selected Renewable Energy Technologies: Modeling, Economic Impacts, and Policy Implications
1. Auflage 2014
ISBN 978-3-942789-22-6

E.ON ERC Band 24
Rosen, C.
Design considerations and functional analysis of local reserve energy markets for distributed generation
1. Auflage 2014
ISBN 978-3-942789-23-3

E.ON ERC Band 25
Ni, F.
Applications of Arbitrary Polynomial Chaos in Electrical Systems
1. Auflage 2015
ISBN 978-3-942789-24-0

E.ON ERC Band 26
Michelsen, C. C.
The *Energiewende* in the German Residential Sector: Empirical Essays on Homeowners' Choices of Space Heating Technologies
1. Auflage 2015
ISBN 978-3-942789-25-7

E.ON ERC Band 27
Rolfs, W.
Decision-Making under Multi-Dimensional Price Uncertainty for Long-Lived Energy Investments
1. Auflage 2015
ISBN 978-3-942789-26-4

E.ON ERC Band 28
Wang, J.
Design of Novel Control algorithms of Power Converters for Distributed Generation
1. Auflage 2015
ISBN 978-3-942789-27-1

E.ON ERC Band 29
Helmedag, A.
System-Level Multi-Physics Power Hardware in the Loop Testing for Wind Energy Converters
1. Auflage 2015
ISBN 978-3-942789-28-8

E.ON ERC Band 30
Togawa, K.
Stochastics-based Methods Enabling Testing of Grid-related Algorithms through Simulation
1. Auflage 2015
ISBN 978-3-942789-29-5

E.ON ERC Band 31
Huchtemann, K.
Supply Temperature Control Concepts in Heat Pump Heating Systems
1. Auflage 2015
ISBN 978-3-942789-30-1

E.ON ERC Band 32
Molitor, C.
Residential City Districts as Flexibility Resource: Analysis, Simulation, and Decentralized Coordination Algorithms
1. Auflage 2015
ISBN 978-3-942789-31-8

E.ON ERC Band 33
Sunak, Y.
Spatial Perspectives on the Economics of Renewable Energy Technologies
1. Auflage 2015
ISBN 978-3-942789-32-5

E.ON ERC Band 34
Cupelli, M.
Advanced Control Methods for Robust Stability of MVDC Systems
1. Auflage 2015
ISBN 978-3-942789-33-2

E.ON ERC Band 35
Chen, K.
Active Thermal Management for Residential Air Source Heat Pump Systems
1. Auflage 2015
ISBN 978-3-942789-34-9

E.ON ERC Band 36
Pâques, G.
Development of SiC GTO Thyristors with Etched Junction Termination
1. Auflage 2016
ISBN 978-3-942789-35-6

E.ON ERC Band 37
Garnier, E.
Distributed Energy Resources and Virtual Power Plants: Economics of Investment and Operation
1. Auflage 2016
ISBN 978-3-942789-37-0

E.ON ERC Band 38
Calì, D.
Occupants' Behavior and its Impact upon the Energy Performance of Buildings
1. Auflage 2016
ISBN 978-3-942789-36-3

E.ON ERC Band 39
Isermann, T.
A Multi-Agent-based Component Control and Energy Management System for Electric Vehicles
1. Auflage 2016
ISBN 978-3-942789-38-7

E.ON ERC Band 40
Wu, X.
New Approaches to Dynamic Equivalent of Active Distribution Network for Transient Analysis
1. Auflage 2016
ISBN 978-3-942789-39-4

E.ON ERC Band 41
Garbuzova-Schiftler, M.
The Growing ESCO Market for Energy Efficiency in Russia: A Business and Risk Analysis
1. Auflage 2016
ISBN 978-3-942789-40-0

E.ON ERC Band 42
Huber, M.
Agentenbasierte Gebäudeautomation für raumlufttechnische Anlagen
1. Auflage 2016
ISBN 978-3-942789-41-7

E.ON ERC Band 43
Soltau, N.
High-Power Medium-Voltage DC-DC Converters: Design, Control and Demonstration
1. Auflage 2017
ISBN 978-3-942789-42-4

E.ON ERC Band 44
Stieneker, M.
Analysis of Medium-Voltage Direct-Current Collector Grids in Offshore Wind Parks
1. Auflage 2017
ISBN 978-3-942789-43-1

E.ON ERC Band 45
Bader, A.
Entwicklung eines Verfahrens zur Strompreisvorhersage im kurzfristigen Intraday-Handelszeitraum
1. Auflage 2017
ISBN 978-3-942789-44-8

E.ON ERC Band 46
Chen, T.
Upscaling Permeability for Fractured Porous Rocks and Modeling Anisotropic Flow and Heat Transport
1. Auflage 2017
ISBN 978-3-942789-45-5

E.ON ERC Band 47
Ferdowsi, M.
Data-Driven Approaches for Monitoring of Distribution Grids
1. Auflage 2017
ISBN 978-3-942789-46-2

E.ON ERC Band 48
Kopmann, N.
Betriebsverhalten freier Heizflächen unter zeitlich variablen Randbedingungen
1. Auflage 2017
ISBN 978-3-942789-47-9